Incident-Related Travel Time Estimation Using a Cellular Automata Model

Zhuojin Wang

Thesis submitted to the falculty of
the Virginia Polytechnic Institute and State University
in partial fulfillment of the requirements for the degree of

Master of Science

in

Civil and Environmental Engineering

Pamela Marie Murray-Tuite

Montasir Mahgoub Abbas

Chang-Tien Lu

June 4, 2009

Falls Church, VA

Keywords: Cellular Automata, incident, travel time

Incident-Related Travel Time Estimation Using a Cellular Automata Model

Zhuojin Wang

Abstract

The purpose of this study was to estimate the drivers' travel time with the occurrence of an incident on freeway. Three approaches, which were shock wave analysis, queuing theory and cellular automata models, were initially considered, however, the first two macroscopic models were indicated to underestimate travel time by previous literature. A microscopic simulation model based on cellular automata was developed to attain the goal. The model incorporated driving behaviors on the freeway with the presence of on-ramps, off-ramps, shoulder lanes, bottlenecks and incidents. The study area was a 16 mile eastbound section of I-66 between US-29 and I-495 in northern Virginia. The data for this study included loop detector data and incident data for the road segment for the year 2007. Flow and speed data from the detectors were used for calibration using quantitative and qualitative techniques. The cellular automata model properly reproduced the traffic flow under normal conditions and incidents. The travel time information was easily obtained from the model. The system is promising for travel time estimation in near real time.

Acknowledgements

I would like to express my sincere gratitude and thanks to my advisor and chair of my committee, Dr. Pamela Murray-Tuite, for her guidance and support during my study at Virginia Tech. I would also like to thank my committee members, Dr. Montasir Abbas and Dr. Chang-Tien Lu for their guidance and help and special thanks to Dr. Chang-Tien Lu for providing me with all the detector data used in this study.

A final thanks my parents and friends. Without their help, I can not reach so far.

Contents

Chapter 1 Introduction 1
1.1 Background 1
1.2 Motivation 2
1.3 Objective 3
1.4 Main Contribution 4
1.5 Organization 4
Chapter 2 Literature Review 6
2.1 Introduction 6
2.2 Previous Approaches 6
2.3 Cellular Automata Models 10
2.3.1 CA Basics 10
2.3.2 CA Models of Single Lane Freeways 10
2.3.3 CA Models of Lane Changing 13
2.3.4 CA Models of Freeway Ramps 15
2.3.5 CA models of Incidents 17
2.4 Summary 18
Chapter 3 Test Site and Data 20
3.1 Introduction 20
3.2 Test Site Description 20
3.3 Data Collection 22
3.3.1 Loop Detector Data 22
3.3.2 Incident Data 23
3.4 Detector Data Processing 23
3.4.1 Detector Data Processing Steps 23
3.4.2 Data Processing 23
3.4.3 Data Processing Results 27
3.5 OD Estimation 32
3.6 Bottleneck Identification 36
3.7 Summary 37
Chapter 4 Methodology 38
4.1 Introduction 38

4.2 Simulation Setup 38
4.3 CA Model Description 40
4.3.1 Initializing the system 40
4.3.2 Updating vehicles 41
4.4 Simulator Description 46
4.5 Summary 48
Chapter 5 Calibration and Validation 50
5.1 Introduction 50
5.2 Evaluation Measurement 50
5.3 Parameter Discussion 52
5.3.1 Slow-to-start Parameters 52
5.3.2 Following Parameters 55
5.3.3 Lane Changing Aggressiveness Parameters 57
5.3.4 Lane Changing Probability Parameters 59
5.3.5 Speed Reduction Parameters 62
5.4 Incident-free simulation 64
5.5 Incident Simulation 67
5.5.1 Incident 1: Weekend Daytime 67
5.5.2 Incident 2: Weekday Off-peak 71
5.5.3 Incident 3: Weekday Peak 72
5.5.4 Incident 4: Weekday Peak 75
5.6 Queue Length 79
5.7 Computational Efficiency 80
5.8 Summary 81
Chapter 6 Summary, Conclusions and Future Work 82
6.1 Summary and Conclusions 82
6.2 Future Work 84
Reference 85

List of Figures

Figure 1.1 Schemes of incident timeline and detailed clearance process (summarized from Hobeika and Dhulopala, 2004) 1
Figure 1.2 Main procedures of the system 4
Figure 3.1 Map of the test site from I-66 (Yahoo) 20
Figure 3.2 Schematic diagram of the test site from I-66 21
Figure 3.3 Station layouts on test site 22
Figure 3.4 Sample volume distribution of stations on mainline and ramps 30
Figure 3.5 Scale factors 31
Figure 3.6 Comparison between volumes from OD tables and from loop detectors 34
Figure 3.7 Speed contour in morning rush hour of April 25, 2007, Wednesday 36
Figure 4.1 Illustration of CA notation 38
Figure 4.2 Schematic diagram of off-ramp influence zone 40
Figure 4.3 Illustration of lane changing priority 44
Figure 4.4 Simulator Interface 47
Figure 4.5 Sample incident input file 47
Figure 5.1 Speed contour plots of morning congestion with different P_0 53
Figure 5.2 speed contour plots of morning congestion with different P_{00} 53
Figure 5.3 Speed contour plots of morning congestion with different $P_{following}$ 56
Figure 5.4 Speed contour plots of morning congestion with different $d_{following}$ 56
Figure 5.5 Speed contour plots of morning congestion with different k 58
Figure 5.6 Speed contour plots of morning congestion with different b 58
Figure 5.7 Speed contour plots of morning congestion with different P_{change_dis} 60
Figure 5.8 Speed contour plots of morning congestion with different P_{change_man} 61
Figure 5.9 Speed contour plots of morning congestion with different P 63
Figure 5.10 Speed contour plot of Wednesday morning congestion 64
Figure 5.11 Traffic flow (veh/5min) at major freeway measurement stations 66
Figure 5.12 Location of Incident 1 67
Figure 5.13 Traffic counts (veh/5min) upstream of the incident location on freeway measurement stations and ramps for incident 1 69
Figure 5.14 Tabular travel time records for incident 1 70

Figure 5.15 Location of Incident 2 71
Figure 5.16 Traffic counts (veh/5min) at upstream of incident location on freeway measurement stations for incident 2 71
Figure 5.17 Tabular travel time records for incident 2 72
Figure 5.18 Location of Incident 3 73
Figure 5.19 Traffic counts (veh/5min) at upstream of incident location on freeway measurement stations for incident 3 74
Figure 5.20 Tabular travel time records for incident 3 75
Figure 5.21 Location of Incident 4 76
Figure 5.22 Traffic counts (veh/5min) at upstream of incident location on freeway measurement stations for incident 4 78
Figure 5.23 Tabular travel time records for incident 4 79
Figure 5.24 Queue length and beginning recovery for Incident 2 80

List of Tables

Table 3.1 Sample incident records for Incident 32421 in April 13, 2007 (IMS) 24
Table 3.2 Station STDEV and relative LSE of stations before and after data modification (Friday) 28
Table 3.3 Mean and variance of gap volume between OD tables and link flow (Friday) 34
Table 4.1 Freeway sections and indicators 40
Table 5.1 Average MAPE value between thirty days and representative flow data 51
Table 5.2 Base values of the parameters for sensitivity analysis 52
Table 5.3 MAPE and GEH analysis on morning congestion with different P_0 54
Table 5.4 MAPE and GEH analysis on morning congestion with different P_{00} 54
Table 5.5 MAPE and GEH analysis on morning congestion with different $P_{following}$ 57
Table 5.6 MAPE and GEH analysis on morning congestion with different $d_{following}$ 57
Table 5.7 MAPE and GEH analysis on morning congestion with different k 59
Table 5.8 MAPE and GEH analysis on morning congestion with different b 59
Table 5.9 MAPE and GEH analysis on morning congestion with different P_{change_dis} 62
Table 5.10 MAPE and GEH analysis on morning congestion with different P_{change_man} 62
Table 5.11 MAPE and GEH analysis on morning congestion with different P 63
Table 5.12 The range of the start time, end time and queue length of four recurring congestion locations 64
Table 5.13 Start time, end time and queue length of four recurring congestion from simulation 65
Table 5.14 The average MAPE and GEH% value of major stations on the mainline 65
Table 5.15 List of final parameter values 66
Table 5.16 Rerouting start time, end time and percentage for Incident 1 67
Table 5.17 MAPE and GEH% of Incident 1 69
Table 5.18 MAPE and GEH% of Incident 2 72
Table 5.19 Rerouting start time, end time and percentage for Incident 3 73
Table 5.20 MAPE and GEH% of Incident 3 75
Table 5.21 Rerouting start time, end time and percentage for Incident 4 76
Table 5.22 MAPE and GEH% of Incident 4 78
Table 5.23 Computational time of four incidents simulation 80

Chapter 1 Introduction

Traffic congestion continues to increase in the United States and worldwide, causing 4.2 billion hours in delays and costing $78 billion in 2005 in 437 urban areas of the U.S (Schrank and Lomax, 2007). The Federal Highway Administration (FHWA) attributes 25% of congestion to incidents (Corbin *et al.*, 2007). Since such a large portion of congestion is ascribed to incidents, prediction and estimation of incident-related effects is critical to road management and can aid the department of transportation with congestion mitigation plans and providing information to the motorists via mass media such as VMS or radio for rerouting purposes.

1.1 Background

Incidents happen everyday. Take Interstate-66, in Northern Virginia, as an example: about 5,000 incidents occurred during 2007, 22% of which are collisions, 48% are disabled vehicles, 15% are congestion, 6% are road work and the rest includes debris, vehicle fires, and police activity. Incidents lead to capacity and speed reduction and queues spilling back on the freeway, thus retarding people's trips, increasing drivers' travel time, reducing the efficiency of the transportation network and causing significant economic loss.

Incident-related delay involves two components: incident clearance duration and recovery time. The incident clearance process can be divided into four periods: detection, dispatch, response and clearance (Hall, 2002). Recovery time, is the time "taken for traffic to reach normal conditions once the incident is cleared" (Hobeika and Dhulopala, 2004, pp.98). Figure 1.1 presents the timeline of an incident along with detailed incident clearance processes from incident occurrence to its clearance. The queue propagates during the incident clearance period and dissipates in the recovery time.

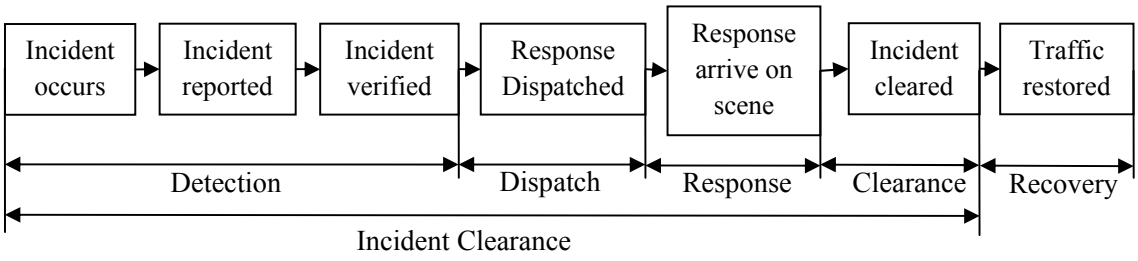

Figure 1.1 Schemes of incident timeline and detailed clearance process (summarized from Hobeika and Dhulopala, 2004)

After an incident occurs, time is key information both for administrators and drivers. The administrator is concerned more about the incident detection, dispatch, response and clearance time while for the drivers, individual travel time information is more desirable, facilitating them to rearrange their schedules or making rerouting decisions. The incident clearance duration from detection to clearance is affected by many factors such as the severity of the incident, the number of responses involved in the rescue, the incident type and occurrence time. For example, planned incidents such as road work normally last much longer than unplanned incidents such as debris, collisions and congestion. The average duration of road work is about 7 hours while it is less than 200 minutes for unplanned accidents according to Virginia Department of Transportation (VDOT) incident records (VDOT, 2007). Numerous studies have contributed to estimate duration which however is out of the scope of this thesis. Instead, travel time from the driver's perspective is the focus of this study with duration as a given value.

1.2 Motivation

Incident-related travel time forecasting is significant for Intelligent Transportation System (ITS) applications on freeway management, facilitating transportation authorities to make congestion mitigation plans and helping individual motorists to reschedule their trips for the purpose of congestion alleviation.

Statistical analysis, macroscopic calculation and microscopic simulation are three main methods to estimate incident-related travel time. Statistical analysis approaches typically consider the entire incident period from incident occurrence to recovery, as such, these are not applicable to the current study which focuses on driver-oriented travel time instead of administrator-oriented incident duration. Though with the computational advantage, macroscopic methods are revealed to underestimate freeway travel time when compared to the field measurements in the presence of ramps along the freeway (Yeon and Elefteriadou, 2006). Therefore, macroscopic models are not applicable when high fidelity results are required. Microscopic simulation, on the other hand, can reproduce the traffic flow more realistically and precisely but with sacrifice on computational efficiency. Furthermore, current existing microscopic simulation packages such as VISSIM and PARAMICS are sufficient for an offline incident simulation, however, inadequate in a near-real time application due to computational effort and difficulty in making frequent changes such as opening or closing lanes in the software.

With these in mind, Cellular Automaton (CA) models are explored in this thesis to develop an accurate and efficient system for near real time forecasting of incident-related travel time, which is expected to avoid drawbacks of previous approaches. Cellular automaton is actually a dynamic

system with discrete and finite features in time and space. “Cellular” points out the discrete feature of the system while “automaton” implies the feature of self-organization, free of requiring extra controls from the outside. Cellular automata are “sufficiently simple to allow detailed mathematical analysis, yet sufficiently complex to exhibit a wide variety of complicated phenomena” (Wolfram, 1983, pp. 601). The discrete feature enables CA models to simulate the network in a more efficient way along with the advantages that microscopic models have. Moreover, CA models can easily capture the features of observed driving behaviors and translate them into model languages. All these advantages make CA models an ideal tool for near real time forecasting.

1.3 Objective

The goal of this study is to develop a CA model for estimating travel time for drivers to get through the incident bottleneck in near real time for I-66 in Northern Virginia. Incident duration is determined externally and is not part of this study. To attain the overall goal, this study addresses the following objectives:

1. Reviewing existing incident-related travel time estimation techniques;
2. Developing origin-destination matrices for the network;
3. Developing CA models to reproduce recurring congestion and non-recurring incident-related congestion;
4. Developing methods to calculate travel time; and
5. Examining the feasibility of the model for near real-time incident simulation.

Input for the simulator includes start time of the incident, clearance duration, location, and status of lane closure. Meanwhile, rerouting information including rerouting start time, end time and percentage of the vehicles for each ramp upstream of the incident location is required in the current system. Outputs of the system are travel time for drivers at different locations passing through the incident bottleneck.

A small user interface was developed in this study. This component to the system provides extra functions for data input and output. For example, the clearance time of the incident may not be accurately determined before the clearance of the incident and lane closure status could change at any time. Under this condition, saving and loading snapshots will be a useful approach to address these problems. The snapshots record the network configuration, vehicles’ distribution and travel time information and are outputted every five minutes. Meanwhile, they also can be loaded into the system for the sake of simulation time, which is an importation issue in near-real time application.

The steps of the system are presented in Figure 1.2. The whole system is developed using the Microsoft Visual Studio 2005 C#.

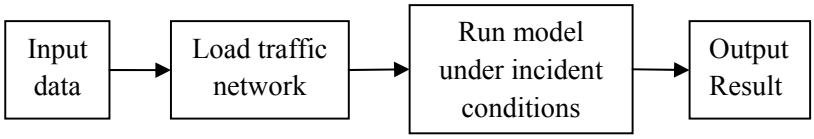

Figure 1.2 Main procedures of the system

1.4 Main Contribution

The main contribution of this study is an original CA model that is capable of real road incident simulation. Several driving behaviors are incorporated into the model, which can be summarized as follows:

1. Slow-to-start
2. Discretionary lane changing behavior on the freeway
3. Mandatory lane changing of exit vehicles near their intended off-ramps
4. Mandatory lane changing of merging vehicles from onramps
5. Merging behavior upstream of the incident locations
6. Brake light effects
7. Driving behavior on shoulder lanes
8. Speed oscillation in ramp influence zones

Driving behaviors 1 to 6 have been studied in the previous literature however different rules are explored in this thesis to catch the features for real traffic simulation. Driving behaviors 7 and 8 are initially proposed in this study.

Based on the CA model, a small simulator was developed for the incident simulation on I-66 for the sake of practical application. After inputting the incident-related information such as start time, end time and location, etc into the simulator via an interface, a readable travel time table will be generated automatically. The output travel time information not only covers the incident clearance duration but also queue dissipation period until the flow recovers to the normal conditions.

1.5 Organization

The remainder of this thesis is organized into five chapters. Chapter 2 presents a brief introduction of previous studies in forecasting incident-related travel time. Advantages and disadvantages of each method are discussed. The remainder of the chapter focuses on an introduction of previous Cellular Automata models for freeways, including models for single lane facilities, lane changing, on- and off-ramps and work zones.

Chapter 3 introduces the test bed for this study, involving the configuration of the road, lane control policies and station layouts, followed by a detailed description of the data processing procedures including data collection, detector data processing and creation of origin-destination

matrices. The results from data processing are presented at the end of the chapter along with bottleneck identification based on speed contour plots generated from detector data.

Chapter 4 presents the framework of the proposed CA model. The initial simulation setup is introduced at first, followed by a detailed illustration of vehicle updating rules in the simulation process, concerning various driving behaviors under different conditions. The function of the simulator is illustrated at the end of chapter 4.

Chapter 5 describes the calibration process, evaluation measures and sensitivity analysis of the parameters. The incident-free condition is simulated first and the corresponding model parameters are calibrated, which are then used in the CA models for incident simulation. Travel time estimation methods are introduced along with sample results from incident simulation.

Chapter 6 presents the summary, conclusions and recommended future work of this study.

Chapter 2 Literature Review

2.1 Introduction

Numerous approaches have been developed to forecast travel time under incident conditions and statistical analysis, macroscopic calculation and microscopic simulation are three main methods to address the issue. Statistical analysis includes probabilistic distributions (Giuliano, 1989; Garib *et al.*, 1997; Sullivan, 1997; Nam and Mannering, 2000), linear regression models (Garib *et al.*, 1997; Ozbay and Kachroo, 1999), time sequential models (Khattak *et al.*, 1995), decision trees (Ozbay and Kachroo, 1999; Smith and Smith, 2001) and Artificial Neural Network (ANN) models (Wei and Lee, 2007). Queuing analysis and shock wave models are two commonly used macroscopic models to estimate the travel time through a bottleneck (Nam and Drew, 1999; Zhang, 2006; Xia and Chen, 2007). Microscopic simulation is normally based on developed simulators such as VISSIM and PARAMICS.

In this chapter, previous approaches are briefly introduced first followed by an introduction of a microscopic simulation approach based on cellular automata (CA) models.

2.2 Previous Approaches

Several methods have been explored to estimate general travel time from detectors. Petty (1998) developed a methodology to estimate link travel time directly from the single loop detector and occupancy (percentage of time when vehicles are detected within a given time) data. The model is based on the assumption that all the vehicles arriving at an upstream point during a certain period of time have a common probability distribution of travel time to a downstream point. The distribution of travel time is calculated by minimizing the difference between actual output volume and estimated output volume speculated from upstream input flow and its travel time distribution. Coifman (2002) explored relationships between travel time and headway, vehicle speed, which are obtained from individual dual loop detectors and speed at capacity, which is derived on the basis of linear approximation of the flow-density relationship. Oh et al. (2003) based their calculations on section density and flow estimates from point detectors. The section-density-based travel time has a linear relation to the section length and the sum of densities in sequential time steps and an inverse relation to the sum of upstream and downstream flows. Though easily used, these previous works applicable for general travel time estimation are not necessarily capable of capturing complex dynamics under incident conditions. Furthermore, they fail to consider the queue effects on the travel time.

Approaches to forecasting travel time specific for incidents scenarios have also been explored. Probabilistic distribution is a statistics-based method to predict incident duration from incident occurrence to recovery. Duration was treated as a random variable and a probability density function was developed to fit the data. Golob et al. (1987), Giuliano (1989) and Garib et al. (1997) deemed that the duration of an incident followed the lognormal distribution while Nam and Mannering (2000) found that the Weibull distribution could also describe the duration.

Linear regression models seek to identify relationships between incident duration and related variables. Garib et al. (1997) incorporated six significant variables into linear regression models, which are the number of lanes affected, the number of vehicles involved, a binary variable for truck involvement, a binary variable for time of day, the natural logarithm of the police response time and a binary variable for weather condition (cited by Smith and Smith, 2001, pp.10).

Time sequential models (Khattak *et al.*, 1995) identified ten distinct stages of the incident and the duration for each stage is calculated on the basis of a specific regression model. The variables used for the regression models are sequentially increasing in accordance to the progression of obtaining the incident information in the field.

Decision tree methods represented a sequential decision process as a tree-shape diagram where the root is the result and each leaf or internal node is labeled with the causes contributing to the occurrence of its upper level event. The inference is processed from the root to leaves and the intermediate events are internal nodes. Once an internal node is reached, an attribute value is assigned to this node and the value is tested to decide "which child node the process should proceed to" (Ohta et al., 2008, pp. 402).

Wei and Lee (2007) used Artificial Neural Network (ANN) approaches to forecast the duration from incident occurrence to clearance. The input variables include incident characteristics, traffic data from loop detectors, time relationship (gap between the time of an incident notification and the recording time of detector data), space relationship (distance between an incident and the detector site) and geometry characteristics (Wei and Lee, 2007).

These approaches typically take into consideration the entire incident period from occurrence to recovery, as such, these are not applicable to the current study which focus on driver-oriented travel time instead of administrator-oriented duration such as response time or clearance time.

Macroscopic models to estimate travel time are developed on the basis of traffic flow theories and the relationships of flow, speed and density. Most of these models are based on comparison between the inflow and outflow of a specific section in sequential time periods. The advantage of these models is their capability of capturing the dynamic characteristics of traffic (Vanajakshi, 2004).

Shock wave theories and queuing models are two generally used macroscopic approaches to forecasting travel time, delay and queue length for individual or total vehicles at a bottleneck. Diagrams developed for the models facilitate the assessment.

Shock wave analysis is based on time-space (t, x) diagrams (see for example Lawson *et al.*, 1997). Parallel continuous lines represent trajectories of sequential vehicles and the slopes of the lines represent the speed of the vehicle. The vehicles drive at free flow speed and reduce their speed when they approach the back of a queue, possibly caused by an infrastructure design or incident related bottleneck. The change in slope of the trajectory line distinguishes the upstream free flow state from the downstream queued state. If these change points are connected among adjacent vehicle trajectories with a line, this line represents the location of the back of the queue as a function of time and its slope indicates the speed of the queue's spilling back. This speed can be calculated numerically as the change in flow divided by the change in density at the interface of the free-flow and queued states (Lawson *et al.*, 1996). Individual delay and total travel time spent in the queue can also be numerically determined from the diagram.

A drawback to using the shock wave approach to forecast the travel time is the tedious and cumbersome work in plotting individual vehicle trajectories. Furthermore, this disaggregate data of each vehicle is not available from detectors which collect aggregated data.

Instead of constructing laborious vehicles trajectories, queuing models are based on input-output (N,t) diagrams (see for example Lawson *et al.*, 1996), also known as cumulative plots (Rakha and Zhang, 2005), which depict the cumulative number of vehicles at two locations: upstream and downstream. The cumulative flows over time at an upstream and a downstream observation point are plotted as A(t) and D(t) on the diagram, recording the arrival and departure time of each vehicle. For an individual vehicle, the horizontal distance between A(t) and D(t) is the total travel time between the two observation points. V(t), obtained by moving A(t) horizontally to the right by the free-flow travel time to the bottleneck, represents the virtual arrival time of each vehicle at the bottleneck without any delay. The horizontal distance between V(t) and D(t) represents the delay for individual drivers. Lawson et al. (1996) also introduced a new curve B(t) into the model, which represents "the number of vehicles to reach the back of the queue by time t, or equivalently the times that each vehicle reached the back of the queue" (Lawson *et al.*, 1996, pp. 5). The horizontal distance and vertical distance between B(t) and D(t) interprets the queue length and the number of vehicles in the queue, respectively.

Using queuing models, Nam and Drew (1999) estimated vehicles' travel times under normal flow conditions and congested flow conditions separately. In normal flow conditions, vehicles are supposed to enter and leave the section within the time interval concerned, while this is not true for

the congestion situation. The area between the cumulative arrival and departure curves from two observation points is considered as total travel time for all vehicles passing through the link.

Rakha and Zhang (2005) pointed out three errors that Nam and Drew (1998, 1999) has made in their research referring to the comparison between shock wave theory and queuing models. Rakha and Zhang claimed that the area between the arrival and departure curves in queuing diagram is the total delay rather than total travel time and based on this point of view, the delay computations for shock wave analysis and queuing models are consistent.

Yeon and Elefteriadou (2006) compared the estimated travel time from shock wave theory and queuing models to field data. The results revealed that neither approach adequately considers the ramp effects along the freeway and both of them underestimate the travel time for congested conditions (Yeon and Elefteriadou, 2006). Based on the results, Yeon and Elefteriadou recommend developing an alternative method which should consider the effects from ramps.

Car-following (CF) are classical microscopic models to simulate traffic and the models have been incorporated into several simulation packages such as VISSIM and PARAMICS. However, despite their capability of capturing vehicle behavior, these existing microscopic simulation packages are excluded as ideal tool for this study due to their run times and difficulty in making some changes or setting some features in the software, especially when near real time simulation is required.

Cellular Automata (CA) models are relatively new methods when compared to CF models with the advantage of computational efficiency. CA models were initially proposed by Von Neumann in 1952 (Ulam, 1952) and introduced into the field of transportation by Cremer and Ludwig in 1986 (Cremer and Ludwig, 1986). CA models have been widely used to simulate a variety of traffic networks including one-way (Nagel and Schreckenberg, 1992; Larraga *et al.*, 2005) and two-way arterials (Simon and Gutowitz, 1998; Fouladvand and Lee, 1999), freeways (Hafstein *et al.*, 2004), intersections (Brockfeld *et al.*, 2001), roundabouts (Fouladvand *et al.*, 2004), toll stations (Zhu *et al.*, 2007) and so forth, and are capable of reproducing various traffic conditions such as congestion and free flow in a microscopic scope. Originally developed CA models allow researchers to make changes in the model, addressing the limitation of using proprietary software and thus becoming an ideal tool for this study.

In this research, CA models specifically applied to freeway traffic are considered. A detailed introduction to CA models is presented in the following section.

2.3 Cellular Automata Models

2.3.1 CA Basics

The CA models separate the roads into a sequence of cells and each cell is either occupied by a vehicle or empty. At each time step, a given vehicle remains in its current cell or moves forward at a speed determined by the relationships between the given vehicle and surrounding vehicles in terms of their relative speed and distance. The relationships are defined in a set of rules. One of the great advantages of CA models is that "the dynamical variables of the model are dimensionless, i.e., lengths and positions are expressed in terms of number of cells, velocity are in terms of number of cells per second, and times are in terms of number of seconds" (Hasfstein *et al*., 2004, pp.341). The dimensionless feature simplifies the application of the models and improves computational efficiency.

Vehicle updating in CA models is either synchronous or sequential. Synchronous updating means in each time step all vehicles are updated in parallel; while in sequential updating, an update procedure is performed sequentially from downstream to upstream. The drivers are assumed to have full information about the behavior of his predecessor in the next time step (Knospe *et al.*, 1999) under sequential updating rules, which yields a higher value of average flow due to a succession of overreactions by the drivers (Jia *et al.,*2007, Knospe *et al.*,1999). Therefore, most CA models follow synchronous updating rules.

The boundary conditions in CA models are categorized into two conditions: periodic and open (Jia *et al.*, 2007). According to periodic boundary conditions, the lead vehicles passing through the end of the road reenter the system at the beginning of the road. The total number of vehicles and density in the system are constant. Under open boundary conditions, new vehicles are injected into the beginning of the road with a probability α and the vehicles are deleted from the system once they reach the end of the road (Jia *et al.*, 2007). Periodic boundary rules are normally used when testing the CA model and calibrating its parameters with a general purpose, where the roads can be hypothetical, and open boundary rules are more adaptable for realistic road networks.

2.3.2 CA Models of Single Lane Freeways

Nagel and Schreckenberg (1992) initially presented a single-lane CA model (NaSch model) for highways in 1992 and most of the later CA models are developed on the basis of this model with additional rules. The rules include four steps, which are presented as follows (Nagel and Schreckenberg, 1992):

Step 1: Acceleration: if the velocity v of a vehicle is lower than the maximum speed ($v_{\max}$) and the gap distance to the next car ahead is larger than its desired speed, the speed is advanced by one ($v+1$).

Step 2: Deceleration: if the forward gap d_n of vehicle n is less than its speed (v), the vehicle reduces its speed to d_n.

Step 3: Randomization: the velocity of each vehicle is decreased by one with probability p if it is greater than zero.

Step 4: Car motion: each vehicle is advanced with its speed (v).

Simple as it is, the cellular automaton model for traffic flow was able to reproduce some characteristics of real traffic, like jam formation (Hafstein *et al.*, 2004). However, NaSch models missed some traffic features, such as the meta-stable state[1], synchronized traffic flow and hysteresis phenomenon[2] encountered in observation.

Numerous efforts have been made to add more rules into the NaSch model to address these limitations. In 1993, Takayasu and Takayasu (1993) introduced slow-to-start rules (TT model). The TT model simply set the maximum speed as 1 cell/s where 1 cell is 7.5 m, and it modified the acceleration step in the NaSch Model, claiming that standing cars accelerate to velocity $v=1$ only if there are at least two empty cells in front. If there is just one free cell in front of the standing cars, it accelerates its speed by one only with a probability q_t. Though the rest of the steps remained the same as the NaSch model, the modification enabled the TT model to present meta-stable states and the hysteresis phenomenon which are missed in the NaSch model.

The BJH model (Benjamin *et al.*, 1996) proposed in 1996 was also capable of simulating the meta-stable status. Unlike the TT model, which combined the slow-to-start rule into the acceleration step of the NaSch model, the BJH model added a slow-to-start rule right after the acceleration step. The rule states: if a vehicle brakes in one time step, then in the next time step the vehicle can advance one cell only with a probability ($1-p_s$), namely, the increase of speed in the first step is zero with a given probability p_s. Like the TT model, the maximum speed was simplified to 1 cell/s where 1 cell is 7.5 m.

The idea behind the modified rules of the BJH and TT models is to mimic the delay of a car in restarting, i.e. due to "a slow pick-up of engine or loss of the driver's attention" (Schadschneider and Schreckenberg, 1999, pp.4).

[1] Meta-stable state is the state region where the traffic flow can be free flow or congestion (Jia *et al.*, 2007).
[2] Hysteresis phenomenon is that the traffic flow in the transferring state from free flow to congestion is higher than that from congestion to free flow (Jia *et al.*, 2007). See for example in Hafstein *et al.*, 2004.

Barlovic et al. (1998) proposed a velocity-dependent-randomization model (VDR model) which modified the randomization step of the NaSch model. The basic idea of the VDR model is that the randomization probability, which is a fixed value in the NaSch model, varies depending on the speed of the vehicle in the previous time step. According to the new rule, the probability for the driver to increase its speed by one is $1-p_0$ if its speed is zero in the previous time step while probability $1-p$ is applied if its previous velocity is greater than zero. The other rules remain the same as the NaSch model. Similar to the TT model and the BHJ model, the VDR model is capable of reproducing meta-stable states.

Li et al. (2001) suggested that the speed of a following vehicle depends not only on the distance between itself and the preceding car but also on the anticipated speed of the preceding car in the next time step. It was confirmed by Li et al. (2001) that neglecting this effect led to underestimation of traffic speed and flow if simulating real road networks. Li et al. (2001) proposed a Velocity Effect (VE) model and addressed the problem by modifying step 2 in the NaSch model. The deceleration rule in the VE model is presented as:

$$v_n \to \min\left(v_{\max}, v_n(t)+1, d_n(t)+v_{n+1}(t+1)\right) \tag{2.1}$$

where $v_{n+1}(t+1)$ is an estimated velocity of the car $n+1$, the car in front of car n, at the $(t+1)$ time step. $v_{n+1}(t+1)$ is given as:

$$v_{n+1}(t+1) = \min\left(v_{\max}-1, v_n(t), \max\left(0, d_{n+1}(t)-1\right)\right) \tag{2.2}$$

Compared with the NaSch model, the output from the VE model was claimed to be consistent with the real data (Li *et al.*, 2001).

The model proposed by Larraga et al. (2005) also takes into consideration the speed of the preceding vehicle. Different from Li's model, Larraga et al. (2005) considers the preceding vehicle's speed at the same time step $\left(v_{n+1}(t)\right)$ rather than the estimated speed at the next time step $\left(v_{n+1}(t+1)\right)$. The new velocity of the vehicle n in the deceleration rule is:

$$v_n(t) = \min\left(v_n(t), \left(d_n(t)+(1-\alpha)\cdot v_{n+1}(t)\right)\right) \tag{2.3}$$

where $d_n(t)$ denotes the empty cells in front of vehicle n at time t. α can be regarded as a safety factor here. Smaller α values represent more aggressive driver behavior. With lower α values, the average speed and flow in the system increase. However, the model is of little use in analyzing traffic flow for it is hard to determine different α for different drivers (Liu, 2006).

Knospe et al. (2000) introduced a comfortable driving (CD) model which takes into account the effects of brake lights. The main idea of the model is summarized as: (1) if the gap in front is large enough, the driver can drive at maximum speed; (2) with an intermediate gap, the following driver is affected by changes in the downstream vehicle's velocity in terms of indication from brake lights; (3) with a small gap, the drivers adjust their velocity for the sake of safety; and (4) the acceleration for a stopped vehicle or a vehicle braking in the last time step is retarded (Knospe *et al.*, 2000). The authors applied three randomization braking parameters p_b, p_0 and p_d in the model, representing the probabilities for the vehicle to reduce its speed by one unit in three conditions respectively: (1) the leading vehicle brakes ($b_{n+1}=1$) and the time headway is shorter than the safe time headway ($t_h < t_s$); (2) the given vehicle is standing still $(v_n = 0)$; and (3) all other cases. The braking parameters are determined for each vehicle before the acceleration step in the NaSch model and used in the randomization step. Moreover, Knospe et al. (2000) proposed an idea of effective distance (d_n^{eff}) taken to define the speed in the deceleration step and determined by a parameter gap_{safety} along with speed and gap distance of the leading vehicle. Compared to the VE model where gap_{safety} is considered as 1 though it is not specifically defined, multiple choices of safety gap, namely, effective gap in Knospe's model, facilitate to calibrate the model and obtain more realistic results. The model proved to be capable of reproducing three phases[3] and hysteresis status (Knospe *et al.*, 2000).

Jiang and Wu (2003) modified Knospe's CD model (MCD) since they deemed that the drivers were still very sensitive to restart their cars when they had just stopped until they reach a certain time, defined as t_c in the model. The modification was made on the first step of Knospe's model, where randomization braking parameters p_0 would be applied to the situation that both $v_n = 0$ and $t_{st} \geq t_c$ are met. t_{st} is the time elapsed after stop of the car. The model successfully simulated synchronized flow and the results were consistent with real traffic data (Jiang and Wu, 2003).

2.3.3 CA Models of Lane Changing

One significant deficiency of single-lane models is that overtaking is not allowed in the system. If a fast vehicle meets a slow one in front, it has to follow the slow vehicle, and queues inevitably spill back. Lane changing models in a multi-lane network can eliminate this effect, thereby having practical meaning to traffic simulation.

[3] Three phases are free flow, synchronized and wide moving jams (Knospe *et al*., 2002).

Lane changing behavior is classified into two categories (Ahmed, 1999): Discretionary Lane Changing (DLC) and Mandatory Lane Changing (MLC). DCL is a positive driving behavior and is normally performed when the driver perceives that the condition in the target lane is better than the current lane, for example, gaining higher speed. MLC is a passive driving behavior which is normally performed under conditions of lane reduction, such as incidents and ramps (Ahmed, 1999).

The rule set defining the vehicles' lane changing can be both symmetric and asymmetric (Rickert *et al.*, 1996). Symmetric rules are used in the systems where lane changing on both sides is permitted while asymmetric rules apply to systems where the motivations of lane changing from left to right or from right to left are different. For example, in Germany, vehicles' passing on the right is illegal, therefore slow moving vehicles always drive on the right and fast vehicles may pass on the left only. However, this is not the case in the US. Nagel et al. (1998) pointed out that American drivers usually do not use the rightmost lane in order to avoid disturbance from ramps. Furthermore, there is no lane changing prohibition rules in the US regulations. Thus, symmetric rules could be more useful to describe actual American driving behavior than the asymmetric rules. In this literature review, only symmetric lane changing rules are studied.

All lane changing rules consist of two parts: A reason or trigger criterion and a safety criterion (Chowdhury *et al.*, 1997). A reason explains why people want to change lanes and a safety criterion determines if it is safe for the driver to do so. If both the subjective motivation and objective condition are fulfilled, the lane change is made.

Rickert et al. (1996) presented a straightforward extension of the NaSch model by introducing a set of lane changing rules. If one vehicle is retarded in its current lane, the travel condition in the target lane is better, and lane changing leads to neither collision nor blockage of other vehicles' way, the vehicle will change to the target lane with probability p_{change}. More specifically, the rules can be defined as: Trigger criteria: (1) the gap in front of vehicle n on the current lane (denoted by d_n) is less than the expected speed for the next time step: $d_n < v_n + 1$; (2) the forward gap of vehicle n on the target lane (denoted by $d_{n,other}$) is larger than the expected speed: $d_{n,other} > v_n + 1$; Safety criteria: (3) the neighbor site of vehicle n in the target lane is empty; (4) the backward gap of vehicle n on the target lane (denoted by $d_{n,back}$) is greater than the maximum speed: $d_{n,back} > v_{\max}$. These rules are adaptable to both changing to the left and to the right lane.

In multilane freeways, inhomogeneous traffic simulation plays an important role. Inhomogeneous traffic refers to the traffic system that consists of various vehicle types such as cars and trucks. Chowdhury et al. (1997) proposed a two-lane model to simulate a traffic network with

two types of vehicles are characterized by different maximum speeds. Cars are defined as fast vehicles and trucks are considered as slow ones. The rules for updating the states of the vehicles in the model are "symmetric with respect to the vehicles as well as with respect to the lanes" (Chowdhury et al., 1997, pp. 417). More specifically, a vehicle changes lanes with probability p_{change} provided: Trigger criteria: (1) $d_n < \min(v_n + 1, v_{\max})$; (2) $d_{n,other} > d_n$; Safety criteria: (3) the neighbor site of vehicle n in the target lane is empty; (4) $d_{n,back} > v_{\max}$.

The model generated good results in homogenous traffic systems but had some problems in simulating inhomogeneous traffic based on the outcomes (Chowdhury *et al.*, 1997; Knospe *et al.*, 1999). Jia et al. (2007) pointed out that the effects of slow vehicles in the system were exaggerated in the model. Even a small number of slow vehicles would initiate the formation of platoons at low densities and the forming queue would not dissipate after a very long time, which was not the case in reality.

Jia et al. (2005) addressed this problem by proposing a two-lane CA model taking into consideration honk effects. Jia's model added two rules to the trigger criteria in Chowdhury's model, which were (1) if the following vehicle $n-1$ blows the horn at the leading vehicle n due to blockage; and (2) the vehicle n can drive at its desired speed on either of the lanes free of collision, the vehicle n changes lanes. The results showed that fast vehicles could pass slow vehicles quickly at low densities and the effects of slow vehicle were suppressed.

Li et al. (2006) pointed out that fast vehicles usually took more aggressive lane changing behavior when its preceding vehicle was a slow vehicle than other cases (i.e., the fast vehicle hindered by a fast one, a slow vehicle hindered by a slow one, or a slow vehicle hindered by a fast one). The model used one parameter T_n to discriminate two types of vehicles: fast $(T_n = 1)$ and slow $(T_n = 0)$ indicated the type of the vehicle n. Provided (1) $T_n = 1$ and $T_{n+1} = 0$; (2) $d_n < \min(v_n + 1, v_{\max}), d_{n,other} > d_n$; (3) $d_{n,back} \geq 2, v_n \geq v_{back,other}$, the following fast vehicle changes lanes with probability $p_{n,change}$. The aggressive lane changing rules for the fast vehicles "enhance the flux of the mixed traffic system in the intermediate density range since the occurrence probability and the lifetime of the plug are suppressed" (Li et al., 2006, pp. 485).

2.3.4 CA Models of Freeway Ramps

The on- and off-ramps are implemented as connected parts of the lattice where the vehicles may enter or leave the system (Diedrich *et al.*, 2000). Diedrich et al. (2000) proposed two different procedures to add cars to the main road when simulating on-ramps. The first procedure searches the lattice successively in the region of the on-ramps (from the location of the first cell to the last cell)

until a vacant cell is found (Diedrich *et al.*, 2000). A vehicle is then inserted into that cell with maximum speed. In the second method, vehicles randomly enter a vacant cell. The second procedure is more realistic than the first because the first does not consider the local density and may greatly disturb the system (Jia *et al.*, 2007).

Campari et al. (2000) extended CA models to two-lane networks with on and off ramps. The study was able to reproduce synchronized flow based on Diedrich's theory. Ez-Zahraouy et al. (2004) also used methods similar to Diedrich's but with an open boundary.

Jiang et al. (2003) argued that the above models only considered the influence of the ramps to the main road. Actually, the main road influenced the ramps in reverse. For example, when the density of the one-lane main road reaches a certain level, it becomes a bottleneck for the ramps (Jia *et al.*, 2007). Jiang et al. (2003) adjusted the vehicle updating sequence based on the estimated travel time for vehicles on the mainline and the ramp to reach the junction point. Vehicles with the shorter travel time are updated first no matter if it is on the mainline or ramp. If the travel time is the same, the sequence is determined by the distance from the junction point. If both travel time and distance are the same, the vehicles on the mainline go first because the ramp traffic should yield to the mainline traffic. Jiang et al. (2003) further modified their model to consider stochastic randomization effects in an on-ramp system, but the essential idea remains the same.

The authors also investigated the on-ramp system where the main road had two lanes. The update rules are based on two steps: (1) the vehicles on the main lanes change lanes according to Chowdhury's lane changing rules (Chowdhury *et al.*, 1997) regardless of the on-ramp; and (2) vehicles on the left lane are updated according to NaSch rules while those on the right follow Jiang's rules (Jiang et al., 2002, 2003).

Jia et al. (2005) first considered the effects of an accelerating lane in an on-ramp system with one lane on the main road. Vehicles are updated according to NaSch models along the mainline and on-ramp (not including the acceleration lane). In the section containing both the mainline and the acceleration lane, which is a two-lane network, the authors proposed two sets of lane changing rules. Rule 1 forbids the vehicles on the main lane to change to the accelerating lane and Rule 2 allows this. More specifically, according to Rule 1 vehicle n changes from the accelerating lane to the main road provided: (1) Trigger: $d_n = d_{n,other} = 0$ or $d_{n,other} \geq 1$; (2) Safety criterion: $d_{n,back} \geq v_{ob}$. v_{ob} denotes the velocity of the following car on the main road at time t. According to Rule 2, the vehicles on the main road switch to the accelerating lane provided: (1) Trigger: $d_n = 0$ and $\left(d_{n,other} - d_n\right) > 2$; (2) Safety criterion: $d_{n,back} \geq v_{ob}$. Comparing the results of simulation with each of these rules, the authors indicated that the lane changing from the main lane to the accelerating

lane should be forbidden and the introduction of an accelerating lane can improve the capacity of the on-ramp system (Jia *et al.*, 2005).

Based on similar rules, Jia et al. (2004) simulated off-ramp systems with a CA model. The authors discuss two off-ramp cases: with and without an exit lane. The exiting vehicles usually change to the right lanes and slow down upstream of the off-ramp. In the case where no exit lane exists, exiting vehicles are not allowed to change from the right lane to the left and they are permitted to change from the left lane to the right provided: Trigger: (1) they are not able to proceed in both lanes; (2) they are able to proceed in the right lane and the difference of speed between the current and the target lane is less than 2 cell/s; and Safety criterion (3) the backward gap is greater than the following vehicle's speed in the target lane. The rules are presented as: Trigger: $d_n = d_{n,other} = 0$; (2) or $d_{n,other} \neq 0$ and $d_n - d_{n,other} \leq 2$; (3) Safety criterion: $d_{n,back} > v_{ob}$. The rule $d_n - d_{n,other} \leq 2$ means the road condition on present lane is not much better than that on the destination lane (Jia *et al.*, 2004). If an exiting vehicle is not able to access the right lane before some given point (could be the last segment where vehicles are allowed to exit), it stops there and waits for an opportunity to change lanes. In the case where an exit lane exists, exiting vehicles which are on the exit lane are not allowed to change to the left and the passing-through vehicles are prohibited to enter the exit lane. The other lane change rules are the same with those in the first case. The simulation results suggest that the traffic conditions are better if an exit lanes exist.

2.3.5 CA models of Incidents

Bottlenecks widely exist in traffic networks. On and off ramps, work zones, accidents, disabled vehicles, and toll booths can be considered typical reasons for the formation of bottlenecks. Bottlenecks reduce the capacity of roads and change driver behavior and thereby the flow pattern. CA models of ramp simulation have been discussed in section 2. 3. 4 and here CA models proposed for incident simulation are presented.

Jia et al. (2003) proposed a model for a two-lane road with a work zone. The authors focused on the upstream section where drivers perceive the work zone and begin to change lanes. According to the rules, the driver on the blocked lane changes to the free lane if the driver perceives that the driving situation is not much better on the blocked lane (the difference of permitted speed is less than 1 cell/s). Moreover, the lane changing behavior should obey the safety criterion: the backward gaps between the vehicle and its following vehicle on the neighbor lane should be large enough to avoid collision. The rules can be specifically described as: (1) Trigger: $d_n - d_{n,other} \leq 1$; (2) Safety criterion: $d_{n,back} > v_{ob}$. The authors also allow the vehicle on the free lane to change to the blocked

lane if the vehicle is blocked on its current lane while the neighbor lane provides better conditions. The rules are: (1) Trigger: $d_n = 0$ and $d_{n,other} > 0$; (2) Safety criterion: $d_{n,back} > v_{ob}$.

Nassab et al. (2006) proposed similar lane changing models referring to a work zone network. Similar with Jia's model, the vehicles are not only allowed to change from the blocked lane to a free lane but also from a free lane to the blocked lane. For the first situation, the authors adopted Rickert's lane changing models and for the second situation, the authors simply negate the criterion of the first situation. More specifically, if conditions (1) $v_n > d_n$; (2) $d_{n,other} > d_n$; (3) $d_{n,back} \geq v_{\max}$ are fulfilled, the vehicles change from the blocked lane to the free lane. Conversely, if conditions (1) $v_n \leq d_n$; (2) $d_{n,other} \leq d_n$; (3) $d_{n,other} \geq v_n$; (4) $d_{n,other} \geq v_{\max}$ are met, the vehicles change from free lane to the blocked lane.

2.4 Summary

Several approaches have been explored to estimate travel time on a freeway. General travel time estimation methods (Petty, 1998; Coifman, 2002; Oh *et al.*, 2003) address the problem by using detector data. Though easily used, these methods are not necessarily capable of capturing complex dynamics under incident conditions. Furthermore, they fail to take into consideration the queue effects on the travel time.

Statistical-oriented methods such as probabilistic distributions (Giuliano, 1989; Garib *et al.*, 1997; Sullivan, 1997; Nam and Mannering, 2000), linear regression models (Garib *et al.*, 1997; Ozbay and Kachroo, 1999), time sequential models (Khattak *et al.*, 1995), and decision trees methods (Ozbay and Kachroo, 1999; Smith and Smith, 2001), Artificial Neural Network (ANN) models (Wei and Lee, 2007) have been developed to forecast incident-related travel time. However, these approaches typically take into consideration the entire incident period from occurrence to recovery, as such, these are not applicable to the current study which focus on driver-oriented travel time instead of administrator-oriented incident duration.

Macroscopic (Nam and Drew, 1999; Zhang, 2006; Xia and Chen, 2007) and microscopic models (Byungkyu and Hongtu, 2006; Khan, 2007) are two types of tools to address the problem. Shock wave theories and queuing models and are two commonly used macroscopic models to estimate the travel time through a bottleneck. They scrutinize the formation and dissipation of the queue and are capable of estimating delay and queue length, along with travel time for both individual and the total vehicles in different states of the system. The shock wave methods are based on time-space diagram and the models are developed from the trajectories of the vehicles. The queuing analysis is based on the input-output diagram on which the arrival and departure at two

observation points are presented. Though with the computational advantage, macroscopic methods underestimated freeway travel time when compared to the field measurements (Yeon and Elefteriadou, 2006) especially in the presence of ramps along the freeway. Therefore, macroscopic models are less capable of yielding high fidelity results compared to the microscopic simulations.

Car Following models are classical microscopic models which are widely used to simulate traffic networks and the models have been incorporated into developed simulation packages such as VISSIM and PARAMICS. However, these existing microscopic simulation packages are excluded as ideal tool for this study, despite their capability of precisely simulating traffic, because of their run times and difficulty in making some changes or setting some features in the software, especially when near real time simulation are required.

Compared with the classical Car Following models, Cellular Automata models are relatively new methods to simulate traffic with the advantage of computational efficiency. A comprehensive literature review of CA models for freeway simulation was presented in this chapter, including single lane models, lane changing models, models for on- and off-ramps and incident models. Some basic characteristics and features of traffic flow are successfully captured by CA models. Furthermore, originally developed CA models have the advantage of computational efficiency and facilitate making changes in the model. All of these previous studies play a role in the rule determination for the proposed CA model in this thesis.

Chapter 3 Test Site and Data

3.1 Introduction

This chapter introduces the selected test site and data utilized for the new proposed CA model for estimating incident-related travel time offline and in near real time. The test site is a section of Interstate 66 in Northern Virginia, USA and the data of interest includes loop detector data collected from the field and related incident data. The test site description, data collection, detector data processing, OD estimation and bottleneck identification are presented sequentially in this chapter.

3.2 Test Site Description

The test site selected for this study is I-66 eastbound from US29 to I-495, a 16-mile stretch of freeway containing 9 on-ramps and 10 off-ramps. The road beyond this range is not under consideration since complete data was unavailable. Figure 3.1 shows the segment of test site I-66 used in this study marked in green. Figure 3.2 presents its schematic diagram where the number above the road represents the number of lanes.

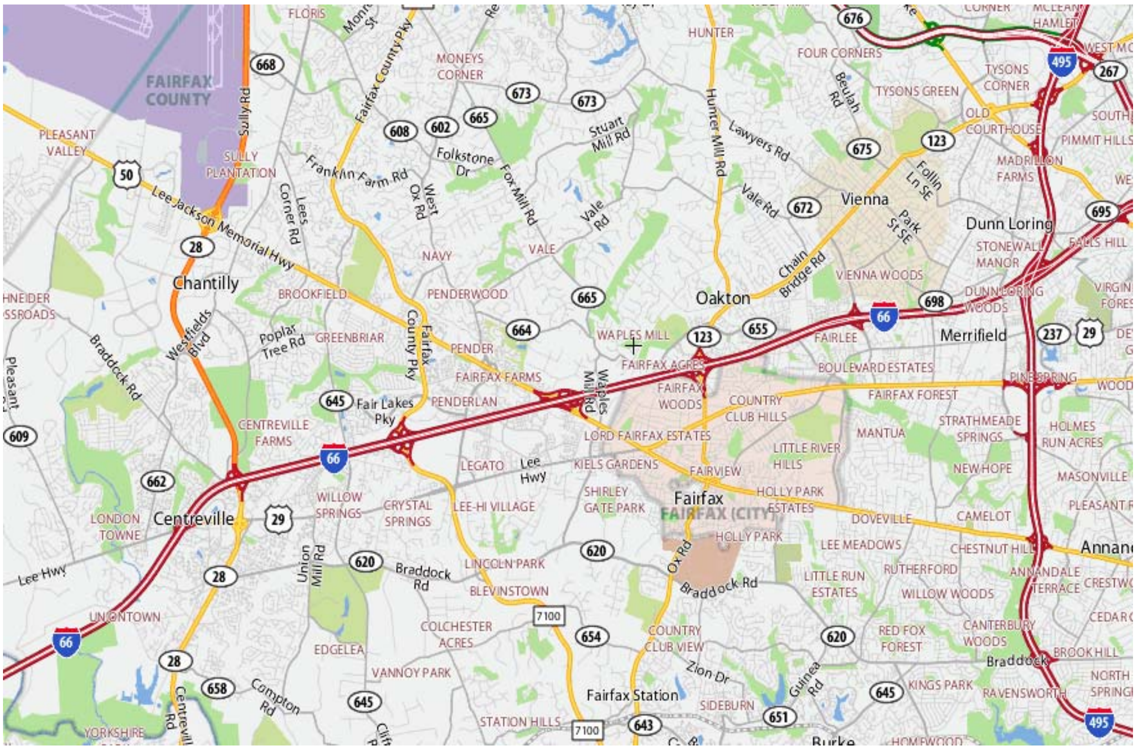

Figure 3.1 Map of the test site from I-66 (Yahoo)

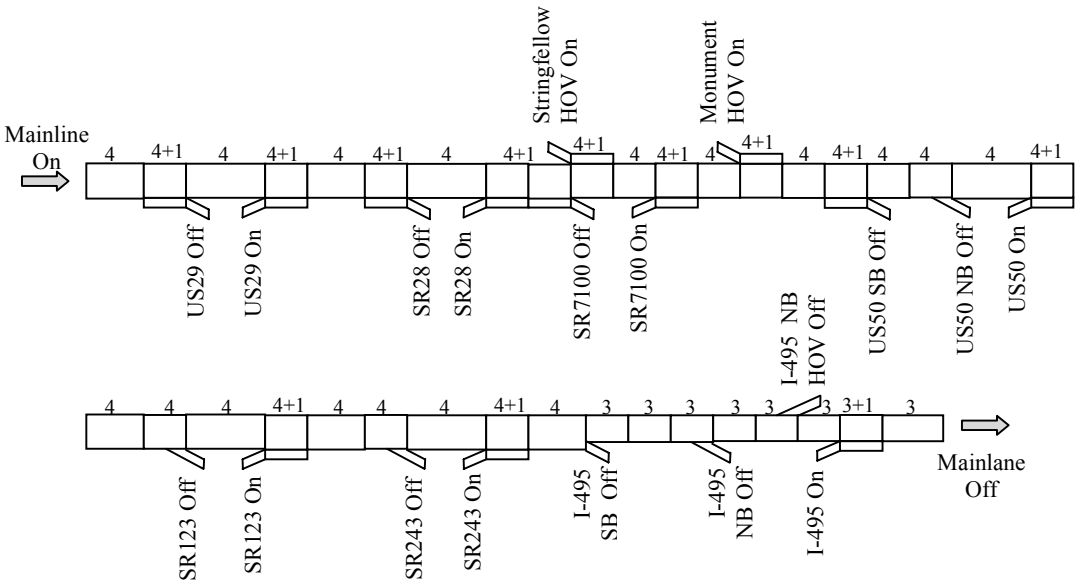

Figure 3.2 Schematic diagram of the test site from I-66

The section from US29 to US50 contains three general purpose (GP) lanes and one HOV lane. The section from US50 to I-495 involves two GP lanes, one HOV lane and one shoulder lane, which is open during the morning peak period to relieve congestion. Normally one additional lane exists in the ramp sections: acceleration lane for on-ramps and exit lane for off-ramps.

Morning congestion of I-66 eastbound starts at about 5:30 am and continues until 11 am on weekdays based on detector data. For the purpose of reducing congestion and making full use of the road, the Virginia Department of Transportation (VDOT) implemented various lane regulations on eastbound of I-66, listed as follows (VDOT, 2008):

1. Inside the Beltway (east of I-495), all eastbound lanes are restricted to vehicles with two or more people (HOV-2) on weekdays from 6:30 am to 9:00 am.

2. Outside the Beltway (west of I-495), the far left lane of the main lanes spanning the entire test site is reserved as an HOV-2 lane during the morning peak from 5:30 am to 9:30 am.

3. The right-side shoulder lane between US50 and the Beltway remains open to all traffic during the morning peak from 5:30 am to 10 am[4] .

4. During weekends, holidays and off-peak hours, shoulder lanes are closed for use and HOV-2 lanes are open to all traffic except trucks.

[4] This regulation is for 2007. For 2008, the period changes to 5:30 am to 11:00 am.

3.3 Data Collection

3.3.1 Loop Detector Data

Inductive loop detectors are the most commonly used equipment to collect traffic measurements on freeways in the USA, probably due to their lower costs and easier interpretation of their working function compared to other detectors, such as AVI (Automatic Vehicle Identification). The test site is equipped with 130 detectors on the mainline along with 21 on the ramps. The loop detectors on the mainline are placed approximately 0.5 miles apart. Parallel detectors with the same milepost, namely, at the same location of the freeway but on different lanes, are grouped into logical units called stations. Each detector belongs to at most one station and each station takes responsibility for only one direction of the freeway. Detectors on the ramps are normally located near the merge or diverge points and detectors on each ramp belong to one station.

The data gathered by the detectors for every minute involves speed, volume and occupancy. Speed is the average value over all the vehicles passing by the detector in a given period, in units of miles per hour. The link speed is the volume weighted speed over all the lanes. Volume is the number of vehicles detected within the defined time frame. Occupancy is the percentage of time that vehicles are detected. Figure 3.3 shows the station layout on the test site. The integers in the figure represent the station ID and the numbers in the parentheses are the milepost of the station.

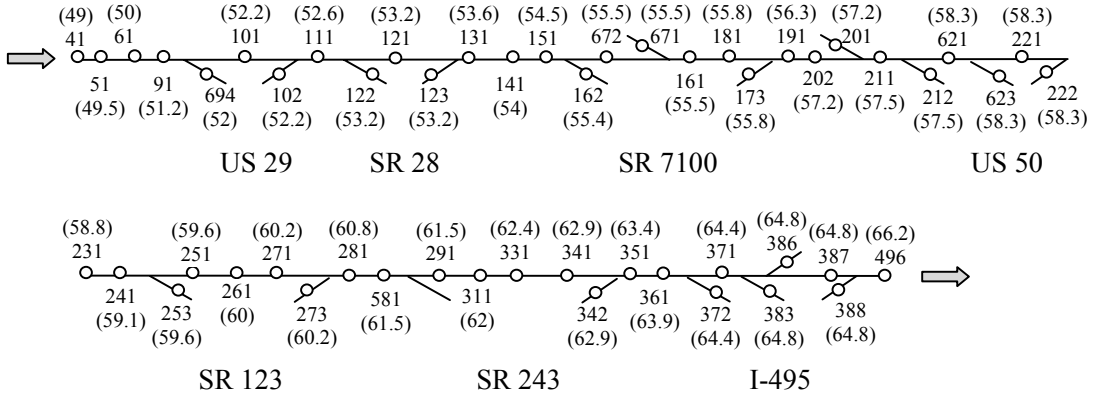

Figure 3.3 Station layouts on test site

The 1-min raw data are collected directly from the loop detectors by VDOT in non-delimited flat formats and then translated into readable format before being stored in the Real-time Freeway Performance Monitoring System (RFPMS), a Microsoft SQL Server database developed by the Virginia Tech Spatial Data Management Lab. This database is used to assemble a history of traffic measurements from all the detectors on I-66 for the most recent five years. The 1-min raw data are preliminarily processed by eliminating abnormal and erroneous data based on rules predefined by the database before being aggregated into 5-min station-level data. The aggregated data is used in

this study to minimize random fluctuations. The data involved in this study covers 2007. Despite preliminary processing, the 5-min data is far from satisfactory for the purpose of this study and further data processing is required. Additional processing procedures are introduced in section 3.4.

3.3.2 Incident Data

Incident data is collected from the Incident Management System (IMS) developed by the University of Maryland CATT Lab and supervised by VDOT. IMS collected incident records on all freeways in Northern Virginia including I-66, I-496, I-395 and I-95 since 2005. Each incident record contains the details of incident-related information including incident ID, incident type and subtype, start time, clear time, close time, location, lane status (closure or open) over time, a brief description of the incident and so forth. An example of incident data is given in Table 3.1.

3.4 Detector Data Processing

3.4.1 Detector Data Processing Steps

The detector data processing takes two steps: data processing and data reorganization. Since preliminary data processing has been conducted on original 1-min detector data before being transformed into 5-min station-level data, data processing here refers to eliminating inconsistent and abnormal source data, possibly caused by malfunction of detectors and incidents, at a system level. System level analysis, differentiated from individual level where erroneous data is identified on the basis of the logical relationship between speed, volume and occupancy data from a single detector, takes into consideration the relations of data among neighboring stations and trends of daily volume distribution. For example, if data from two stations on the same link, a road section between two junctions within which the configuration of the road is uniform, is significantly different, the data should be further scrutinized and justified on its consistency. Data reorganization means transforming flow data into Origin-Destination (OD) formats required as input for the CA model. QueensOD, a software package, is utilized in this study to develop the OD trip tables from the detector flow data.

3.4.2 Data Processing

The objective of data processing is to compile a complete and representative set of flow data for each day of the week representing the normal non-incident daily travel pattern. The data set covering all inflow and outflow in the network is generated as a base case for the CA incident model simulation.

Table 3.1 Sample incident records for Incident 32421 in April 13, 2007 (IMS)

Incident ID	**Incident Type - Subtype**	**Severity**	**Start Time**	**Clear Time**	**Closed Time**	**Location**
32421	Collision - Personal Injury	High Profile	2007-04-13 17:46:16-04	2007-04-13 19:12:16-04	2007-04-13 19:19:39-04	East @ Chain Bridge Rd
32421	Collision - Personal Injury	High Profile	2007-04-13 17:46:16-04	2007-04-13 19:12:16-04	2007-04-13 19:19:39-04	East @ Chain Bridge Rd
32421	Collision - Personal Injury	High Profile	2007-04-13 17:46:16-04	2007-04-13 19:12:16-04	2007-04-13 19:19:39-04	East @ Chain Bridge Rd
32421	Collision - Personal Injury	High Profile	2007-04-13 17:46:16-04	2007-04-13 19:12:16-04	2007-04-13 19:19:39-04	East @ Chain Bridge Rd
32421	Collision - Personal Injury	High Profile	2007-04-13 17:46:16-04	2007-04-13 19:12:16-04	2007-04-13 19:19:39-04	East @ Chain Bridge Rd
32421	Collision - Personal Injury	High Profile	2007-04-13 17:46:16-04	2007-04-13 19:12:16-04	2007-04-13 19:19:39-04	East @ Chain Bridge Rd
Milemarker	**Latitude**	**Longitude**	**Link ID**	**WB Shoulder Closed**	**WB Lanes Closed**	**WB Ramps Closed**
60.00	38.8695468	-77.3091462	159	X	X	X
60.00	38.8695468	-77.3091462	159	0	0	0
60.00	38.8695468	-77.3091462	159	0	0	0
60.00	38.8695468	-77.3091462	159	0	0	0
60.00	38.8695468	-77.3091462	159	0	0	0
60.00	38.8695468	-77.3091462	159	0	0	0
HOV Shoulders Closed	**HOV Lanes Closed**	**HOV Ramps Closed**	**EB Shoulders Closed**	**EB Lanes Closed**	**EB Ramps Closed**	**Duration**
X	X	X	X	X	X	00:05:07
0	0	0	2	3	0	00:00:13
0	0	0	2	3	0	00:00:09
0	0	0	1	3	0	00:54:07
0	0	0	1	1	0	00:24:21
0	0	0	0	0	0	00:09:26
Remark						
There is a vehicle crash on I-66 East at Chain Bridge Road (exit 60). All Lanes are blocked. Traffic is backed up to Fairfax County parkway.						

In the previous studies, one specific day is selected as the typical day after considering the completeness of the data and justifying if its flow data faithfully follows the daily trend (Gomes *et al.*, 2004). However, this method is not suggested for this study due to: 1) no single day has absolute complete data; 2) no single day is incident free throughout the test site; and thus 3) fluctuation of the flow from day to day can not guarantee the representativeness of the data.

The procedures to compile a representative data set in this study are: 1) integrating data from the same station, same day of a week (except holidays) and same time of a day into one group; 2) eliminating outliers for each group; and 3) averaging flow for each group. Then the average flow data of the same day is arranged chronologically and the combination of data is considered as the

representative entity used for OD estimation for each day of the week. The main advantage of this method is that it dramatically reduces the risks of biased representative data but requires more efforts in data processing. The most challenging part of data processing is identifying abnormal data.

The detailed data processing procedure used in this study is described as follows. This procedure is applied to most stations which have good data quality and small data variance. For some stations with less reliability of data quality or mass loss of data, probably caused by detector malfunction, different approaches are utilized, which are indicated in the following procedure.

Step 1: choose representative station data for each link

This applies to the condition that more than one station is located on one link which is a road section with uniform configuration. For example, in Figure 3.3, stations like 131, 141, 151 or 251, 261, 271 are located on the same link and only data from one station is selected as representative data for that link. The selection standard is based on the comparison among these station data assuming the flows should be close to each other since there is no flow increase or decrease within the link. In other words, if one station's flow is much smaller than the other two, this station should not be selected even if the lower flow is caused by downstream congestion and the data is valid. The higher value should be closer to the theoretical flow rate, which is equal to flow under normal condition. If all the stations have similar data, the station in the middle is chosen since the flow is less likely to be influenced by the ramps located at the ends of the link. If one link has only one station on it without competitors, this station is selected.

Step 2: process station data

Data from the same station, same day of a week (except holidays) and same time of a day is integrated into one group. Thus there are at most 52 data sets for each group corresponding to 52 weeks of a year. The detailed steps are listed as follows:

(1) eliminating data in the group where flow equals zero;

(2) calculating the average flow and finding the maximum gap between data points and the average;

(3) deleting the data with the maximum gap if the gap value is greater than a defined threshold;

(4) repeating (2) and (3) until the maximum gap is less than the threshold; and

(5) calculating average flow of the reduced data group.

The flow data may be zero on some ramps at night. However, eliminating these valid zero data does not affect the results of flow estimation since the average flow on these ramps is low and so is the standard deviation of its flow rate. The results from (5) are considered as the representative link volume for a specific time of day and "normal" conditions. The maximum gap and threshold were used here to obtain a data set with higher convergence in order to increase the reliability of the

results. The thresholds are defined as: 1) if the average volume is greater than 250 veh/5min, the threshold is 100; 2) if the average is greater than 150 but less than 250, 80 is used; and 3) if the average is less than 150, 50 is used as the threshold.

The determination of thresholds is based on preliminary manual tests on multiple data sets of different days of the week and different time of the day. Some abnormal data which can be easily observed from the data set, for example, the data which is 200 veh/5min higher or lower than the other values, are initially identified. Several sets of thresholds are tested and the one which can exclude all the identified abnormal data and meanwhile keep most of the valid data is finalized. Then the finalized thresholds are applied to all the station data and verified by analyzing the least square error, standard deviation and percentage of the values excluded from the data set. The evaluation is based on the comparison of these results before and after the data processing. The threshold of the least square error for the mainline flow data uses 20%. The threshold of the standard deviation is set as 50 veh/5min for the mainline data and 20 veh/5min for the ramps. The threshold to evaluate the percentage of data elimination is defined as 80%, namely, more than 80% of data should be kept.

However, this method is not applicable to some stations with a variety of false data. These stations should be identified and specific methods applied. For example, data from the first half year of Station 387 doubles the value from the second half year. In this case, the first half year data should be eliminated before the method is applied since the data is much higher than the realistic value when checking with downstream and upstream links.

Step 3: processing data on a system level

The average flow data of the same day of the week is organized chronologically (covering 24 hours). The basic idea of system-level data calibration is that the inflow should be close to outflow for each merge or diverge point. For example, in Figure 3.3, the flow data of Station 91 should be similar with the sum of Station 694 and 101 at the US29 off-ramp. Similarly, Station 111 data should be similar with the sum of Station 101 and 102 at the US29 on-ramp. On the basis of this approach, it is easy to identify the erroneous data in stations, which is replaced with an average value calculated from neighboring stations. For example, the erroneous data in Station 101 can be replaced by [(St. 91 – St. 694) + (St. 111 – St. 102)] / 2. Apart from using the spatial relations among stations, daily trend is another method to identify the abnormal data. If the flow at one time increases or decreases unaccountably and is much higher or lower than the value in its neighboring time steps, the volume is considered abnormal and substituted by interpolation from the data in neighboring time steps. Reasonable flow fluctuation within the boundary of 100 veh/5min on the mainline is not eliminated since it is possibly caused by platoon or queue discharge.

3.4.3 Data Processing Results

3.4.3.1. Standard deviation and relative Least Square Error

The convergence of link flow data used to calculate the average flow is important to justify the reliability of results since the flows of one location are normally similar from day to day. In order to quantify the variability in flow data, standard deviation (STDEV), relative least- squares error (LSE) and percentage of data eliminated in data processing (indicated as deletion% below) are utilized. LSE is computed by dividing the average squared error by the average flow volume, as indicated in Equation 3.1(Rakha *et al.*, 1998).

$$LSE = \frac{\sqrt{\frac{\sum_i (q_i - \overline{q})^2}{n}}}{\overline{q}} \tag{3.1}$$

Where q_i is the link flow, $\overline{q}$ is the average link flow, n is the total number of data involved and i indicates the individual data at different times of the day.

Standard deviation represents the absolute variation of the data set while relative LSE stands for the relative variation related to its average value. Relative LSE value is more applicable to justify the data sets with higher average values while STDEV provides more intuitional judgments on data sets with lower values. Therefore, in this study, comparison between original data and processed data of mainline stations is mainly based on relative LSE and comparison of ramp data is mainly based on STDEV value. Table 3.2 lists the average STDEV, relative LSE value and deletion% for each station before and after data processing for Friday. The stations lacking complete data are not listed.

When statistics were compared from the above table, the STDEV and relative LSE were found to decrease dramatically in most cases. Most STDEV values are less than 30 veh/5min. Relative LSE for most stations decrease below 20%, which means the average variance of data is less than 20% of the mean flow. The decrease of STDEV and LSE for ramp stations is not as dramatic as mainline stations due to the relative lower flow on ramps. STDEV for all stations are less than 20 veh/5min. The results show that the link flow comes to a satisfactory convergence level after data processing and yield a reliable data set over which the representative flow is averaged.

Table 3.2 Station STDEV and relative LSE of stations before and after data modification (Friday)

Mainline	**61**	**111**	**121**	**141**	**672**	**161**	**191**
STDEV Before(veh/5min)	44.07	44.35	41.27	48.56	37.04	37.83	46.33
STDEV After(veh/5min)	26.69	26.51	21.96	28.76	23.53	23.67	28.34
LSE Before	23.62%	23.47%	26.06%	22.36%	25.95%	24.52%	25.85%
LSE After	15.10%	14.88%	16.32%	13.71%	16.56%	15.32%	16.36%
Deletion%	4.89%	5.05%	4.78%	5.23%	3.88%	3.79%	5.72%
Mainline	**211**	**221**	**231**	**261**	**291**	**351**	
STDEV Before(veh/5min)	53.01	38.79	58.58	65.46	48.85	52.96	
STDEV After(veh/5min)	37.25	24.23	30.65	30.31	28.21	30.29	
LSE Before	31.16%	23.55%	21.47%	25.54%	22.86%	21.58%	
LSE After	21.69%	14.55%	11.67%	12.97%	13.67%	12.70%	
Deletion%	11.41%	4.04%	6.50%	8.03%	5.34%	6.13%	
Ramp	**102**	**122**	**123**	**162**	**173**	**212**	**623**
STDEV Before(veh/5min)	8.01	13.60	19.78	9.22	5.83	9.59	7.01
STDEV After(veh/5min)	7.10	9.70	16.10	8.39	5.08	6.73	5.11
LSE Before	35.92%	31.55%	23.72%	31.50%	44.51%	46.43%	50.95%
LSE After	32.79%	24.79%	19.55%	29.53%	44.22%	42.97%	50.58%
Deletion%	0.78%	3.08%	2.24%	0.92%	0.05%	0.96%	0.09%
Ramp	**222**	**273**	**342**	**386**	**388**		
STDEV Before(veh/5min)	28.20	7.83	14.00	43.19	18.89		
STDEV After(veh/5min)	19.17	6.90	10.71	11.26	7.55		
LSE Before	23.28%	37.90%	30.20%	55.81%	73.15%		
LSE After	17.74%	36.95%	28.13%	25.62%	36.61%		
Deletion%	2.80%	0.29%	1.06%	3.41%	4.34%		

3.4.3.2. Representative Daily Flow

Figure 3.4 presents a sample volume distribution of stations on mainline and ramps after data processing.

Mainline Stations:

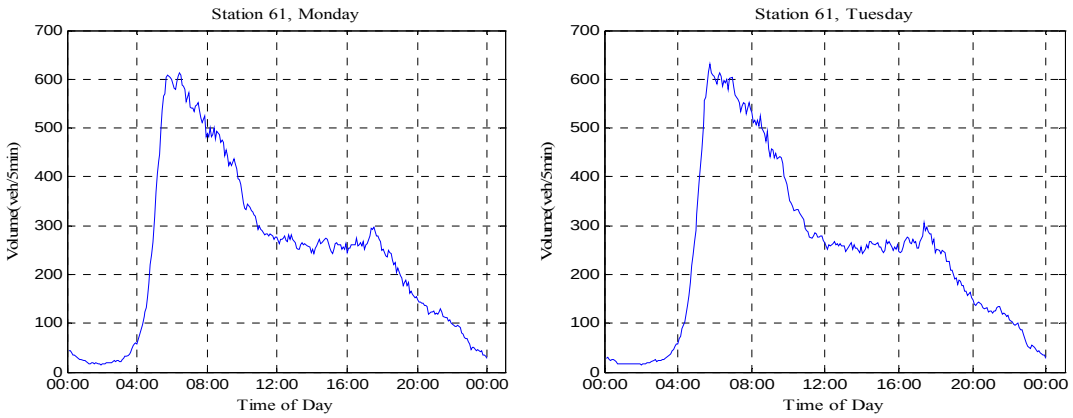

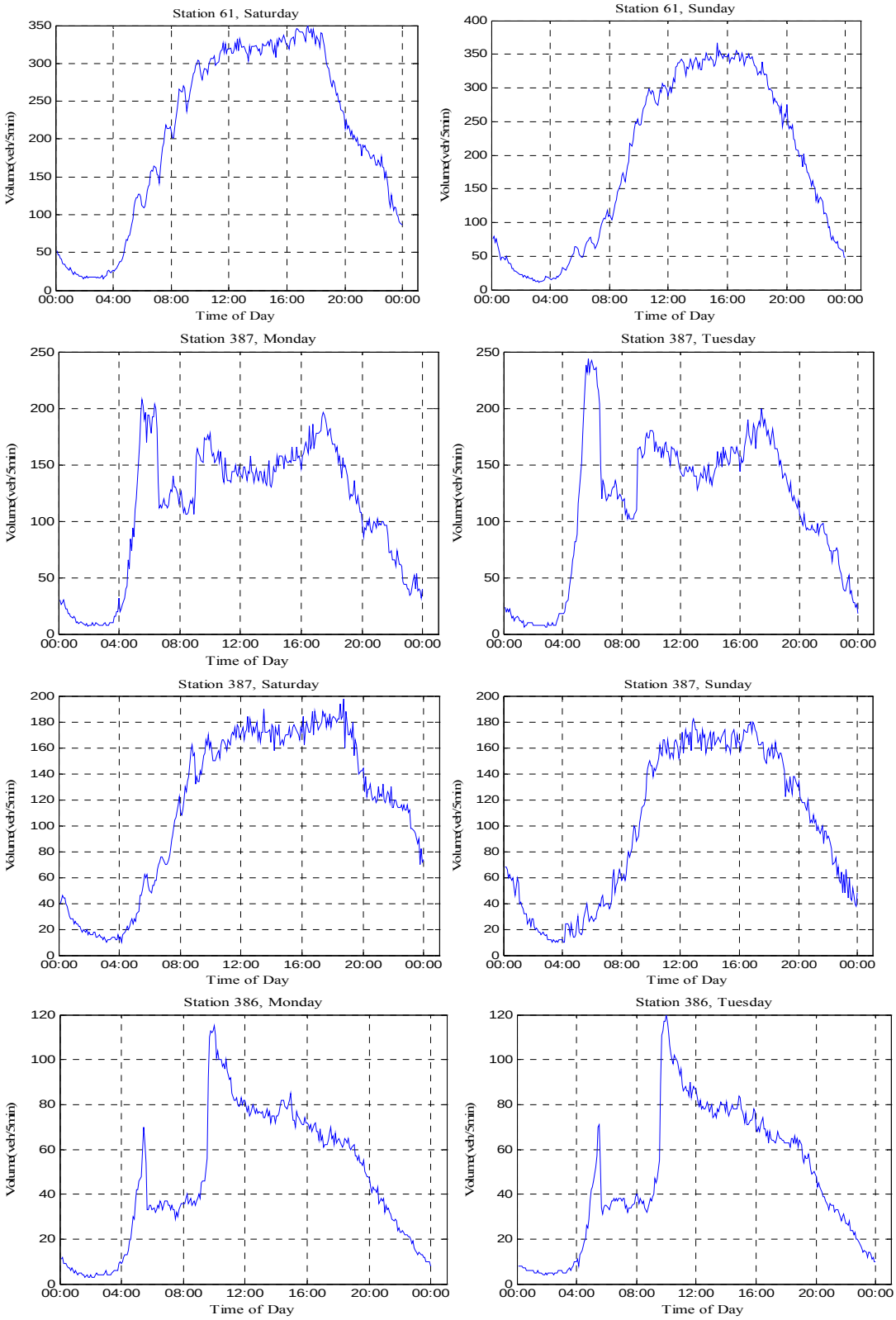
Station 61, Saturday
Volume(veh/5min)
Time of Day
Station 61, Sunday
Volume(veh/5min)
Time of Day
Station 387, Monday
Volume(veh/5min)
Time of Day
Station 387, Tuesday
Volume(veh/5min)
Time of Day
Station 387, Saturday
Volume(veh/5min)
Time of Day
Station 387, Sunday
Volume(veh/5min)
Time of Day
Station 386, Monday
Volume(veh/5min)
Time of Day
Station 386, Tuesday
Volume(veh/5min)
Time of Day
00:00 04:00 08:00 12:00 16:00 20:00 00:00

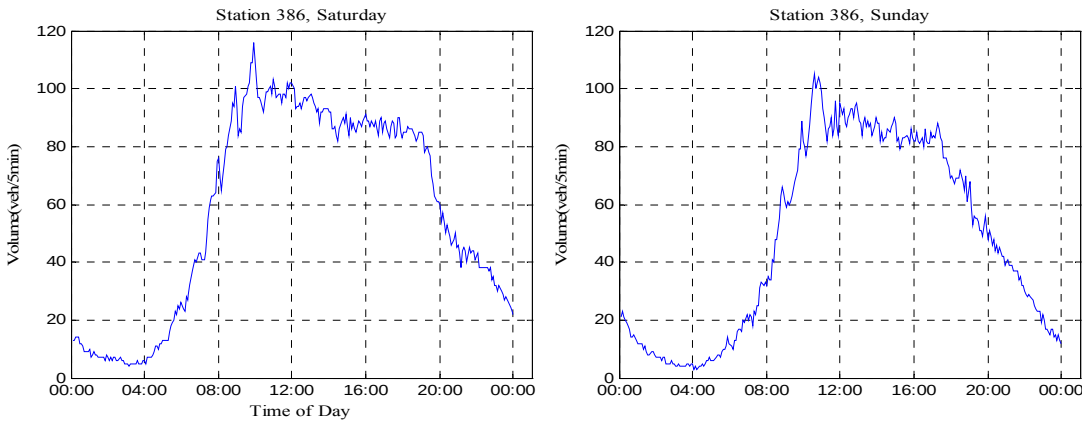

Figure 3.4 Sample volume distribution of stations on mainline and ramps

Three stations are selected and flow from these stations is plotted for Monday, Tuesday, Saturday and Sunday. Station 61 is at the beginning of the mainline and station 387 is at the end. Station 386 is located on the off ramp of I-495 NB HOV lane. The flow pattern between weekends and weekdays are different. In weekdays, the flow increases dramatically in the morning rush hour and drops to half in the afternoon. In weekends, however, plots from all stations show that the flow gradually increases in the morning and reaches the apex in the afternoon. Station 387 on the mainline and station 386 on the I-495 off-ramp are selected since the flow patterns of these stations are different from others. The reason for abrupt drop of flow after 6:00 am on weekdays is due to HOV restrictions east of I-495.

3.4.3.3. Scale factor

Scale factors, defined as the ratio of the total inflow of the system to the total outflow for each given interval, can be used to identify possible problems with the real data (Gomes *et al.*, 2004). The scale factor is expected to fall within 10% of 1.00 for an incident-free condition and the average over a day should be close to 1.00 (Gomes *et al.*, 2004). The scale factors of Wednesday, Friday and Sunday are shown in Figure 3.5.

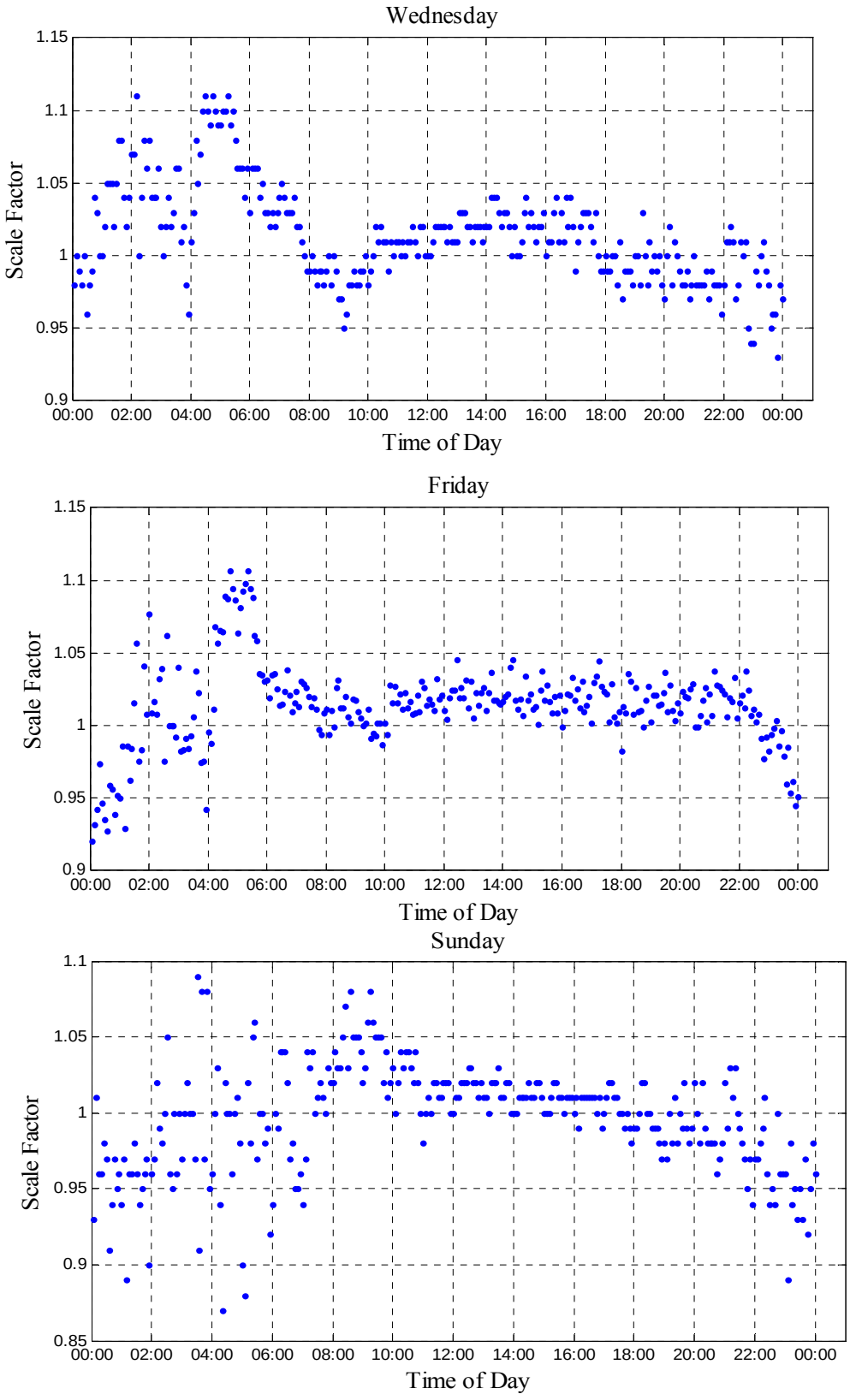

Figure 3.5 Scale factors

From Figure 3.5, the scale factors around midnight for all days are relatively low because the absolute flow value is small and the quotient of two small values exaggerates the difference between the numerator and denominator. On the contrary, the scale factors are relatively high from 4:00 to 6:00 am for weekdays and 8:00 to 10:00 am for all days due to the morning congestion. By and large, scale factors are within the reasonable range, justifying the calibrated link flow and qualifying the data as inputs for OD estimation.

3.5 OD Estimation

QueensOD is a macroscopic statistic OD estimation model developed by M. Van Aerde and his colleagues at Queens University (M. Van Aerde & Assoc., 2005). It is used to convert the observed link traffic flows to the set of OD matrices, which are required for the proposed CA models in this study.

In this study, QueensOD is used to convert the on- and off-ramp flow data into a sequence of 2016 OD matrices for a whole week – 288 for each day and one for each 5-min time interval in the 24 hour period. The dimension of each matrix is 21*21, including 10 origins and 11 destinations (all origins and destinations are listed in both the rows and columns).

Volumes calculated from OD tables are compared with loop detector data to justify the assignment results and evaluate the performance of QueensOD. Figure 3.6 shows the results for four example locations and presents their volumes from OD tables and from detectors.

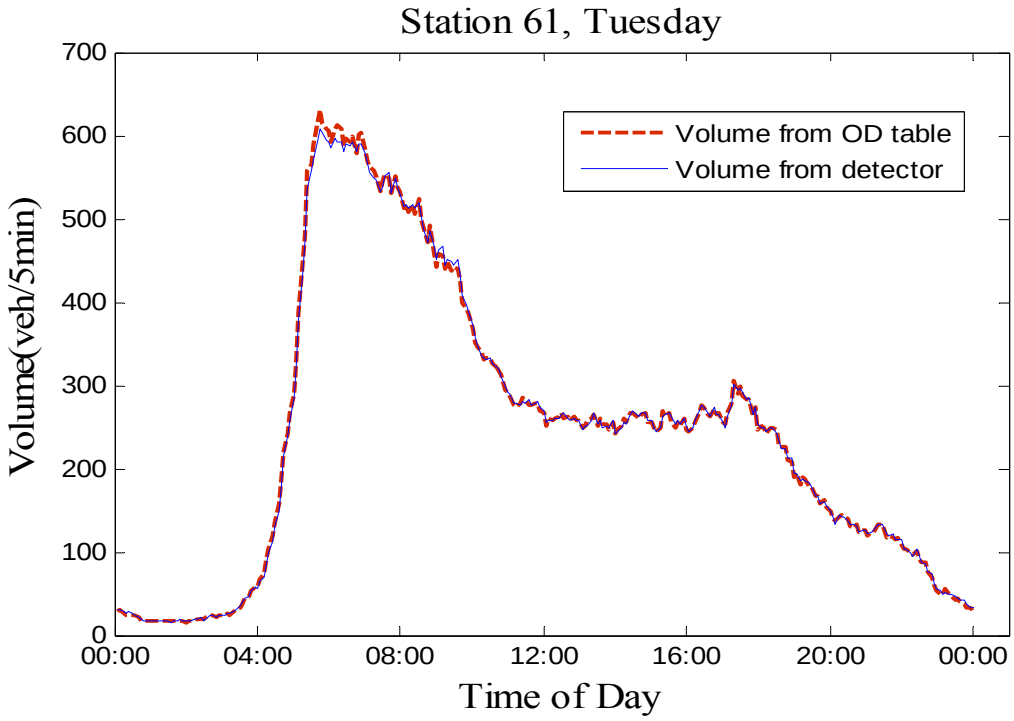

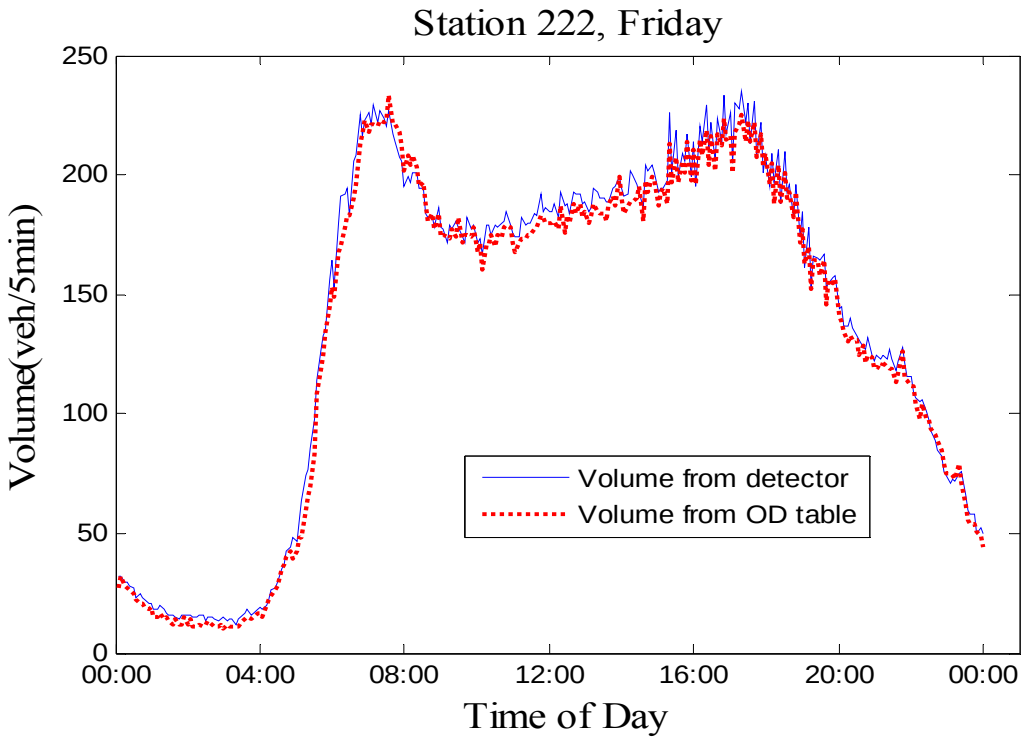
Station 222, Friday
Volume(veh/5min)
250
200
150
100
50
0
00:00
04:00
08:00
12:00
16:00
20:00
00:00
Time of Day
Volume from detector
Volume from OD table

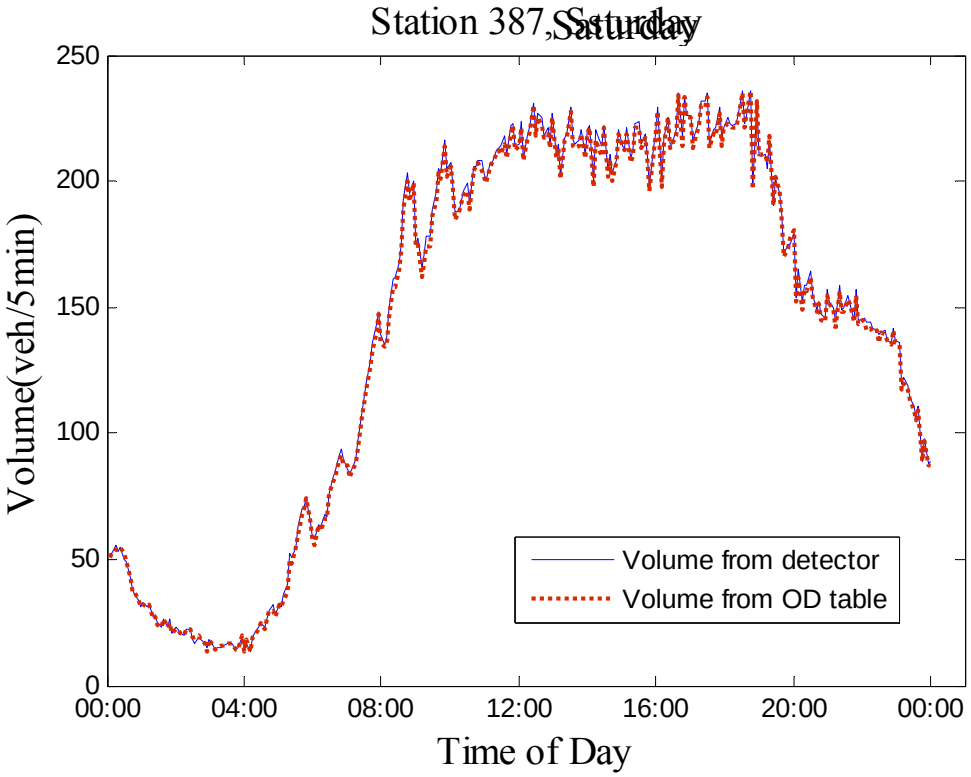
Station 387, Saturday
Volume(veh/5min)
250
200
150
100
50
0
00:00
04:00
08:00
12:00
16:00
20:00
00:00
Time of Day
Volume from detector
Volume from OD table

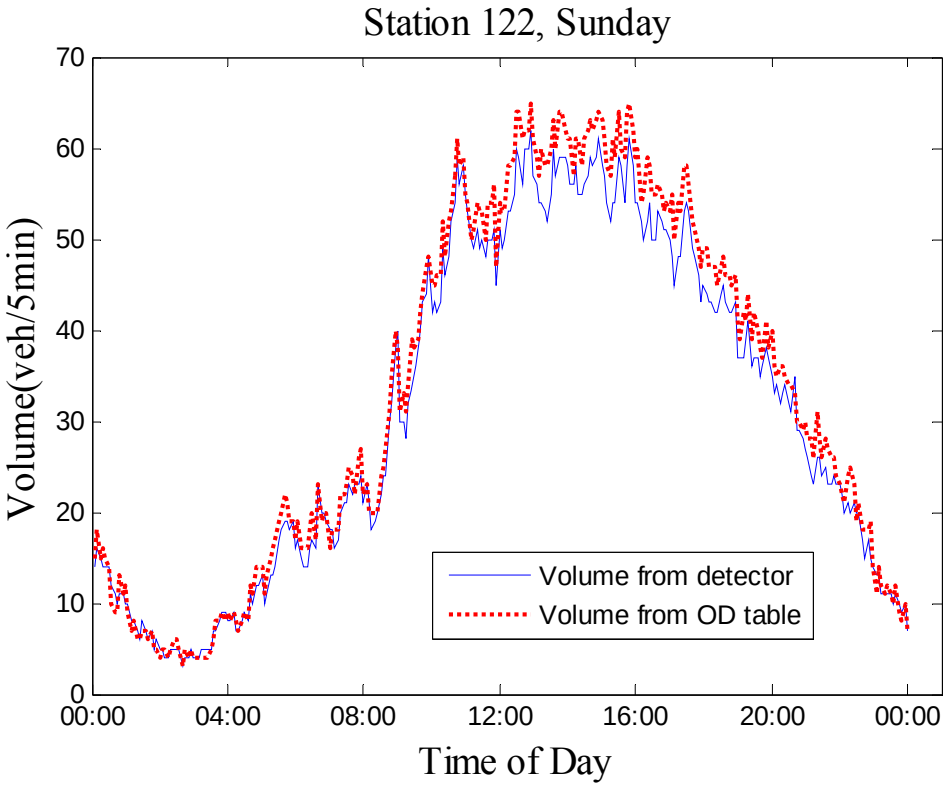

Figure 3.6 Comparison between volumes from OD tables and from loop detectors

As can be seen from Figure 3.6, the volume calculated from OD tables matches the detector flow data very well. Table 3.3 presents the absolute average ("Avg" in units of veh/5min) and standard deviation of volume difference ("Std" in units of veh/5min) of all the ramps based on 24 hours (288 data sets).

Table 3.3 Mean and standard deviation of gap volume between OD tables and link flow

Sun	I-66 On	US29 Off	US29 On	SR28 Off	SR28 On	SR7100 Off	Stringfellow HOV On	SR7100 On	Monument HOV On	US50 SB Off	US50 NB Off
Avg	1	0	2	2	1	2	0	0	0	1	2
Std	3	2	2	2	3	2	0	2	0	2	2
Sun	US50 On	SR123 Off	SR123 On	SR243 Off	SR243 On	I-495 SB Off	I-495 NB Off	I-495 NB HOV Off	I-495 On	I-66 Off	
Avg	2	1	1	0	1	1	1	0	0	1	
Std	4	2	3	2	2	3	2	1	0	1	
Mon	I-66 On	US29 Off	US29 On	SR28 Off	SR28 On	SR7100 Off	Stringfellow HOV On	SR7100 On	Monument HOV On	US50 SB Off	US50 NB Off
Avg	0	0	1	3	2	2	1	0	1	1	2
Std	5	2	2	4	4	3	1	3	1	4	2
Mon	US50 On	SR123 Off	SR123 On	SR243 Off	SR243 On	I-495 SB Off	I-495 NB Off	I-495 NB HOV Off	I-495 On	I-66 Off	
Avg	2	2	1	1	0	2	2	0	1	1	
Std	5	3	3	3	2	4	4	2	1	2	

Tue	I-66 On	US29 Off	US29 On	SR28 Off	SR28 On	SR7100 Off	Stringfellow HOV On	SR7100 On	Monument HOV On	US50 SB Off	US50 NB Off
Avg	0	1	1	3	2	2	1	0	0	1	2
Std	5	2	2	4	4	4	1	2	1	4	2
Tue	US50 On	SR123 Off	SR123 On	SR243 Off	SR243 On	I-495 SB Off	I-495 NB Off	I-495 NB HOV Off	I-495 On	I-66 Off	
Avg	2	3	2	2	0	3	2	0	1	1	
Std	5	3	4	3	3	5	5	2	1	2	
Wed	I-66 On	US29 Off	US29 On	SR28 Off	SR28 On	SR7100 Off	Stringfellow HOV On	SR7100 On	Monument HOV On	US50 SB Off	US50 NB Off
Avg	1	1	1	3	1	2	1	0	1	1	2
Std	5	2	2	4	4	4	2	3	1	4	2
Wed	US50 On	SR123 Off	SR123 On	SR243 Off	SR243 On	I-495 SB Off	I-495 NB Off	I-495 NB HOV Off	I-495 On	I-66 Off	
Avg	2	3	3	1	1	3	2	0	1	1	
Std	6	4	4	3	3	5	5	2	1	2	
Thu	I-66 On	US29 Off	US29 On	SR28 Off	SR28 On	SR7100 Off	Stringfellow HOV On	SR7100 On	Monument HOV On	US50 SB Off	US50 NB Off
Avg	0	0	1	3	2	1	1	0	1	1	2
Std	5	2	2	4	4	5	2	4	1	4	2
Thu	US50 On	SR123 Off	SR123 On	SR243 Off	SR243 On	I-495 SB Off	I-495 NB Off	I-495 NB HOV Off	I-495 On	I-66 Off	
Avg	3	3	4	0	1	3	2	0	1	1	
Std	6	3	4	4	3	6	5	2	1	2	
Fri	I-66 On	US29 Off	US29 On	SR28 Off	SR28 On	SR7100 Off	Stringfellow HOV On	SR7100 On	Monument HOV On	US50 SB Off	US50 NB Off
Avg	1	0	1	3	1	1	1	1	1	2	2
Std	4	1	2	3	4	3	1	2	1	3	2
Fri	US50 On	SR123 Off	SR123 On	SR243 Off	SR243 On	I-495 SB Off	I-495 NB Off	I-495 NB HOV Off	I-495 On	I-66 Off	
Avg	4	4	5	3	0	1	2	3	2	4	
Std	4	3	4	4	3	2	2	4	1	4	
Sat	I-66 On	US29 Off	US29 On	SR28 Off	SR28 On	SR7100 Off	Stringfellow HOV On	SR7100 On	Monument HOV On	US50 SB Off	US50 NB Off
Avg	1	0	1	2	1	0	0	0	0	2	2
Std	3	1	1	2	3	2	0	2	0	2	2
Sat	US50 On	SR123 Off	SR123 On	SR243 Off	SR243 On	I-495 SB Off	I-495 NB Off	I-495 NB HOV Off	I-495 On	I-66 Off	
Avg	3	3	2	2	0	2	2	1	1	1	
Std	3	2	3	2	1	2	2	1	0	1	

As indicated in the table, all of the standard deviations are within the range of 10 veh/5min and the average is no more than in 5 veh/5min. The difference between volumes of these two sources is within a small scope, indicating QueensOD is capable of estimating OD demands and the results are consistent with the detector data.

3.6 Bottleneck Identification

Speed contour plots are used to help visualized congestion indicated by the detector data. The x axis is the list of stations on the mainline from upstream to downstream and the y axis is the time of day with 5-min intervals. The number in the table represents the average vehicle weighted speed for each specific location on the freeway and time of day. The speed contour plots can easily identify the location and time of congestion by marking the segments with speed less than 45 mph, which is the same threshold used by VDOT.

The speed limit on I-66 is defined as 55 mph though the average free flow speed is about 65 mph. Identifying daily flow patterns on I-66 eastbound provides a guide for future parameter calibration in the model simulation process. The morning peak period is the focus since recurring congestion emerges every weekday. Figure 3.7 shows a sample congestion pattern where average vehicle speed drops below 45 mph from 5:40 am to 10:35 am throughout the whole test site. From this and other similar contour plots, four distinct bottlenecks were identified, which are (listed from downstream to upstream):

Bottleneck 1: upstream of Station 361 (near I-495 off-ramps)

Bottleneck 2: upstream of Station 581 (near SR243 off-ramp)

Bottleneck 3: upstream of Station 231 (near US50 on-ramp)

Bottleneck 4: upstream of Station 131 (near SR28 on-ramp)

Station	49(41)	49.5(51)	50(61)	51.2(91)	52.2(101)	52.8(111)	53.2(121)	53.6(131)	54(141)	54.5(151)	55.5(672)	55.4(161)	56.3(191)	57.5(211)	58.3(621)	58.2(221)	58.8(231)	59.1(241)	60(261)	60.2(271)	60.8(281)	61.5(581)	61.5(291)	62(311)	62.4(331)	62.9(341)	63.4(351)	63.9(361)	64.8(387)
5:45	61	62	63	63	60	59	59	46	49	51	61	62	55	64	60	52	46	58	56	57	63	57	59	62	58	62	61	59	46
5:50	62	62	64	58	57	51	50	32	41	50	61	61	52	61	56	55	54	61	59	60	63	60	58	61	58	59	56	53	50
5:55	61	61	62	60	44	33	35	35	54	55	62	61	44	61	57	44	42	48	54	50	61	58	57	61	60	63	63	55	48
6:00	60	61	62	29	20	21	54	54	61	60	63	63	52	61	54	31	37	49	56	57	58	51	52	56	51	53	53	54	50
6:05	51	42	31	22	26	41	54	53	59	58	62	62	55	63	51	28	41	55	55	57	60	56	56	59	52	42	46	40	47
6:10	25	19	18	51	46	39	52	45	56	56	59	58	53	59	35	24	35	52	56	58	60	55	54	60	54	46	49	36	48
6:15	22	25	30	61	57	44	53	49	54	53	59	48	54	46	24	21	41	56	58	59	60	58	58	63	59	47	50	45	50
6:20	37	38	53	56	54	56	55	47	56	56	44	20	53	43	22	20	40	55	57	58	60	54	57	63	59	62	57	47	52
6:25	53	55	59	60	46	37	54	50	58	55	34	19	53	37	26	23	40	54	58	59	62	56	58	64	59	60	57	55	49
6:30	60	63	64	60	24	35	53	48	54	43	32	26	50	39	24	19	40	53	58	58	60	57	57	64	59	62	60	54	53
6:35	59	62	64	63	33	38	55	49	51	45	49	27	49	28	17	19	39	51	57	58	59	56	58	64	59	62	61	39	49
6:40	57	60	61	63	43	41	51	37	48	45	54	32	25	27	18	18	37	54	55	56	54	55	53	61	58	59	43	26	54
6:45	55	59	60	60	43	34	48	40	49	42	58	47	18	28	18	19	38	53	57	58	57	53	58	64	59	49	26	22	57
6:50	59	59	61	51	31	33	48	35	37	45	57	32	16	28	22	18	36	52	56	58	58	51	57	64	58	48	19	20	53
6:55	58	61	62	39	34	28	27	35	35	42	54	25	13	29	18	17	36	49	56	57	57	45	55	64	58	15	19	23	54
7:00	58	61	61	44	14	16	45	27	35	40	52	16	23	28	19	17	36	53	58	58	57	39	54	64	56	10	24	17	62
7:05	55	58	60	26	7	10	53	50	53	46	50	20	15	32	15	17	39	52	56	56	50	34	55	64	50	11	18	20	49
7:10	55	52	34	17	7	12	52	51	58	56	56	17	9	36	28	16	37	51	55	54	31	30	53	63	39	13	22	19	55
7:15	36	19	20	18	9	12	52	53	59	58	46	7	20	34	19	17	38	52	53	33	26	30	50	61	39	14	18	22	49
7:20	23	21	21	17	13	21	49	46	56	54	27	15	22	33	18	16	36	51	35	21	22	31	50	63	41	10	16	15	53
7:25	20	21	25	27	32	26	46	45	44	42	33	19	18	29	20	17	36	47	27	20	35	29	51	61	33	11	15	15	46
7:30	23	21	22	45	33	34	44	30	35	41	28	14	17	30	24	16	31	38	25	16	31	26	50	60	20	9	18	15	56
7:35	26	29	31	55	44	35	23	26	35	40	26	13	19	28	13	15	33	48	29	15	22	26	47	52	14	7	16	15	52
7:40	36	37	39	59	50	33	19	23	38	39	33	15	16	30	14	17	35	41	18	16	24	25	48	40	9	11	17	14	54
7:45	46	36	30	58	33	28	25	28	34	42	36	15	19	30	15	14	31	36	17	10	27	27	50	34	9	7	19	17	48
7:50	43	39	39	58	18	30	24	29	38	41	40	15	16	24	13	15	24	37	20	13	25	25	54	31	10	9	21	19	55
7:55	44	36	52	52	22	34	29	28	31	39	49	14	12	27	9	16	38	39	17	13	23	29	48	27	11	10	31	18	54
8:00	55	59	57	41	27	30	23	24	33	42	58	18	15	27	12	16	32	33	19	14	26	23	48	37	15	12	20	13	54
8:05	55	61	63	38	15	32	25	32	39	43	56	19	18	29	12	15	31	36	13	11	23	28	49	50	13	7	16	13	53
8:10	54	59	52	38	29	39	32	29	45	48	50	16	19	28	13	15	37	33	13	14	25	26	51	51	11	6	14	12	50
8:15	53	46	31	50	46	33	28	31	43	44	58	26	14	27	17	15	27	35	12	13	26	26	50	52	12	6	15	14	53
8:20	32	35	55	46	41	41	33	33	37	43	59	21	18	21	15	16	26	24	14	10	26	21	52	52	10	7	14	12	48
8:25	53	56	60	46	48	31	33	27	35	41	59	35	15	27	12	16	28	25	11	11	21	23	49	56	11	6	16	11	47
8:30	54	60	62	45	39	37	32	28	36	44	58	36	17	31	16	14	17	23	15	13	25	24	50	49	10	6	16	15	47
8:35	57	61	62	44	38	34	30	29	37	41	59	29	19	23	8	12	28	26	15	16	26	23	48	43	9	7	18	14	47
8:40	58	59	48	44	38	35	32	30	35	42	60	37	17	26	10	13	20	31	19	17	24	26	50	39	11	7	16	14	53
8:45	45	37	37	53	44	33	30	29	36	41	60	51	22	23	10	18	34	39	16	18	27	27	49	44	11	6	15	13	53
8:50	33	31	41	53	50	38	26	27	37	40	59	45	25	31	16	18	34	39	16	17	31	25	47	45	8	5	16	14	52
8:55	51	39	39	61	43	31	22	26	37	45	58	53	25	28	22	19	32	37	14	15	32	25	52	45	11	5	14	12	50
9:00	40	44	54	56	32	27	25	34	49	44	59	50	29	31	15	20	29	33	18	18	31	25	47	40	8	5	17	13	50
9:05	56	58	60	38	25	31	31	31	40	42	57	55	25	27	18	21	39	47	17	19	40	30	48	37	11	4	21	18	51
9:10	58	61	55	46	11	31	45	29	43	44	59	58	24	30	21	23	34	36	20	22	49	35	48	31	12	12	23	16	46
9:15	51	48	48	34	22	43	49	32	39	40	58	58	29	32	22	22	26	40	25	24	48	33	47	31	12	11	21	16	49
9:20	62	61	44	50	38	44	37	32	36	47	59	60	32	24	8	17	18	44	58	50	50	41	42	31	16	14	21	19	51
9:25	64	65	67	62	42	43	38	35	43	48	60	60	25	19	8	14	19	47	62	62	62	56	52	29	19	13	21	17	49
9:30	64	66	66	68	61	47	46	29	37	45	60	60	20	20	11	10	15	44	62	63	65	63	62	52	13	12	31	22	50
9:35	64	64	65	67	61	61	54	46	44	42	59	59	13	25	10	16	16	46	63	64	65	63	63	65	35	18	31	22	50
9:40	65	64	65	68	63	63	61	53	54	47	60	34	12	25	8	13	14	45	62	62	66	62	63	64	55	33	29	24	47
9:45	65	66	67	68	63	63	62	57	63	60	50	25	20	25	7	9	12	44	62	63	64	62	63	66	61	62	49	23	50
9:50	65	65	65	69	65	64	63	59	63	60	62	36	14	22	12	7	12	46	62	64	66	64	63	66	60	62	65	47	44
9:55	67	67	67	69	65	63	62	60	64	63	66	43	15	23	9	5	7	40	65	66	68	67	64	65	62	64	66	62	46
10:00	65	66	65	69	65	64	63	58	63	62	67	47	13	21	7	4	6	42	68	70	68	67	65	68	62	66	67	65	61
10:05	65	66	66	69	65	65	63	60	65	61	66	55	10	17	12	9	8	44	66	70	71	66	66	69	63	65	66	62	54
10:10	67	66	66	70	64	64	63	60	65	64	68	51	5	16	10	17	14	45	65	69	66	63	66	66	60	65	65	63	51
10:15	66	67	66	70	65	65	63	59	63	62	60	14	6	20	10	17	21	46	62	65	67	64	62	68	62	65	60	62	49
10:20	66	66	65	69	64	64	63	62	65	62	44	7	11	20	15	27	31	44	59	61	56	53	57	63	56	63	59	60	52
10:25	66	66	66	69	65	64	63	59	65	64	27	10	10	27	31	22	51	58	61	62	54	50	56	62	56	62	59	58	49
10:30	66	66	67	70	65	64	62	58	64	63	51	10	21	29	25	24	51	59	62	64	66	60	62	65	57	58	46	58	51
10:35	67	68	68	71	66	65	63	60	65	63	57	41	22	28	36	31	39	53	60	62	60	57	61	68	57	58	47	58	46
10:40	65	66	65	68	63	65	62	59	64	61	64	64	21	33	35	32	29	47	58	62	57	55	61	66	55	54	49	57	54
10:45	64	67	67	69	64	64	63	61	64	62	65	64	50	32	34	28	33	46	59	61	54	53	59	65	51	43	47	57	52
10:50	65	66	66	68	64	65	62	61	66	64	64	65	58	59	44	36	30	45	59	62	57	52	53	48	28	42	44	55	45
10:55	65	66	66	70	66	65	63	59	65	63	65	63	57	62	57	59	38	46	57	59	61	57	52	46	30	34	47	55	51
11:00	65	66	65	68	63	64	63	61	66	64	67	65	58	64	57	60	59	61	56	58	62	57	53	43	33	36	47	55	49

Figure 3.7 Speed contour in morning rush hour of April 25, 2007, Wednesday

Bottleneck 1 which is close to the I-495 off-ramps is mainly caused by the high volume of vehicles leaving the I-66 via the I-495 off-ramps. The high frequencies of lane changing in this ramp influence area bring about high speed oscillation. Meanwhile, the congestion on I-495 also affects the traffic on I-66 when the queue spills back on the ramps. Bottleneck 2 is also caused by high volume of vehicles taking the SR243 off-ramps. The congestions near Bottleneck 3 and Bottleneck 4 are attributed to high demand coming from the US50 on-ramp and SR28 on-ramp, creating merging congestion on both the mainline and ramp.

3.7 Summary

The test site description, data collection, detector data processing, OD estimation and bottleneck identification were presented sequentially in this chapter.

The test site selected for this study is a 16-mile stretch of freeway I-66 eastbound in Northern Virginia, USA. The data of interest includes loop detector data along with incident data from Incident Management System. Detector data is processed before being imported into the model including eliminating erroneous data and compiling a complete and representative set of flow data for each day of the week representing the normal non-incident daily travel pattern. Standard deviation, relative Least Square Error, deletion%, daily flow trend and scale factors justify the data processing procedures and qualify the results from the data processing. Link flow data is then transferred to OD formats by using QueensOD, a developed OD estimation method to generate OD tables. The results show the model is capable of generating OD tables and the outcomes are consistent with link flow data.

Speed data from the detectors are arranged as speed contours where congestion can be easily identified. The flow and speed data will be used for the model calibration and validation later on.

Chapter 4 Methodology

4.1 Introduction

The Cellular Automata model developed for this study is introduced in this chapter. The proposed CA model is based on NaSch models (Nagel and Schreckenberg, 1992) and incorporates lane changing rules. The simulation setup is introduced followed by detailed illustration of the functions of the incident simulator.

4.2 Simulation Setup

The length for each cell is 7.5 m (24.6 ft), which is the average length occupied by one vehicle in a complete jam condition (Nagel and Schreckenberg, 1992). Each cell is occupied by one vehicle or empty. The maximum speed defined here is 4 cell/s which is equivalent to 67 mph rather than 5 cell/s (84 mph) normally used in the previous studies. Since the speed limit of the test site is 55 mph and the average free flow speed observed is about 65 mph, 4 cell/s is consistent with realistic conditions in the US. The time step is one second.

The notation is visually represented in Figure 4.1 where "X" in bold indicates the given vehicle under concern.

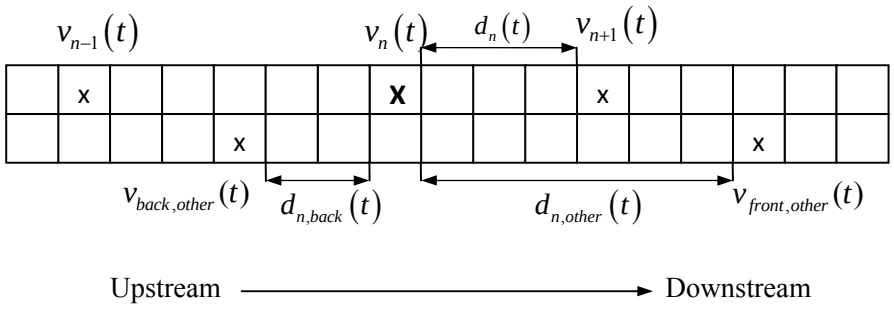

Figure 4.1 Illustration of CA notation

$v_n(t)$: speed of the given vehicle n at time t, in units of cells/second;

$v_{n+1}(t)$: speed of the leading vehicle $n+1$ at time t, in units of cells/second;

$v_{n-1}(t)$: speed of the following vehicle $n-1$ at time t, in units of cells/second;

$v_{front,other}(t)$: speed of the leading vehicle in the neighboring lane at time t, in units of cells/second;

$v_{back,other}(t)$: speed of the following vehicle in the neighboring lane at time t, in units of cells/second;

$d_n(t)$: distance between the given vehicle and its leading vehicle at time t, in units of cells;

$d_{n,other}(t)$: distance between the given vehicle and its leading vehicle in the neighboring lane at time t, in units of cells;

$d_{n,back}(t)$: distance between the given vehicle and its following vehicle in the neighboring lane at time t, in units of cells;

The distance between the given vehicle and its following vehicle $n-1$ is not given specific notation since it can be expressed as $d_{n-1}(t)$.

Look-back distance, look-ahead distance and ramp influence zones are used in the model. Each off-ramp has a look-back distance where the corresponding exiting vehicles will change lanes in advance to reach their intended off-ramp. In this study, a uniform value of 60 cells (450 m) is applied to all of the off-ramps. Look-ahead distance is applied in the bottleneck sections with lane reduction, where the drivers on the blocked lane can observe the lane closure and start to switch. In this case, the look-ahead distance is 30 cells (225 m).

On-ramp and off-ramp influence zones are defined as "(1) an area that incurs operational impacts of merging vehicles in the mainline of the freeway and the acceleration lane for 1,500 ft from the merge point downstream; (2) an area that incurs operational impacts of diverging vehicles in the mainline of the freeway and the deceleration lane for 1,500 ft from the diverge point upstream" (HCM2000, 2000, pp.5-7). In this system, the on-ramp influence zone length is set as 60 cells (1476 ft) from the merge point downstream. The off-ramp influence zone not only covers 60 cells (1476 ft) from the diverge point upstream, equivalent to the look back distance, but also includes the freeway section with a deceleration lane since speed oscillation from frequent lane changes occurrs in this section as well. Figure 4.2 presents the schematic diagram of off-ramp influence zone.

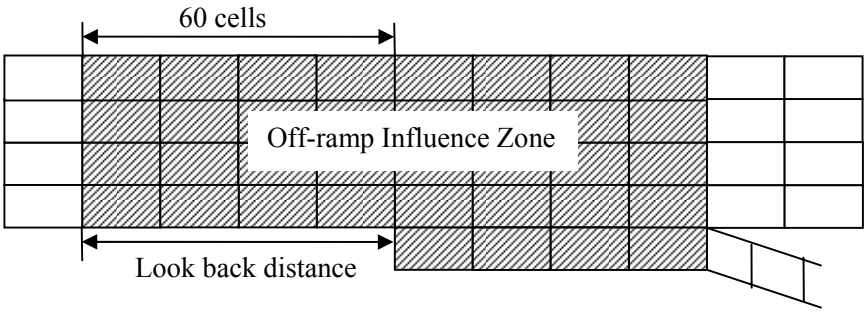

Figure 4.2 Schematic diagram of off-ramp influence zone

Since various features of the freeway are involved in the system (i.e. on-ramp, off-ramp, shoulder lane, etc), indicators are used in the model to discriminate the vehicles under different conditions with different driving behavior. Table 4.1 lists the sections on the freeway and their corresponding indicators.

Table 4.1 Freeway sections and indicators

Freeway Section	Indicator
shoulder lane	-5
look-ahead distance	-4
on-ramp influence zone	-3
no vehicle permission zone	-2
acceleration lane	on-ramp ID
off-ramp influence zone	off-ramp ID
all other sections	-1

Minus 2 indicates the freeway sections where no vehicles are permitted, including incident zones, shoulders and imaginary sections. Since the test site is presented as a 6*3600 matrix, some lanes in this uniform six-lane network which do not exist in reality are also presented in the network, such as rightmost lane between US 50 and I-495. These lanes are defined as imaginary sections where no vehicles are allowed to enter.

4.3 CA Model Description

4.3.1 Initializing the system

The network is initially empty at the beginning of the simulation. The system is initialized by injecting vehicles into the network based on open boundary condition, which is also used throughout the whole simulation process. The probability that a vehicle is injected to a lane in every second is α , defined as total demand divided by the corresponding time interval. For example, if the demand on one lane is 150veh/5min, the value of α is 150/(5*60) = 50%.

In a four lane system, injection probability α of each lane is not only determined by the total link demand but also the vehicle distribution over the lanes, namely, the percentage of vehicles assigned. For example, in the eastbound direction of I-66, approximated 30% of the vehicles drive on each of the two middle lanes and 20% on the leftmost and rightmost lane. If the link demand is 600 veh/5min, the injection probability of each lane for every second is 40% (600*20%/(5*60)), 60%, 60% and 40%, respectively. The vehicles are injected randomly into one of the western most first four cells, corresponding to the farthest location that a vehicle can reach in one time step, only if these cells within a lane are all empty. However, if the first four cells already contain some vehicles, the system will navigate to the location of the last vehicle. So long as blank cells are available behind it, a vehicle will be injected into any cell upstream of the last vehicle.

The destination of the new injected vehicle is determined based on volume-weighted percentage, which is calculated from OD matrices. For example, a demand of 100 vehicles from one origin has two destinations: 30 vehicles will go to destination 1 and the rest 70 will go to destination 2. A vehicle will choose destination 1 and 2 with probability 30% and 70%, respectively.

Similar injection approach is applied to vehicles from the on-ramps. The only difference is that the initial maximum speed for the vehicles from the mainline is 4 cell/s while 3 cell/s is applied to those from the on-ramps, considering slower speed of vehicles on the acceleration lane.

4.3.2 Updating vehicles

The updating rules are based on the NaSch model (Nagel and Schreckenberg, 1992) and Chowdhury's lane changing model (Chowdhury *et al.*, 1997) while some modifications have been made. The lane changing models have been incorporated into the NaSch four-step models, making the total updating steps become five. In the following steps, all the values at time $t-1$ are defined and the values labeled with t are to be determined. The initial value of $v_n(t)$ is defined as the same with $v_n(t-1)$ and is to be updated from step to step.

Step 1: Acceleration

If the vehicle's speed in the last time step is less than the maximum speed $v_{\max}$, the vehicle will increase its speed by 1 cell/s in the current time step. The rule is expressed as:

$$\text{If } v_n(t-1) < v_{\max}, \text{ then } v_n(t) \to \min\left(v_n(t-1)+1, v_{\max}\right)$$

$v_n(t-1)+1$ indicates the desired speed of the vehicle in the current time step, which is restricted by the maximum speed.

Step 2: Lane Changing

Lane changing behavior is classified into discretionary and mandatory. Mandatory lane changing includes changing from the on-ramps to the mainline, from the mainline to the intended off-ramps, and from one lane to another near a bottleneck with lane reduction. Other cases where lane changing is not necessarily required are considered discretionary.

The given vehicle will change lanes with probability $P_{change,dis}$ (probability for discretionary lane changing) if the following conditions are met:

Trigger criteria:

(1) the forward gap is less than the desired speed of the given vehicle: $d_n(t) < v_n(t)$;

(2) the forward gap in the neighboring lane is greater than current lane: $d_{n,other}(t) > d_n(t)$;

Safety criteria:

(3) the neighboring site of the given vehicle n is empty;

(4) the backward gap in the neighboring lane is greater than or equal to the following vehicle's speed at time $t-1$: $d_{n,back}(t) \geq v_{back,other}(t-1)$.

The inequality $d_n(t) < v_n(t)$ equals $d_n(t) < v_n(t) \times \Delta t$. The term Δt is omitted since the minimum time unit defined in the model is 1 second, namely, $\Delta t = 1s$. Similar omission is applied to all of the following inequalities and equations where both speed and distance variables are involved.

The criteria (4) is less restrictive compared to Chowdhury's model (Chowdhury *et al.*, 1997) which is $d_{n,back} \geq v_{\max} + 1$. In the proposed rule, the leading vehicle will switch given the lane changing behavior does not lead to speed reduction for the following vehicle in the target lane, implying that the following vehicle will not be cut off based on its current speed. Discretionary lane changing behavior is more freely used here and the frequency should be higher compared to Chowdhury's models given the same lane changing probability $P_{change,dis}$ which indicates the aggressiveness of the lane changing maneuvers.

Mandatory lane changing behavior is more aggressive than the discretionary type, thereby following less restrictive lane changing rules, which is reflected by the tolerance of the current and following vehicles to speed reduction. The vehicles which are to enter the mainline from an acceleration lane, to reach the intended off-ramps from the mainline, or to divert to an unblocked lane near a bottleneck will take the lane change maneuver with probability $P_{change,man}$ if (1) the speed of the lane changing vehicle drops by less than k cell/s in the current time step; and (2) the speed of

the following vehicle in the target lane drops by less than b cell/s in the current step. The criteria is expressed as:

$$d_{n,other}(t) \geq v_n(t-1) - k \text{ and } d_{n,back}(t) \geq v_{back,other}(t-1) - b$$

The parameter $P_{change,man}$ represents the probability of mandatory lane changing, which should be greater than $P_{change,dis}$. The parameters k and b are the maximum speed reduction that the given vehicle and the following vehicle can tolerate due to the lane changes. Higher values lead to higher frequency of lane changing maneuvers. These rules reflect the following vehicle showing courtesy to mandatory lane changing drivers and implicitly incorporate the effect of mandatory merging into the model.

In this model, a specific mandatory lane changing rule is applied to vehicles unintentionally driving on the shoulder lane when the lane is closed. Shoulder lane control is a freeway management strategy on I-66. When the shoulder lane status switches from open to closed in the off-peak, vehicles are not allowed to access the shoulder lane. However, abruptly closing the shoulder lane and setting it as an impenetrable barrier in the model will cause great congestion. Therefore, the closed shoulder lane in the off-peak is defined as a special area which vehicles are permitted, however, they are forced to leave as soon as possible. More aggressive lane changing rules are used: the vehicles on the shoulder lane will change to the general purpose lane given the number of forward and backward blank cells in the target lane are greater than or equal one. The rule is expressed as:

$$d_{n,other}(t) \geq 1 \text{ and } d_{n,back}(t) \geq 1$$

The purpose of this rule is to force the vehicles to leave the shoulder lane with high lane changing rates without causing great oscillation on the other lanes. Once the vehicles leave the shoulder lane, they are not allowed to reenter again. However, if the lane change maneuver can not be finished due to congestion condition and high density of vehicles on the target lane, for example, an incident occurred, the vehicles will continue on the shoulder lane. This driving behavior is consistent with vehicles will normally using shoulder lanes when congestion is aroused by an incident.

The lane change direction is determined based on the current vehicle's location. The rules are listed as follows:

(1) If the vehicle is on the right acceleration lane, the lane change direction is left.

(2) If the vehicle is on the left acceleration lane, the lane change direction is right.

(3) If an exit vehicle is within the look-back distance of its intended off-ramp, which is on the right side, the vehicle will follow a uniform right lane change; if the off-ramp is on the left, the vehicle will keep changing left until it reaches the exit lane.

(4) If a vehicle is within the look-ahead distance of a blocked lane, the vehicle will follow a uniform direction and keep changing until it reaches an unblocked lane. The direction could be either left or right, based on the location of the unblocked lane.

(5) If a vehicle is on a shoulder lane, the lane change direction is left since all the shoulder lanes are rightmost.

(6) A vehicle is not permitted to change to acceleration lanes, exit lanes, shoulder lanes and all road segments indicated as -2.

(7) On a uniform section with no presence of ramps and incidents, the vehicle can choose either left or right.

One conflict exists in determining the lane change direction when an exit vehicle within the look-back distance meets a blocked lane section (as shown in Figure 4.3). The exit vehicle which is supposed to move to the right should turn to the left lane first. After bypassing the closed section, it will keep moving right until it reaches the exit lane.

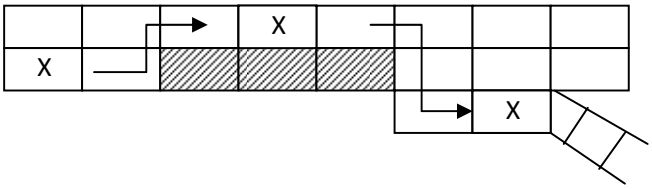

Figure 4.3 Illustration of lane changing priority

Once the lane changing criteria are met, the vehicle's location will change from its current cell to its adjacent cell. The updating order for all the vehicles in the network is from downstream to upstream, consistent with the following vehicle making a lane change decision depending on the leading vehicle's behavior. The updating sequence implicitly takes into consideration the interaction between leading and following vehicles.

Step 3: Deceleration

If the desired speed of vehicle n exceeds the forward gap, the vehicle will reduce its speed to the gap. The rule is expressed as:

$$\text{If } d_n(t) < v_n(t), \text{ then } v_n(t) \to d_n(t).$$

This rule indicates that the vehicle's desired speed should not exceed the forward gap and overtaking in a single lane is prohibited in the model.

Step 4: Randomization

The randomization step decreases a vehicle's speed by 1 cell/s with a certain probability considering possible oscillations on the freeway. The rule is expressed as:

$$v_n(t) \to \max\left(v_n(t)-1, 0\right)$$

Nagel and Schreckenberg pointed out the importance of this step in simulating realistic traffic flow since without this rule, "the dynamics is completely deterministic" (Nagel and Schreckenberg, 1992, pp.2222). Six probabilities are defined in this study considering the different probabilities in several conditions, which are:

(1) P_0 : if the speed of vehicle n at time $t-1$ is zero and its forward gap at time t is 1;

(2) P_{00} : if the speed of vehicle n at time $t-1$ is zero and its forward gap at time t is greater than 1;

(3) P_{onramp} : if the vehicle is in on-ramp influence zone;

(4) $P_{offramp}$: if the exit vehicle is in off-ramp influence zone;

(5) $P_{following}$: if the brake lights of the leading vehicle are turned on;

(6) P : in all other circumstances;

The parameters P_0 and P_{00} are used to mimic the "slow-to-start" behavior caused by the reaction time taken to restart stopped vehicles. The adoption of P_{00} avoids excessive reaction time since if the vehicles have taken "slow-to-start" rules in the last time step, the vehicle should move forward in the current time while allowing the possibility that some drivers will take more time to start their vehicles.

The parameters P_{onramp} and $P_{offramp}$ reflect the possible oscillation in ramp influence areas. In the study, specific values are assigned to four bottlenecks in the morning congestion, which are presented as $P_{offramp\_B1}$, $P_{offramp\_B2}$, P_{onramp_B3} and P_{onramp_B4}. The rest of the on-ramps and off-ramps use uniform P_{onramp} and $P_{offramp}$ value.

The parameter $P_{following}$ accounts for the effect of brake lights of leading vehicles. If the front vehicle within the distance of $d_{following}$ has brake lights on, the following vehicle is more likely to reduce its speed, preventing from abrupt stop. The parameter $d_{following}$ is the threshold distance in which the brake lights of leading vehicle affect the following vehicles. If the vehicles are under both effects of P_{onramp} and $P_{following}$ or $P_{offramp}$ and $P_{following}$, the higher one is selected. The brake

lights will turn on if (1) the vehicle is stopped ($v_{n+1}(t)=0$); or (2) the speed in the current time step is less than that in the previous time step ($v_{n+1}(t)<v_{n+1}(t-1)$).

The parameter P is applied to all other normal conditions where vehicles are driven on a uniform section with no ramps and lane reductions.

Step 5: Car motion

The vehicles advance with their speed obtained from the previous steps. If a vehicle leaves the system, it is deleted from the network.

After one loop of updating existing vehicles in the system at one time step, new vehicles are injected with probability determined by the lane demand as described in the section 4.2.1.

4.4 Simulator Description

A simulator was developed in this study and its functionality will be introduced in this section.

The required inputs for the incident simulator are: (1) incident ID; (2) day of the week; (3) simulation start time; (4) simulation end time; (5) incident start time; (6) incident end time; (7) incident location; (8) incident zone length; and (9) lane closure status.

Simulation start time and simulation end time determine the simulation period which should cover the whole incident duration. If the incident duration is not known prior to the clearance of the incident, a rough simulation end time should be selected. Based on (2) and (3), corresponding OD tables will be loaded into the system. At the beginning of the simulation, the initial network can be either empty or initialized by loading snapshots saved from previous incident-free simulation. The snapshots include the layouts of the vehicles and their related information such as origins, destinations, trajectories and so forth. The simulation start time should be at least half an hour earlier than the incident start time if the simulation is initiated with an empty network in order to distribute vehicles throughout the network. This advance time is not required if snapshots are loaded. Incident start and end times, the corresponding incident location, zone length (how long the lanes are occupied), and lane closure status (which lanes are closed) will be applied to the system. If the incident end time is not available initially, an estimated time can be used.

Two approaches are available for inputting the incident information: (1) coding via the interface; and (2) reading from a file. For approach (1), the data of incident start and end time, incident location, incident zone length and lane closure status are directly typed into the system through the interface which is presented in Figure 4.4. However, only a single lane closure record can be input at one time. If multiple lane closure information is required, approach (2) will be used

in conjunction with the interface and the “Read Incident Data From File” box is checked. A sample input incident file is presented in Figure 4.5.

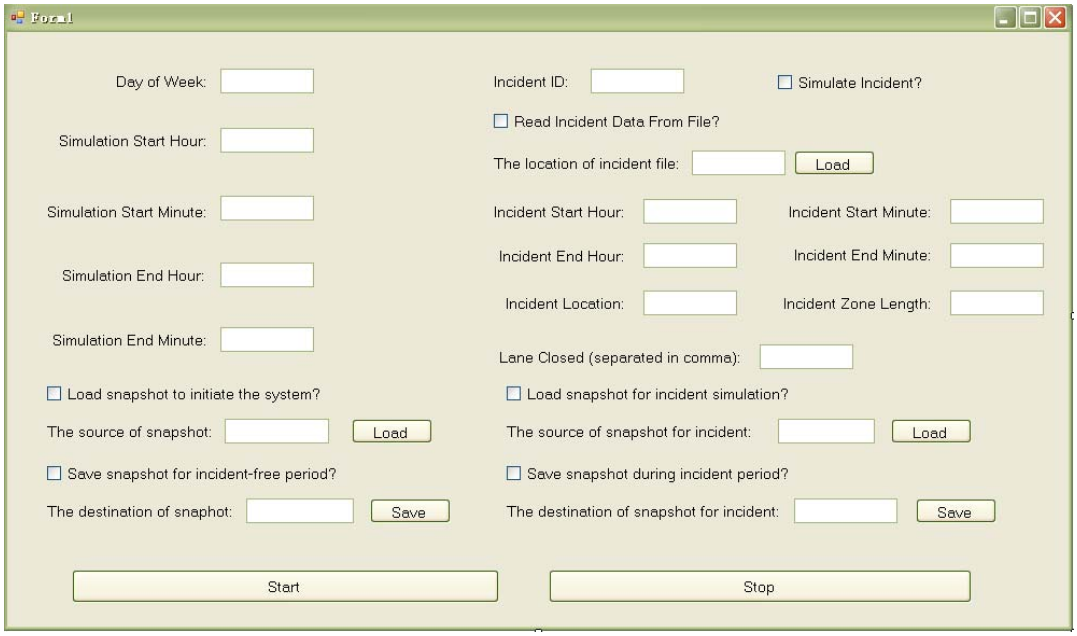

Figure 4.4 Simulator Interface

*Incident 33910 Wednesday,

*Start Time; End Time; Location; Incident Zone Length; Lane Closure

8:20;8:45;1410;10;1,2,3

Figure 4.5 Sample incident input file

The comments are indicated with a “*” in the front. The system ignores these comments and will automatically navigate to the incident inputs. Five inputs required are start time, end time, location of the incident, incident zone length and lane closure status, which are separated with semicolons. The start time and end time should be written without any additional zeros or “AM” and “PM” in it. For example, five past three in the afternoon should be expressed as “15:5” rather than “15:05” or “3:5 pm”. The location of the incident is expressed by the cell indicator in the system. The incident zone length is also input in the unit of cells rather than meter or feet. Lane closure status lists the closed lane number where 1 represents the leftmost lane and these numbers are separated with comma.

The outputs from the simulator include travel time information in terms of time of day and distance upstream from the incident location.

Normally, incident end time and lane closure information throughout the incident duration is not known prior to clearance. Therefore, flexible information input methods are provided for the

system. Two options can be used to address the issue: (1) saving and loading snapshots; and (2) re-run the simulator from the beginning. Option 1 is operated through interface and option 2 normally uses the incident file. In order to illustrate the function of option 1, one example is provided. Assume an incident occurred at 13:00 and the lanes 3 and 4 are closed initially. The clearance time is not available but estimated to be 14:00. The incident end time, which can be defined as "14:0", and lane closure status which is "3, 4" are typed in via the interface. When the simulator is running, snapshots of the network are saved every five minutes, including all vehicle-related information along with estimated travel time. However, if lane closure status is changed at 13:30 when all lanes are closed, The simulation should be stopped first via the "Stop" button on the interface and the incident start time and lane closure status are changed to "13:30" and "1,2,3,4" via the interface. Then the snapshot saved for 13:30 should be loaded into the network. When the simulation continues, the snapshots are saved similarly. The procedures for option 2 are: (1) creating a flat incident file including information of lane closure phases; (2) loading the file into the network; and (3) re-running the system from the beginning. Both methods are efficient and convenient to get the travel time results when the lane closure status needs to be changed.

4.5 Summary

The proposed CA models are based on the NaSch four-step models (Nagel and Schreckenberg, 1992) with the incorporation of a lane changing step between the acceleration and deceleration step. The models use an open boundary condition to match the real traffic network.

The rules of acceleration and deceleration remain the same as NaSch models. Lane changing rules are based on Chowdhury's model (Chowdhury *et al.*, 1997). The proposed rules and parameters are developed based on previous studies, empirical perspective and practical observation. The rules are summarized as: 1) slow-to-start; 2) discretionary lane changing behavior on the freeway; 3) mandatory lane changing of exit vehicles near their intended off-ramps; 4) mandatory lane changing of merging vehicles from onramps; 5) merging behavior upstream of the incident locations; 6) brake light effects; 7) driving behavior on shoulder lanes; and 8) speed oscillation in ramp influence zones. Driving behaviors 1 to 6 have been studied in the previous literature however different rules are explored in this thesis to catch the features for real traffic simulation. Driving behaviors 7 and 8 are initially proposed. A CA model was previously used to simulate work zones. However, it was initially used to simulate other types of incidents such as collision and disabled in this study.

The model can not only be used in off-line simulation, it is also applicable to the near-real time case. A simulator was developed with the presence of an interface, via which inputs can be put into the simulator. Snapshots are important supplementary tools for this practical application.

Chapter 5 Calibration and Validation

5.1 Introduction

In this chapter, the parameters introduced in the previous chapter are calibrated and validated to reproduce morning recurring congestion and various incident conditions. Model calibration is based on comparison of vehicle counts between field data and simulation results. Speed contours are supplementary tools used for model evaluation for incident-free days. Congestion is identified by marking cells where the average speed is less than 45 mph in speed contour plots. In the MUTCD, speed of 50 mph is used as the threshold to discriminate the normal condition and freeway congestion and speed less than 30 mph is an indicator of severe congestion (MUTCD, 2003, pp. 4H-1). VDOT uses 45 mph as the threshold considering possible factors that may affect the oscillation of the speed, such as weather conditions and seasonal variations. In order to be consistency with VDOT applications, 45 mph is selected as the threshold in this study.

5.2 Evaluation Measurement

Calibration of the model is based on trial-and-error with different sets of parameter values. Several evaluation measurements were used to assess the performance of the proposed models and evaluate the parameter values and are listed as follows.

1. Mean Absolute Percentage Error (MAPE)

The average Mean Absolute Percentage Error (MAPE) value is defined as (Wikipedia):

$$MAPE = \frac{1}{n}\sum_{t=1}^{n}\left|\frac{A_t - F_t}{A_t}\right| \tag{5.1}$$

where A_t is the actual value and F_t is the forecast value, n is the total number of paired data and t indicates a single pair-wise data set. The MAPE is computed by summing up the absolute values of all the percentage errors and getting the average, indicating the overall fitness of the results.

The MAPE value is used to evaluate the model in simulating the recurring morning congestion and incident bottlenecks. In the first case, A_t uses flow data from OD inputs and F_t is substituted with the simulation results. The average MAPE value of each station is computed by averaging all MAPE values ranging from 5:00 am to 11:00 am with a resolution of 5 minutes. In the second case, A_t are replaced with flow data from the detectors of the incident day and F_t is the simulation result. The data involved is the flow data with 5-min resolution, covering the whole incident duration

along with half an hour before the occurrence of the incident and half to one hour after the incident clearance, depending on the queue dissipation duration.

A MAPE value of 20% or less is considered acceptable. This threshold is the approximate maximum MAPE value between the field volume and OD inputs among major mainline stations, reflecting the normal oscillation of traffic flow in the network. In this case, A_t are substituted by field data and F_t use OD inputs. The computation is based on the entire flow data of thirty days with a resolution of 5 minutes. Table 5.1 lists the results of average MAPE values between station data from thirty days and OD inputs.

Table 5.1 Average MAPE value between thirty days and representative flow data

	61	111	141	161	191	231	261	291	351	Average
MAPE	17.30%	16.73%	16.16%	16.36%	19.50%	14.19%	16.76%	16.41%	15.50%	16.55%

The average MAPE value of each station varies from 14% to 20% and the total average is approximate 17%. The maximum value 20% is chosen as the threshold to evaluate the simulation results considering the possible variance of the MAPE value over different stations. If the average MAPE value for each station is less than 20%, the results are considered acceptable.

2. GEH statistics

GEH statistics can also be used to evaluate simulation results. GEH is defined as (Chu, 2004):

$$GEH = \sqrt{\frac{\left(Vol_{obs} - Vol_{sim}\right)^2}{\left(Vol_{obs} + Vol_{sim}\right)/2}} \tag{5.2}$$

The GEH calculation is also based on station-level flow data with 5-min resolution. According to Chu's definition, if more than 85% of the GEH values are less than 5, the results are acceptable. The percentage of GEH values less than 5 will be indicated as GEH% in the following contents.

One advantage of GEH% over MAPE is that it is not highly affected by the input value. MAPE will exaggerate the difference between two values if the denominator in the equation is small (Wikipedia). Therefore, GEH% is more adaptable to evaluate the small values such as station data from ramps.

3. Speed Contour

Due to the discrete feature of the CA model, where the speed is only defined with four or five values and considering that the speed from the site data is more precise than the simulation, speed data will not be used to calibrate the model in a numerical approach. Instead, speed contours will be used as a visual tool to examine the daily morning congestion of the network in terms of initial time and end time of the congestion along with queue length. Due to the possible oscillation of this information from day to day, reflected by the severity of the congestion, a range was set. If the

simulation results are located within these ranges, the model is considered to be capable of reproducing the morning bottlenecks.

5.3 Parameter Discussion

As indicated in Chapter 4, fifteen parameters are used in the simulation. The initial range of each parameter and sensitivity analysis is discussed in this section. Speed contour plots and MAPE and GEH analysis are used to evaluate the effects of each parameter on simulation results. The speed contour plots provide intuitive judgments on how the parameters affect the average speed and MAPE and GEH analysis investigate the effects on the traffic flow.

5.3.1 Slow-to-start Parameters

Two parameters P_0 and P_{00} are used to mimic the slow to start driving behavior of the vehicles and they affect the reaction time of a diver to start its vehicle from stop. In order to test the effects of the parameter on the simulation results, the parameter under concern changes with different values while the other parameters remain the same. A set of parameters values is selected as the base case for this sensitivity analysis. Table 5.2 lists the base values of the parameters for sensitivity analysis.

Table 5.2 Base values of the parameters for sensitivity analysis

P_0	P_{00}	P	$P_{offramp}$	$P_{offramp\_B1}$	$P_{offramp\_B2}$	P_{onramp}	P_{onramp_B3}
0.8	0.1	0.1	0.1	0.3	0.3	0	0.1
P_{onramp_B4}	$P_{following}$	$d_{following}$	k	b	$P_{change,man}$	$P_{change,dis}$	
0.25	0.4	8	2	1	0.9	0.5	

Figure 5.1 and Figure 5.2 presents the speed contour plots of morning peak with different P_0 and P_{00} values while other parameters remain uniform. The P_0 and P_{00} values ranging from [0.6, 0.8] and [0.1, 0.2], respectively, are initially tested.

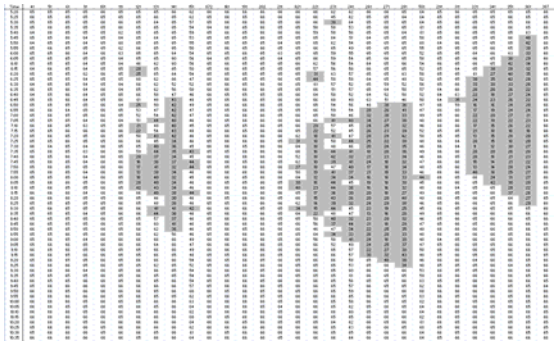

(a) $P_0 = 0.6$

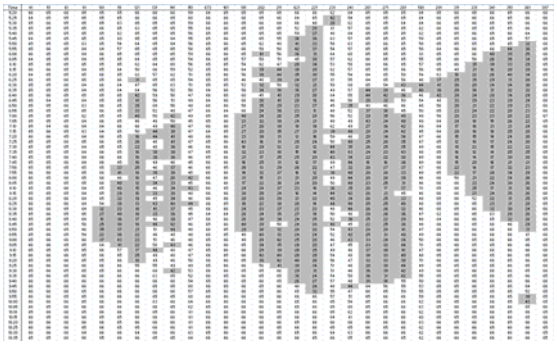

(b) $P_0 = 0.7$

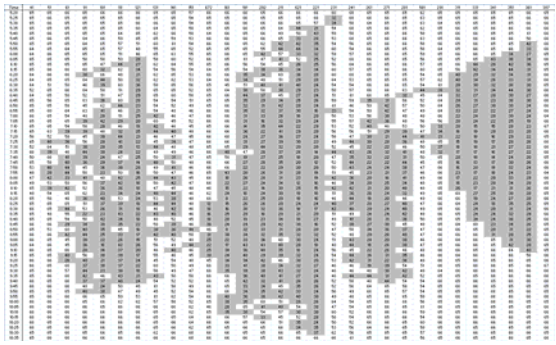

(c) $P_0 = 0.8$

Figure 5.1 Speed contour plots of morning congestion with different P_0

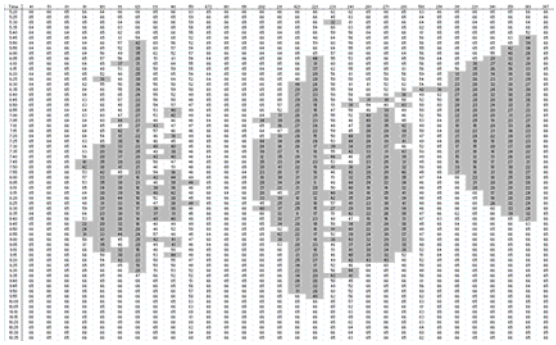

(a) $P_{00} = 0$

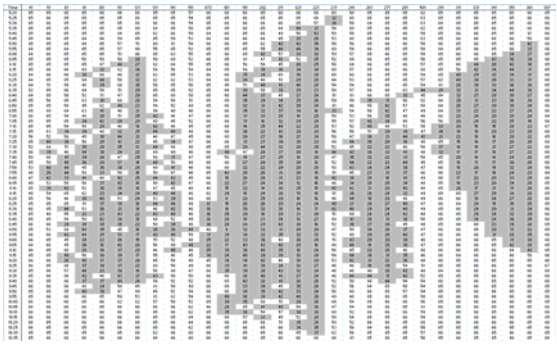

(b) $P_{00} = 0.1$

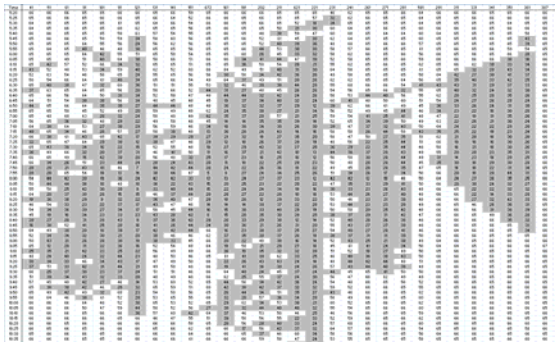

(c) $P_{00} = 0.2$

Figure 5.2 speed contour plots of morning congestion with different P_{00}

P_0 and P_{00} affect the congestion duration and queue length. Bottleneck 3 (second from the left) and bottleneck 4 (left most) are more sensitive to these two parameters in terms of the speed reduction. The queue spill back distance extends to two more stations in bottleneck 4 when P_0 increased from 0.6 to 0.7. Bottleneck 3 almost disappears when $P_0 = 0.6$ is applied. However, the difference between $P_0 = 0.7$ and $P_0 = 0.8$ is not as dramatic but the increase in congestion still can be observed such as in bottleneck 3 and bottleneck 4. The impact of P_{00} on the speed can be noticed from the speed contours, indicated by the aggravation of congestion at bottleneck 3 and 4 with the increase of P_{00} value.

The effects of the two parameters on flow are presented in Table 5.3 and Table 5.4 which list the MAPE and GEH analysis for different scenarios. Different stations reflect different bottleneck traffic conditions. Station 61, 111 and 141 are located within the influence of bottleneck 4 and Station 161, 191 and 231 reflect bottleneck 3. Station 261 and 291 are affected by bottleneck 2 and Station 351 represents the traffic at bottleneck 1.

Table 5.3 MAPE and GEH analysis on morning congestion with different P_0

$P_0 = 0.6$	61	111	141	161	191	231	261	291	351
MAPE	5.0%	5.1%	5.6%	6.2%	5.6%	6.8%	8.8%	8.2%	8.2%
GEH%	100.0%	100.0%	100.0%	100.0%	100.0%	96.0%	96.0%	98.7%	98.7%
$P_0 = 0.7$	61	111	141	161	191	231	261	291	351
MAPE	5.1%	6.4%	6.7%	7.5%	8.5%	8.7%	9.7%	10.4%	9.4%
GEH%	100.0%	98.7%	100.0%	100.0%	96.0%	93.3%	93.3%	94.7%	97.3%
$P_0 = 0.8$	61	111	141	161	191	231	261	291	351
MAPE	7.5%	8.6%	8.3%	11.1%	11.3%	10.7%	11.8%	10.6%	10.1%
GEH%	98.7%	96.0%	96.0%	94.7%	96.0%	86.7%	90.7%	94.7%	100.0%

Table 5.4 MAPE and GEH analysis on morning congestion with different P_{00}

$P_{00} = 0$	61	111	141	161	191	231	261	291	351
MAPE	4.8%	6.8%	6.3%	7.3%	6.8%	7.8%	8.6%	8.9%	7.8%
GEH%	100.0%	100.0%	100.0%	100.0%	100.0%	94.7%	94.7%	100.0%	98.7%
$P_{00} = 0.1$	61	111	141	161	191	231	261	291	351
MAPE	7.5%	8.6%	8.3%	11.1%	11.3%	10.7%	11.8%	10.6%	10.1%
GEH%	98.7%	96.0%	96.0%	94.7%	96.0%	86.7%	90.7%	94.7%	100.0%
$P_{00} = 0.2$	61	111	141	161	191	231	261	291	351
MAPE	11.8%	13.9%	11.5%	14.3%	14.1%	12.1%	13.3%	11.5%	10.6%
GEH%	84.0%	73.3%	88.0%	86.7%	82.7%	84.0%	88.0%	97.3%	93.3%

Since the higher MAPE value and lower GEH% value indicate the good match of the data, increasing P_0 and P_{00} values decreases the fitness of the data, as indicated in Table 5.3 and Table 5.4. Meanwhile, parameter P_{00} has greater impact on flow than P_0 since all of the MAPE values and GEH% values meet the threshold when P_0 changes from 0.6 to 0.8 while the GEH% values of some stations drop below the threshold when P_{00} increases to 0.2.

5.3.2 Following Parameters

Parameters $P_{following}$ and $d_{following}$ reflect the cautiousness of the following drivers when approaching the leading vehicles. Normally, the safety following distance is determined with "three–second rule" which indicates that the safety time headway to the leading vehicle is three seconds. Therefore, if the forward gap of the following vehicle is less than the safety distance, vehicles are more likely to reduce its speed especially when the leading vehicles brakes. In this study, the $d_{following}$ is set to a range from 6 cells to 12 cells, equivalent to 150 ft to 300 ft, corresponding to the safety distance when the current vehicle's speed is 2 cell/s to 4 cell/s. Uniform values of $d_{following}$ are used for all the vehicles with different speeds. The initial range of $P_{following}$ is from 0 to 1 and four values were tested. Figure 5.3 and Figure 5.4 present the speed contour plots of morning peak with different $P_{following}$ and $d_{following}$ values while other parameters remain uniform.

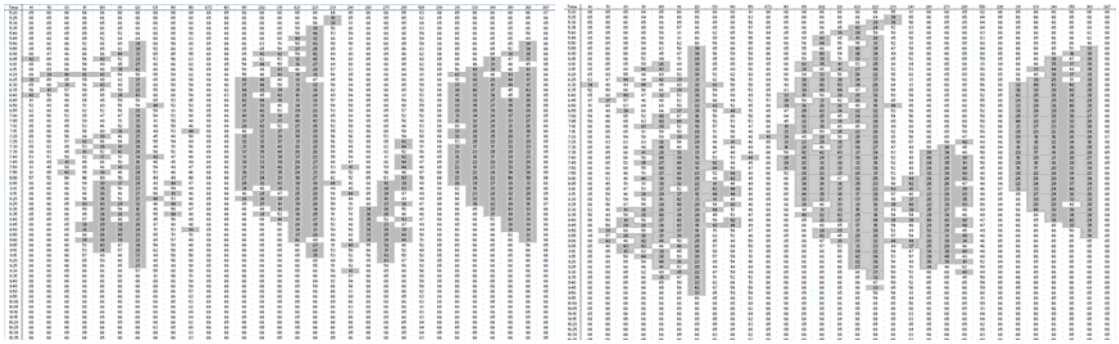

(a) $P_{following} = 0$ (b) $P_{following} = 0.2$

(c) $P_{following} = 0.4$ (d) $P_{following} = 0.7$

Figure 5.3 Speed contour plots of morning congestion with different $P_{following}$

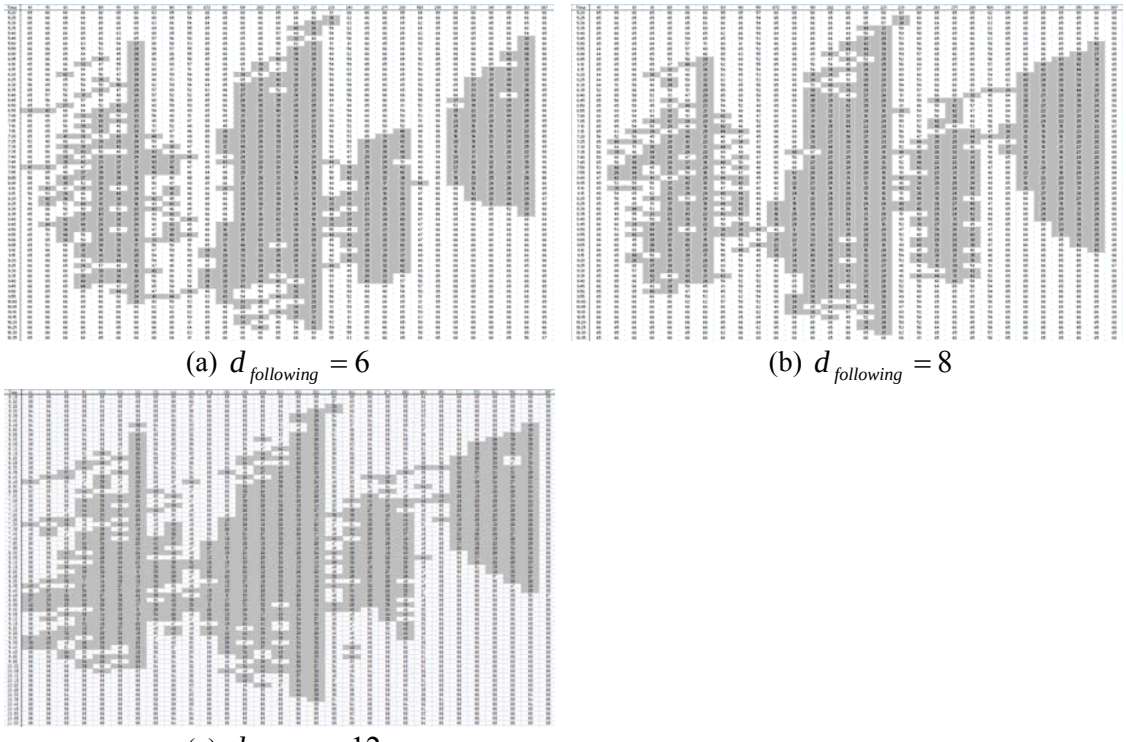

(a) $d_{following} = 6$ (b) $d_{following} = 8$

(c) $d_{following} = 12$

Figure 5.4 Speed contour plots of morning congestion with different $d_{following}$

Increasing $P_{following}$ and $d_{following}$ will expediate the queue spilling back speed, but aggravate the congestion in terms of the congestion duration and queue length. Aggravation of congestion at bottleneck 2, 3 and 4 can be easily identified in Figure 5.3 with the increase of the $P_{following}$ value. The parameter $d_{following}$ has slightly impacts on speed at four bottlenecks. Table 5.5 and Table 5.6 present the MAPE and GEH analysis on morning congestion with different $P_{following}$ and $d_{following}$. As shown in the tables, the parameters have similar effects on the flow as the speed.

Table 5.5 MAPE and GEH analysis on morning congestion with different $P_{following}$

$P_{following}=0$	61	111	141	161	191	231	261	291	351
MAPE	6.2%	7.8%	6.8%	7.8%	8.3%	8.1%	8.9%	8.7%	9.0%
GEH%	97.3%	93.3%	100.0%	100.0%	98.7%	93.3%	97.3%	97.3%	97.3%
$P_{following}=0.2$	61	111	141	161	191	231	261	291	351
MAPE	7.3%	8.6%	7.7%	9.2%	10.9%	8.7%	9.8%	9.4%	9.2%
GEH%	93.3%	94.7%	98.7%	97.3%	93.3%	90.7%	97.3%	97.3%	94.7%
$P_{following}=0.4$	61	111	141	161	191	231	261	291	351
MAPE	7.5%	8.6%	8.3%	11.1%	11.3%	10.7%	11.8%	10.6%	10.1%
GEH%	98.7%	96.0%	96.0%	94.7%	96.0%	86.7%	90.7%	94.7%	100.0%
$P_{following}=0.7$	61	111	141	161	191	231	261	291	351
MAPE	10.7%	13.2%	11.3%	13.9%	13.9%	13.0%	13.9%	12.1%	10.2%
GEH%	89.3%	88.0%	92.0%	92.0%	88.0%	82.7%	84.0%	97.3%	97.3%

Table 5.6 MAPE and GEH analysis on morning congestion with diffe**rent** $d_{following}$

$d_{following}=6$	61	111	141	161	191	231	261	291	351
MAPE	7.8%	8.7%	7.5%	10.4%	11.6%	10.5%	11.5%	10.7%	9.5%
GEH%	93.3%	93.3%	98.7%	96.0%	90.7%	90.7%	94.7%	98.7%	97.3%
$d_{following}=8$	61	111	141	161	191	231	261	291	351
MAPE	7.5%	8.6%	8.3%	11.1%	11.3%	10.7%	11.8%	10.6%	10.1%
GEH%	98.7%	96.0%	96.0%	94.7%	96.0%	86.7%	90.7%	94.7%	100.0%
$d_{following}=12$	61	111	141	161	191	231	261	291	351
MAPE	10.7%	11.0%	10.1%	12.9%	13.1%	11.6%	12.6%	11.4%	9.4%
GEH%	86.7%	85.3%	92.0%	86.7%	88.0%	86.7%	90.7%	97.3%	98.7%

5.3.3 Lane Changing Aggressiveness Parameters

k and b define the aggressiveness of mandatory lane changing behaviors. k represents the personal desire for lane changing while b indicates the tolerance of following vehicle in the target lane. Higher values of k and b lead to higher frequency of lane changing and reduce the waiting time for a switch, however generating more speed oscillation on the freeway. Figure 5.5 and Figure

5.6 present the speed contour plots of morning peak with different k and b value while other parameters remain uniform.

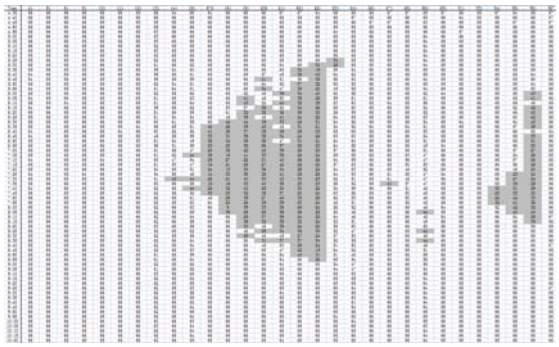

(a) $k = 0$

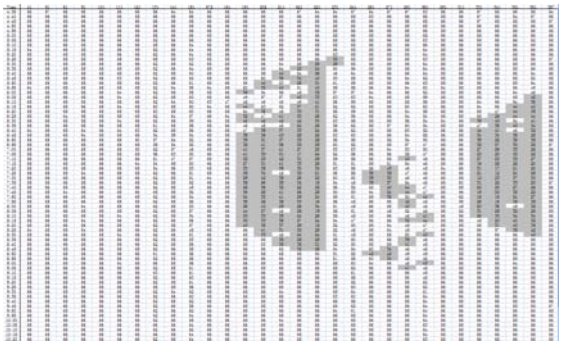

(b) $k = 1$

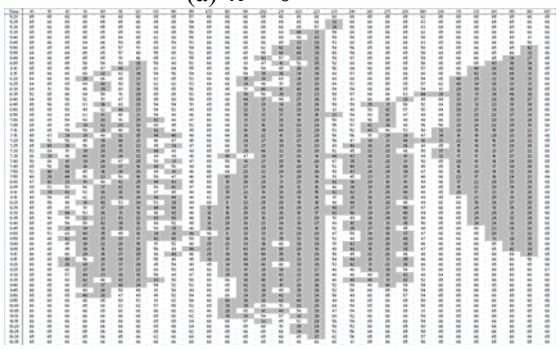

(c) $k = 2$

Figure 5.5 Speed contour plots of morning congestion with different k

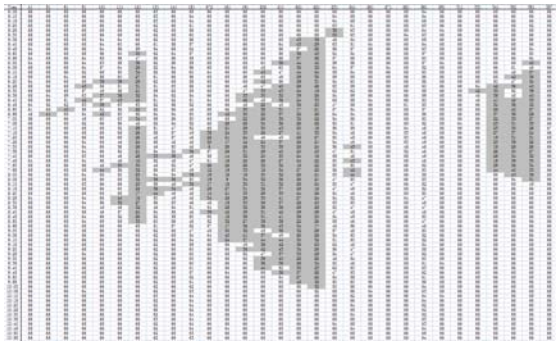

(a) $b = 0$

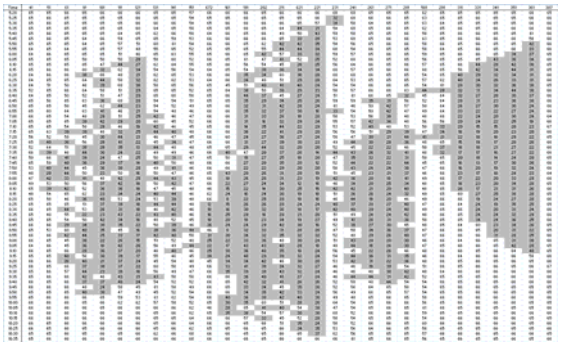

(b) $b = 1$

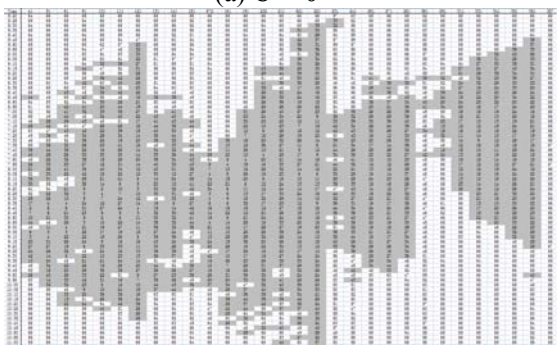

(c) $b = 2$

Figure 5.6 Speed contour plots of morning congestion with different b

As indicated in Figure 5.5 and Figure 5.6, k and b highly affect the severity of the congestion at four bottlenecks, representing the nature of congestion where merging and diverging near the ramps generated great speed oscillation on the freeway. This effect is eliminated when either k and b are set to zero and the congestion in bottleneck 2 and bottleneck 4 almost disappear in Figure 5.5 and Figure 5.6. The recommended values of k and b are 2 and 1, respectively. k and b also affect the location where vehicles choose to change the lane. For example, the merging vehicles from an on-ramp will change to mainline at the beginning of accelerating lane with higher values of k and b. However, if the values are small, vehicles will probably change lanes close to the end of the accelerating lane or even be blocked until a proper gap emerges. Table 5.7 and Table 5.8 present the MAPE and GEH analysis on morning congestion with different k and b.

Table 5.7 MAPE and GEH analysis on morning congestion with different k

$k=0$	61	111	141	161	191	231	261	291	351
MAPE	5.3%	4.9%	5.4%	7.9%	7.4%	7.9%	8.9%	7.8%	7.5%
GEH%	100.0%	100.0%	100.0%	98.7%	96.0%	94.7%	96.0%	97.3%	98.7%
$k=1$	61	111	141	161	191	231	261	291	351
MAPE	5.3%	4.7%	4.8%	6.2%	6.5%	7.3%	8.3%	7.6%	9.2%
GEH%	100.0%	100.0%	100.0%	100.0%	97.3%	96.0%	97.3%	97.3%	97.3%
$k=2$	61	111	141	161	191	231	261	291	351
MAPE	7.5%	8.6%	8.3%	11.1%	11.3%	10.7%	11.8%	10.6%	10.1%
GEH%	98.7%	96.0%	96.0%	94.7%	96.0%	86.7%	90.7%	94.7%	100.0%

Table 5.8 MAPE and GEH analysis on morning congestion with different b

$b=0$	61	111	141	161	191	231	261	291	351
MAPE	5.2%	6.6%	5.7%	8.7%	9.4%	9.1%	9.4%	7.9%	7.6%
GEH%	98.6%	97.3%	100.0%	97.3%	98.6%	97.3%	95.9%	98.6%	100.0%
$b=1$	61	111	141	161	191	231	261	291	351
MAPE	7.5%	8.6%	8.3%	11.1%	11.3%	10.7%	11.8%	10.6%	10.1%
GEH%	98.7%	96.0%	96.0%	94.7%	96.0%	86.7%	90.7%	94.7%	100.0%
$b=2$	61	111	141	161	191	231	261	291	351
MAPE	17.1%	18.9%	16.4%	19.1%	17.8%	15.3%	15.8%	14.4%	11.9%
GEH%	77.3%	64.0%	78.7%	73.3%	74.7%	76.0%	80.0%	93.3%	92.0%

As indicated in Table 5.8, the value of k did not have a great impact on traffic flow. However, when the value of b increases from 1 to 2, the GEH% value dramatically reduced and dropped below the threshold. Therefore, the value of b should be less than 2.

5.3.4 Lane Changing Probability Parameters

Increasing the lane changing probability will smooth the flow and alleviate the congestion on the freeway. The value of P_{change_dis} ranges from 0 to 1 and three values are tested. The mandatory

lane change probability is higher than the discretionary one and close to 1. Figure 5.7 and Figure 5.8 present the speed contour plots of morning peak with different P_{change_dis} and P_{change_man} value while other parameters remain uniform.

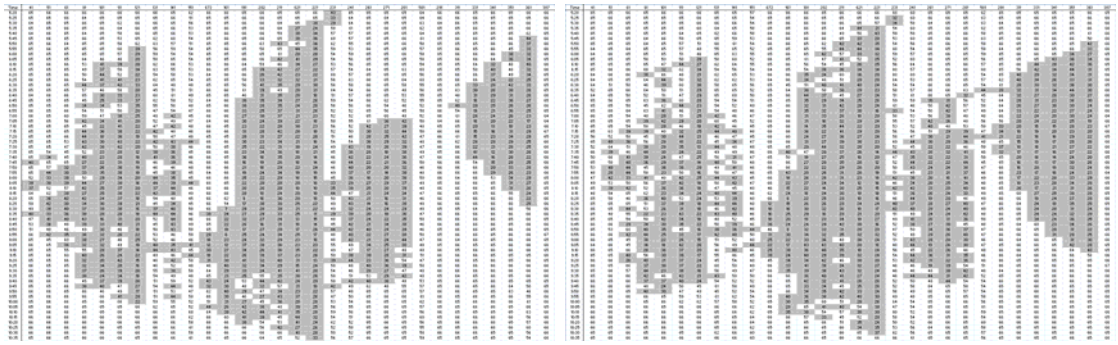

(a) $P_{change\_dis} = 0.3$ (b) $P_{change\_dis} = 0.5$

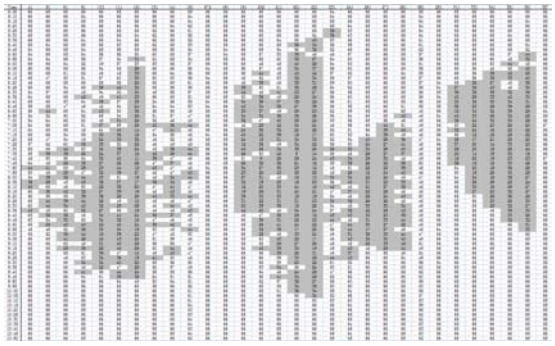

(c) $P_{change\_dis} = 0.7$

Figure 5.7 Speed contour plots of morning congestion with different P_{change_dis}

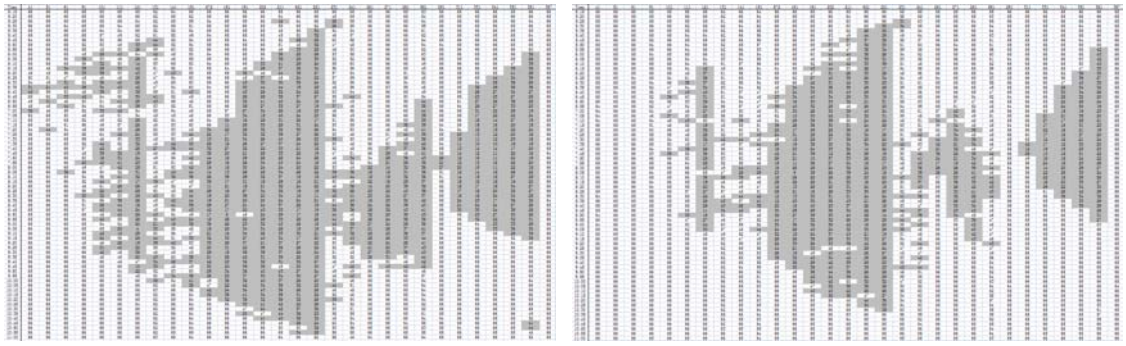

(a) $P_{change\_man} = 0.3$ (b) $P_{change\_man} = 0.5$

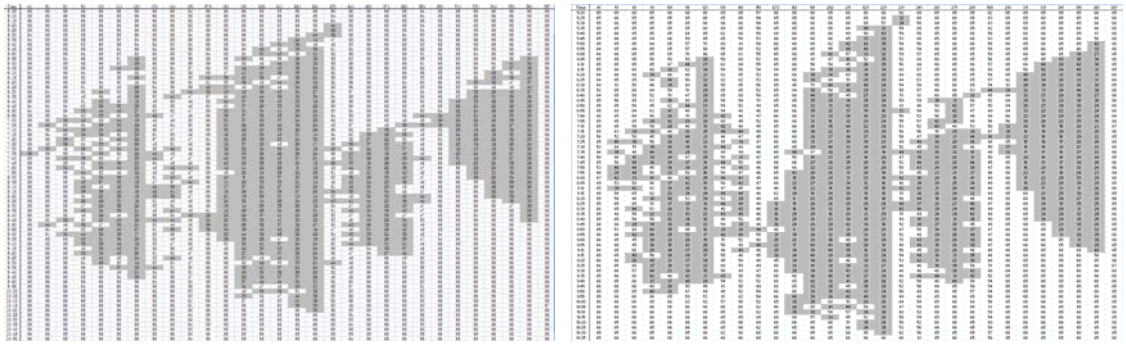

(c) $P_{change\_man} = 0.7$ (d) $P_{change\_man} = 0.9$

Figure 5.8 Speed contour plots of morning congestion with different P_{change_man}

The congestion is mitigated with the increase of P_{change_dis} especially at Bottleneck 3.

The congestion at bottleneck 4 is aggravated with the increase of P_{change_man} value, indicating that higher P_{change_man} values will create more speed oscillation near ramps. Three downstream bottlenecks are affected by this bottleneck. Normally the downstream congestion will increase given the upstream congestion are mitigated since more vehicles will surge to the downstream bottlenecks. Table 5.9 and Table 5.10 present the MAPE and GEH analysis on morning congestion with different P_{change_dis} and P_{change_man}. From Table 5.9 and Table 5.10, the change on the flow is not as obvious as speed contours.

Table 5.9 MAPE and GEH analysis on morning congestion with different P_{change_dis}

$P_{change\_dis} = 0.3$	61	111	141	161	191	231	261	291	351
MAPE	8.5%	10.3%	9.2%	11.9%	12.4%	11.8%	13.5%	11.9%	9.1%
GEH%	98.7%	93.3%	98.7%	96.0%	92.0%	88.0%	90.7%	94.7%	94.7%
$P_{change\_dis} = 0.5$	61	111	141	161	191	231	261	291	351
MAPE	7.5%	8.6%	8.3%	11.1%	11.3%	10.7%	11.8%	10.6%	10.1%
GEH%	98.7%	96.0%	96.0%	94.7%	96.0%	86.7%	90.7%	94.7%	100.0%
$P_{change\_dis} = 0.7$	61	111	141	161	191	231	261	291	351
MAPE	7.4%	8.1%	7.8%	9.1%	9.3%	9.4%	10.7%	9.6%	8.6%
GEH%	97.3%	96.0%	97.3%	97.3%	96.0%	96.0%	96.0%	98.7%	98.7%

Table 5.10 MAPE and GEH analysis on morning congestion with different P_{change_man}

$P_{change\_man} = 0.3$	61	111	141	161	191	231	261	291	351
MAPE	7.0%	9.3%	8.6%	12.0%	12.2%	13.0%	13.6%	11.4%	11.7%
GEH%	94.7%	90.7%	92.0%	94.7%	90.7%	85.3%	88.0%	96.0%	94.7%
$P_{change\_man} = 0.5$	61	111	141	161	191	231	261	291	351
MAPE	5.2%	6.1%	6.7%	11.3%	10.2%	10.6%	11.5%	10.2%	10.3%
GEH%	100.0%	100.0%	96.0%	93.3%	93.3%	90.7%	94.7%	97.3%	97.3%
$P_{change\_man} = 0.7$	61	111	141	161	191	231	261	291	351
MAPE	7.4%	7.3%	7.4%	10.7%	11.5%	10.8%	11.2%	10.5%	10.0%
GEH%	96.0%	96.0%	98.7%	96.0%	92.0%	90.7%	93.3%	93.3%	92.0%
$P_{change\_man} = 0.9$	61	111	141	161	191	231	261	291	351
MAPE	7.5%	8.6%	8.3%	11.1%	11.3%	10.7%	11.8%	10.6%	10.1%
GEH%	98.7%	96.0%	96.0%	94.7%	96.0%	86.7%	90.7%	94.7%	100.0%

5.3.5 Speed Reduction Parameters

The three parameters P, P_{onramp} and $P_{offramp}$ represent possible speed reductions when vehicles approach the different sections of the freeway. Several specific ramps use distinct P_{onramp} and $P_{offramp}$ values in order to simulate the recurring morning congestion on weekdays. These parameters have similar impacts on the congestion, namely, higher values indicate more speed drop and congestion in the bottlenecks. Figure 5.9 presents the speed contour plots of the morning peak with different P values while other parameters remain uniform.

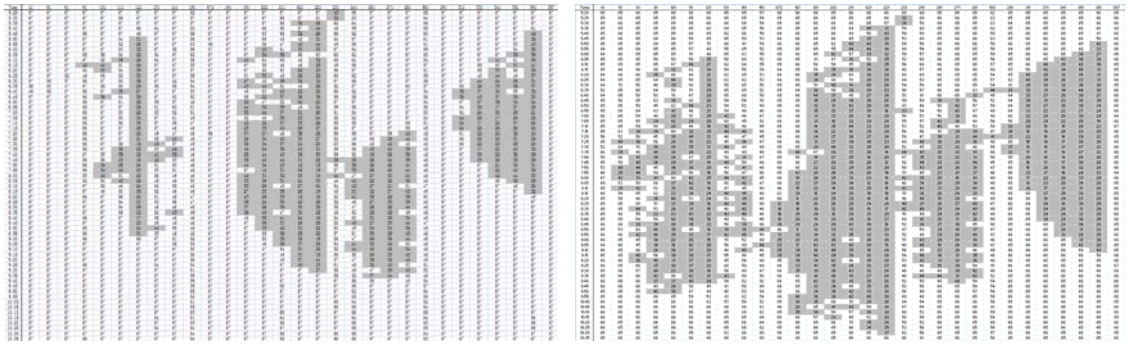

(a) $P = 0$ (b) $P = 0.1$

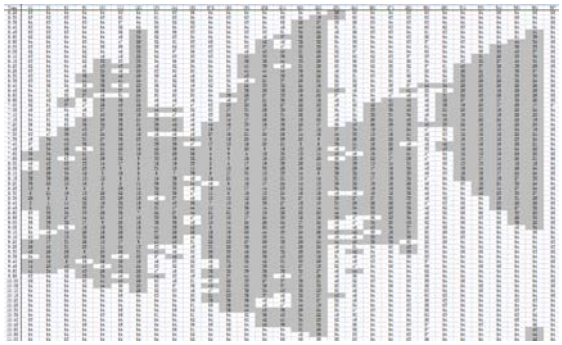

(c) $P = 0.2$

Figure 5.9 Speed contour plots of morning congestion with different P

With the increase of P, the congestion at bottlenecks have consistently increased based on the speed values. Table 5.11 presents the MAPE and GEH analysis on morning congestion with different P values.

Table 5.11 MAPE and GEH analysis on morning congestion with different P

$P = 0$	61	111	141	161	191	231	261	291	351
MAPE	5.0%	5.6%	5.2%	6.9%	8.2%	7.5%	9.0%	8.4%	7.9%
GEH%	100.0%	97.3%	100.0%	100.0%	96.0%	94.7%	96.0%	97.3%	96.0%
$P = 0.1$	61	111	141	161	191	231	261	291	351
MAPE	7.5%	8.6%	8.3%	11.1%	11.3%	10.7%	11.8%	10.6%	10.1%
GEH%	98.7%	96.0%	96.0%	94.7%	96.0%	86.7%	90.7%	94.7%	100.0%
$P = 0.2$	61	111	141	161	191	231	261	291	351
MAPE	14.5%	15.3%	13.2%	14.9%	14.9%	13.7%	13.8%	12.0%	11.0%
GEH%	81.3%	82.7%	89.3%	85.3%	80.0%	85.3%	90.7%	98.7%	97.3%

As indicated in Table 5.11, the value of P has consistent impact on flow, especially at bottleneck 3 and 4, since the GEH% values of stations between 61 and 231 decrease below 90% and MAPE exceed 10% when P is 0.2. The other speed reduction parameters have similar effects on speed and flow as parameter P.

5.4 Incident-free simulation

Incident-free simulation uses the OD inputs to reproduce the typical day free of incidents on the freeway. It is used as the base for incident simulation. The most important part of incident-free simulation is to reproduce the morning congestion in the eastbound direction of I-66, ranging from 5:30 am to 11:00 am. Four bottlenecks which generated recurring morning congestion are easily identified from the speed contour plots.

The initial and end time of the congestion at each bottleneck is within a certain range but varies regarding the severity of the congestion in terms of queue length and duration from day to day. Weekdays follow similar traffic congestion. Table 5.12 displays the range of start time, end time and queue length observed from the site based on thirty weekdays.

Table 5.12 The range of the start time, end time and queue length of four recurring congestion locations

	Bottleneck 1	Bottleneck 2	Bottleneck 3	Bottleneck 4
Start Time	5:35 am – 6:40 am	5:25 am – 6:30 am	6:15 am – 7:15 am	5:30 am – 7:30 am
End Time	8:00 am – 9:45 am	8:45 am – 10:55 am	9:00 am – 10:45 am	8:45 am – 10:10 am
Queue Length	2.7 – 4.6 mile	2.9 – 4.7 mile	1.5 – 2.4 mile	1.9 – 2.8 mile

Figure 5.10 shows a simulation result of morning congestion on Wednesday and the initial time, end time and queue length of each bottleneck are listed in Table 5.13.

Time	41	51	61	91	101	111	121	131	141	151	672	161	191	202	211	621	221	231	241	261	271	281	581	291	311	331	341	351	361	387
5:20	65	65	66	65	66	66	66	65	65	57	66	66	66	65	66	66	66	60	60	65	65	65	62	65	65	65	65	65	66	65
5:25	65	66	66	65	65	65	66	65	65	54	65	65	66	65	65	65	66	32	60	66	66	65	63	65	65	66	65	65	66	66
5:30	65	66	65	65	65	65	66	66	66	54	65	66	66	66	66	65	57	34	59	64	65	65	63	64	65	65	65	65	66	66
5:35	65	65	65	65	65	65	60	64	65	58	65	65	66	65	64	44	21	54	60	65	66	65	62	65	66	65	66	66	66	66
5:40	65	66	65	65	65	64	65	62	66	58	64	66	65	66	49	50	43	59	58	65	65	66	58	65	66	66	65	65	61	66
5:45	65	66	65	64	66	59	65	65	59	53	66	66	66	66	65	33	28	53	60	65	66	66	63	65	66	66	66	66	50	66
5:50	65	65	65	64	65	57	51	60	61	54	66	66	65	62	42	42	35	54	56	65	66	66	58	66	65	66	65	65	42	66
5:55	64	65	64	65	65	57	48	55	65	52	65	65	65	55	44	44	34	60	54	66	65	65	58	64	65	66	65	66	33	66
6:00	64	66	65	65	65	51	46	65	63	55	65	66	65	42	57	33	32	59	57	65	66	65	59	65	66	66	65	34	27	65
6:05	65	65	65	58	50	50	28	58	60	52	66	65	61	47	41	52	25	52	60	66	65	65	56	65	65	65	43	36	34	66
6:10	65	65	65	65	47	44	27	62	64	55	65	66	56	54	45	26	25	56	64	66	65	66	57	65	66	44	28	42	36	65
6:15	65	66	66	60	32	62	34	54	56	54	64	65	54	38	36	34	34	60	57	65	66	66	60	65	56	42	34	44	31	65
6:20	64	66	66	38	66	48	21	62	65	53	66	66	35	34	60	36	28	60	60	66	65	65	54	65	40	29	32	34	31	66
6:25	64	65	65	64	44	50	32	62	62	53	64	66	34	48	51	29	28	64	53	65	65	65	57	62	40	34	26	33	31	66
6:30	64	51	50	46	39	60	36	58	65	56	65	45	51	40	41	40	24	54	54	66	66	65	54	61	28	30	32	36	30	65
6:35	52	65	66	64	58	51	29	65	65	52	65	64	38	50	38	29	23	59	57	66	66	63	44	28	32	31	34	44	30	66
6:40	64	65	50	52	51	47	29	65	60	50	65	66	44	37	45	27	24	51	61	66	65	32	45	64	32	27	28	30	27	66
6:45	65	56	65	63	36	60	28	54	54	51	65	65	35	29	34	25	26	59	59	35	31	56	52	64	28	31	23	36	30	66
6:50	65	65	59	45	62	44	23	54	52	49	65	66	32	31	42	28	24	61	46	50	42	57	50	64	26	27	30	30	24	66
6:55	65	60	64	63	41	46	21	54	48	46	66	66	35	32	37	30	16	33	54	50	42	47	49	64	33	22	22	27	24	66
7:00	66	65	54	48	28	51	25	42	46	47	66	66	31	33	26	18	20	58	53	56	38	48	48	66	22	24	20	30	24	64
7:05	65	65	65	33	42	29	20	60	45	52	66	66	31	18	32	29	24	55	57	42	36	48	56	56	20	24	22	25	19	66
7:10	65	65	54	58	28	46	19	42	46	45	65	66	14	35	44	22	29	53	52	40	48	53	50	33	20	15	15	28	23	67
7:15	65	63	39	39	48	32	25	44	40	48	66	66	36	22	41	29	20	56	56	51	29	39	47	34	18	19	20	23	20	66
7:20	56	52	58	45	30	44	21	46	47	45	66	60	24	27	36	27	24	58	47	30	21	44	41	21	22	18	16	29	22	65
7:25	65	40	36	56	28	41	22	45	34	47	66	66	31	27	39	30	23	49	44	30	28	36	48	65	15	19	17	28	26	66
7:30	52	64	51	38	28	35	13	44	48	48	65	65	29	44	32	20	20	52	45	22	22	46	50	37	18	18	21	27	22	66
7:35	66	39	46	44	30	24	22	49	49	46	66	40	47	20	37	26	14	44	43	26	32	41	48	32	17	17	16	27	22	66
7:40	50	66	41	39	24	47	25	50	31	47	65	50	19	27	25	18	20	47	35	32	22	31	50	65	20	18	14	24	20	65
7:45	65	58	40	36	29	37	14	40	50	48	66	66	27	20	35	20	12	52	44	22	22	44	45	65	16	13	17	30	26	66
7:50	53	40	44	45	36	38	28	49	41	46	66	66	22	22	29	20	20	50	43	24	24	38	47	66	16	20	19	32	24	66
7:55	48	28	44	50	23	50	16	50	47	46	65	43	20	26	31	28	19	51	45	23	21	37	46	66	23	17	18	24	23	64
8:00	47	42	33	41	48	42	25	44	43	45	66	18	26	28	31	23	19	42	36	20	18	41	49	66	17	22	20	33	29	66
8:05	49	53	50	56	37	42	18	50	42	47	66	22	27	24	34	12	16	46	34	20	25	34	48	65	18	23	20	34	28	65
8:10	65	39	45	52	36	36	18	47	45	48	66	15	22	14	30	25	15	42	42	21	20	40	48	65	26	17	21	31	26	66
8:15	48	54	65	62	23	34	24	40	44	46	62	24	16	24	30	19	18	51	36	26	24	32	49	65	60	27	25	38	28	65
8:20	65	58	46	36	40	53	24	53	39	48	66	8	22	25	29	18	16	46	44	19	20	46	49	66	66	19	24	27	28	66
8:25	65	65	65	51	37	39	18	44	44	48	12	15	26	26	29	24	24	40	37	28	27	40	47	66	64	24	19	35	25	65
8:30	66	65	44	53	26	31	18	46	42	46	18	16	30	32	36	18	17	42	40	29	24	40	49	65	66	24	20	31	24	66
8:35	65	48	55	22	23	43	22	43	40	46	16	25	29	18	29	21	20	51	49	24	24	42	48	66	65	24	24	32	29	66
8:40	65	65	54	50	42	34	18	48	52	45	18	20	19	23	34	19	27	49	41	26	31	36	50	65	65	34	24	38	25	66
8:45	66	66	29	34	30	35	22	50	39	46	36	24	24	29	42	30	16	52	38	27	30	45	48	65	64	60	23	34	26	65
8:50	65	53	60	40	35	45	16	38	36	44	46	8	32	33	31	28	20	47	50	34	36	37	47	66	66	65	20	31	22	65
8:55	66	66	42	44	25	33	17	42	40	50	31	30	34	32	35	32	32	52	48	29	26	40	47	66	66	66	31	28	25	66
9:00	66	65	45	38	22	26	15	51	52	48	25	22	33	36	48	30	24	51	43	28	20	30	46	66	64	66	65	31	30	66
9:05	64	66	45	36	18	42	26	56	49	44	22	17	43	43	40	28	18	48	44	19	26	30	47	65	66	66	66	42	28	65
9:10	66	65	66	28	36	37	20	46	40	46	25	38	36	40	35	18	24	56	45	22	26	45	48	66	66	65	66	64	40	65
9:15	65	65	40	56	30	39	17	55	46	45	38	24	40	29	39	32	24	54	44	36	31	35	46	66	64	66	66	66	58	66
9:20	66	66	26	40	21	37	24	45	54	48	45	34	34	42	46	30	20	53	42	31	22	36	48	66	65	66	65	66	65	66
9:25	66	65	66	37	38	37	22	60	50	49	66	33	41	38	34	32	27	46	46	19	39	54	51	66	65	66	66	65	66	67
9:30	65	66	57	44	23	38	18	56	49	47	66	35	39	38	43	32	24	46	46	48	38	42	48	64	66	66	66	66	66	66
9:35	65	66	66	42	46	43	21	43	50	50	66	66	36	40	41	27	24	46	44	44	31	42	52	65	65	65	66	66	66	66
9:40	66	65	66	37	37	40	24	54	52	52	66	65	42	32	41	26	26	52	50	48	44	54	54	66	65	66	66	65	66	66
9:45	66	66	66	48	24	50	45	61	58	49	66	65	33	34	45	35	26	52	56	64	65	58	54	65	66	66	65	65	65	65
9:50	65	65	65	40	30	47	49	45	52	54	66	66	34	35	42	33	24	56	49	66	65	57	54	65	65	66	66	65	66	65
9:55	65	66	66	66	65	59	53	61	62	54	66	40	36	38	42	40	30	49	48	65	66	65	58	66	66	66	66	66	66	66
10:00	66	66	66	65	66	62	62	57	58	52	65	30	35	60	51	28	26	64	54	65	66	66	56	65	66	66	66	66	65	65
10:05	66	66	66	66	65	66	66	66	66	62	46	28	65	41	40	54	38	47	54	65	66	65	61	66	65	66	65	65	65	66
10:10	66	66	66	66	66	66	66	65	66	62	65	35	38	54	57	30	30	60	52	66	66	66	58	65	65	66	65	66	66	66
10:15	66	66	66	66	66	66	66	65	65	64	66	66	57	33	45	52	28	58	54	65	65	66	54	66	66	66	66	66	65	65
10:20	66	65	66	66	66	66	66	65	66	64	66	66	65	66	51	35	24	50	52	66	66	65	60	66	66	66	66	66	65	66
10:25	66	65	66	65	66	66	66	65	66	62	65	65	66	65	66	34	35	53	56	64	66	65	58	65	65	65	66	65	65	66
10:30	65	65	66	65	66	65	66	62	66	60	66	66	65	65	66	65	37	62	56	65	65	65	57	66	66	66	65	66	66	65
10:35	65	66	66	66	66	66	66	66	66	60	66	66	66	65	66	66	66	66	61	65	66	65	56	65	66	65	65	66	65	66

Figure 5.10 Speed contour plot of Wednesday morning congestion

Table 5.13 Start time, end time and queue length at four bottlenecks based on simulation

	Bottleneck 1	Bottleneck 2	Bottleneck 3	Bottleneck 4
Start Time	6:05 am	5:35 am	6:40 am	5:50 am
End Time	9:40 am	10:30 am	9:35 am	9:10 am
Queue Length	4.2 mile	3.7 mile	2.0 mile	2.8 mile

Compared with Table 5.12, the simulation results are located within the range of oscillation, indicating the capability of the model to appropriately reproduce the traffic pattern of weekday morning peak.

Apart from the qualitative analysis based on speed contours, MAPE values and GEH% calculation justify the model quantitatively. Table 5.14 summarizes the average MAPE and GEH% values of major measurement stations on the mainline. The comparison is based on simulation results and OD inputs ranging from 5:00 am to 11:00 am with a resolution of 5 minutes. Figure 5.11 presents the corresponding flow plots between these two data sets.

Table 5.14 The average MAPE and GEH% value of major stations on the mainline

	61	111	141	161	191	231	261	291	351
MAPE	7.5%	8.6%	8.3%	11.1%	11.3%	10.7%	11.8%	10.6%	10.1%
GEH	98.7%	96.0%	96.0%	94.7%	96.0%	86.7%	90.7%	94.7%	100.0%

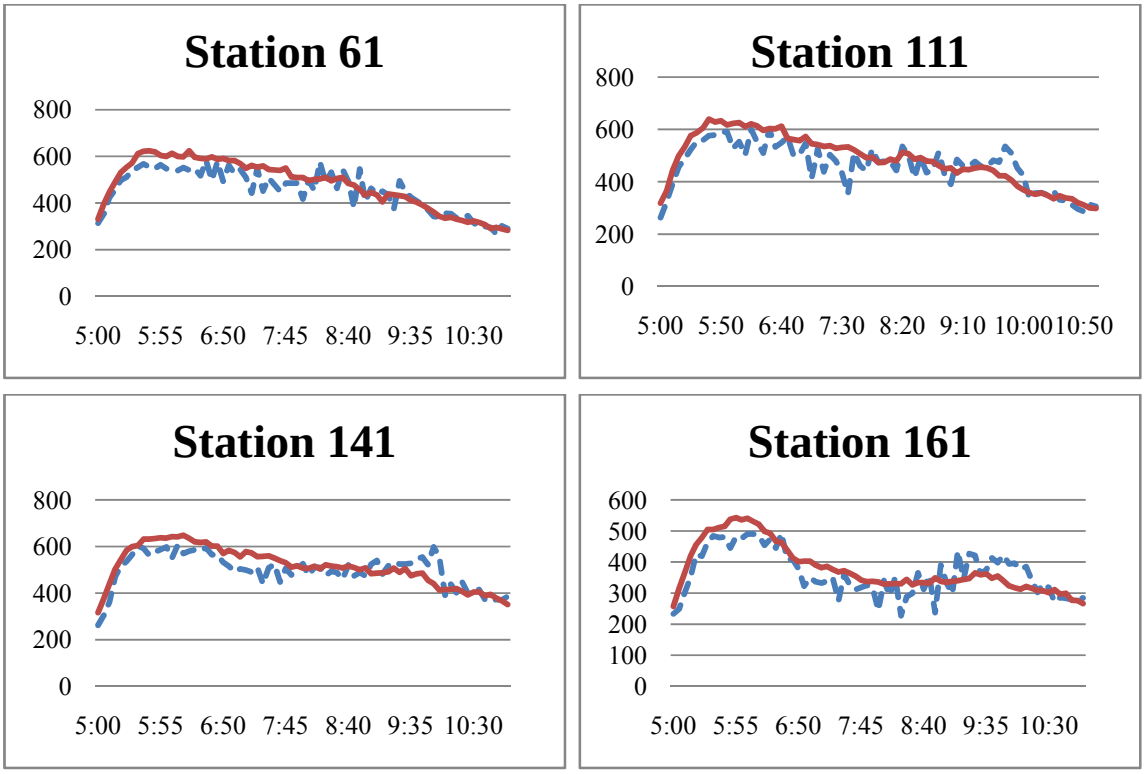

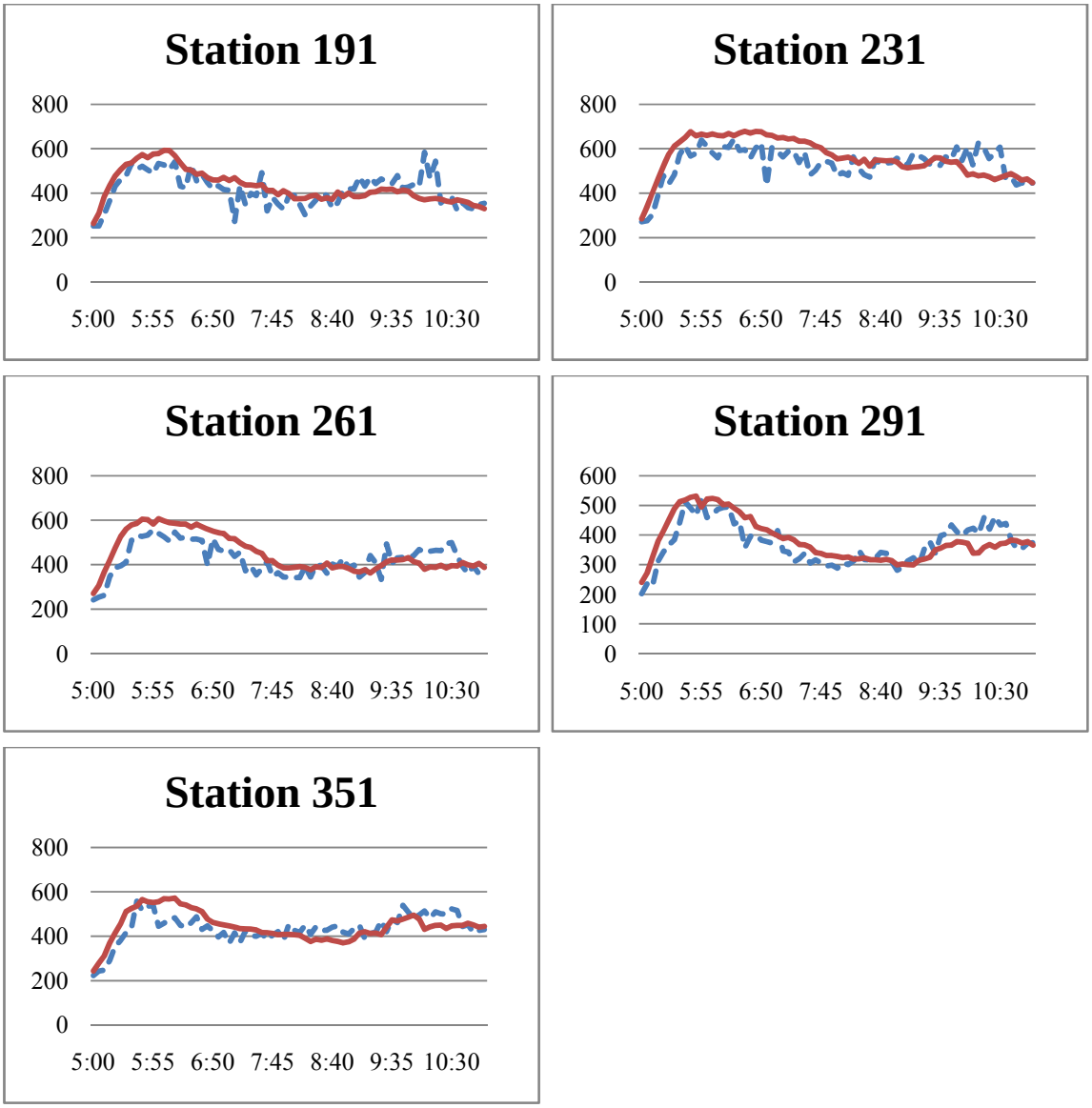

Figure 5.11 Traffic flow (veh/5min) at major freeway measurement stations
(Solid line: field data; Dashed line: simulation results)

According to Table 5.14, the MAPE and GEH% values meet the thresholds since MAPE values are less than 20% and GEH% exceed 85%. Flow plots in Figure 5.11 present good matches between simulation results and field observation. Table 5.15 gives the corresponding values of parameters on which the following incident simulation is based.

Table 5.15 List of final parameter values

P_0	P_{00}	P	$P_{offramp}$	$P_{offramp\_B1}$	$P_{offramp\_B2}$	P_{onramp}	P_{onramp_B3}
0.8	0.1	0.1	0.1	0.3	0.3	0	0.1
P_{onramp_B4}	$P_{following}$	$d_{following}$	k	b	$P_{change,man}$	$P_{change,dis}$	
0.25	0.4	8	2	1	0.9	0.5	

5.5 Incident Simulation

The parameters listed in Table 5.15 were used in the simulation of the incidents. The rerouting information is defined as inputs in this study, such as rerouting start time, end time and the percentage of vehicles choosing to reroute will be assigned to each of the ramps upstream of the incident locations. The rerouting inputs for the following incident simulation are determined using a trial and error approach. The initial values of rerouting percentage are set 0%. Different sets of values are input into the model and the one which makes the ramp flow of the simulation results consistent with the field data, evaluated based on MAPE and GEH analysis, is used as the final rerouting inputs. If the rerouting inputs are justified, the incident is simulated and the capability of the model is evaluated in terms of the consistency of mainline flow between the simulation results and field data.

5.5.1 Incident 1: Weekend Daytime

The description of Incident 1 is shown as follows:

- Incident ID: 35091
- Duration: 12:50 - 13:55, May 19, 2007, Saturday
- Location: Between US50 On-ramp and SR243 Off-ramp
- Type: Disabled
- Severity: Major
- Lane closure status:

  12:50 – 13:55 (65 min) One lane was blocked

The location of incident 1 is displayed in Figure 5.12.

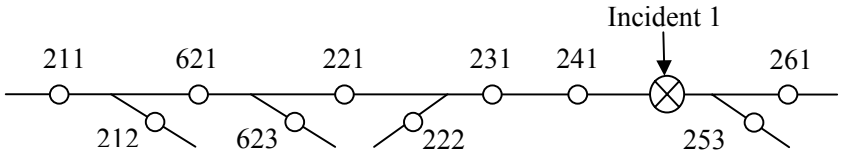

Figure 5.12 Location of Incident 1

Two off-ramps in the upstream of the incident location are affected by the incident: US50 NB Off-ramp (Station 623) and US50 SB Off-ramp (Station 212). Rerouting inputs for relevant ramps are listed in Table 5.7.

Table 5.16 Rerouting start time, end time and percentage for Incident 1

	US50 NB Off (623)	US50 SB Off (212)
Start Time	13:00	13:05
End Time	13:25	14:20
Percentage	10%	18%

The flow plots comparing the detector data and simulation results are presented in Figure 5.13. The stations involved cover all the mainline stations upstream of the incident with reliable detector data and all ramps affected by the incident.

Ramps:

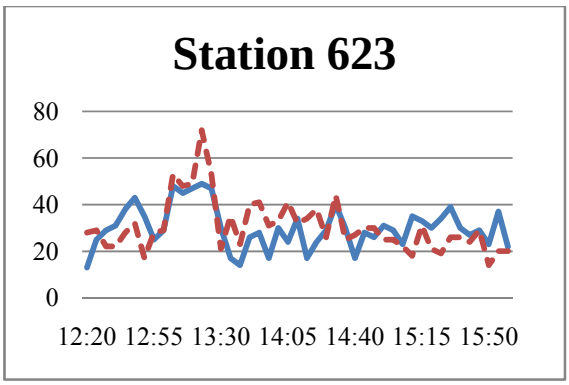

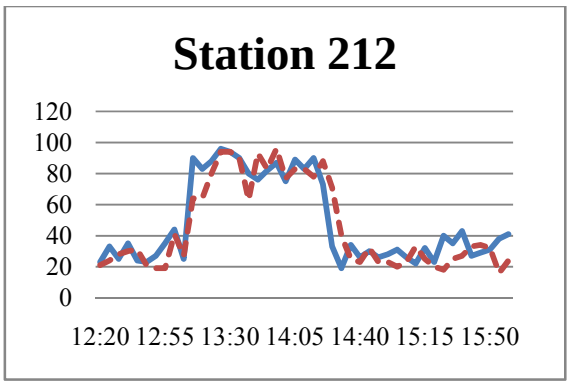

Mainline:

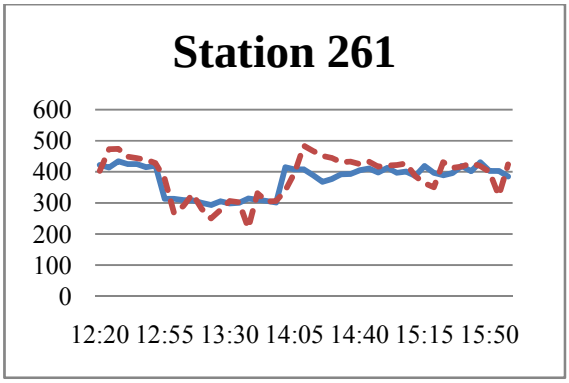

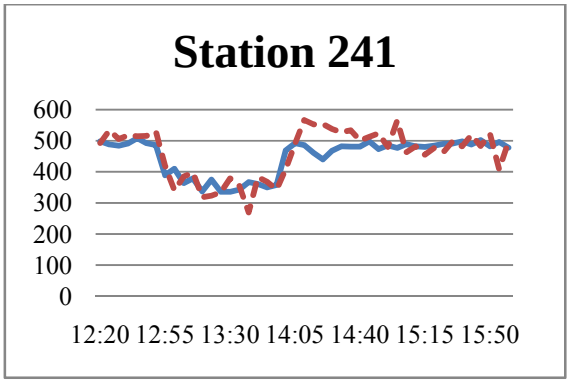

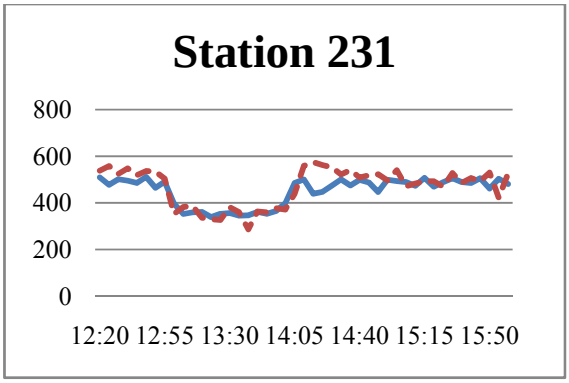

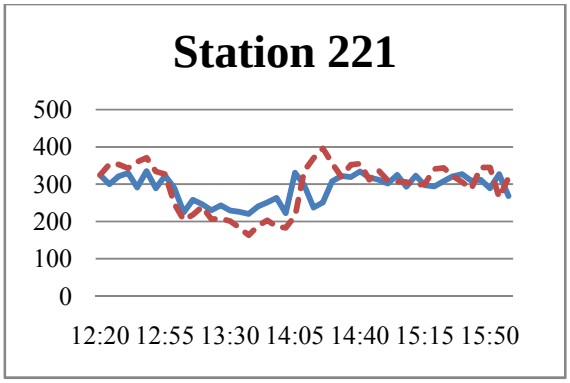

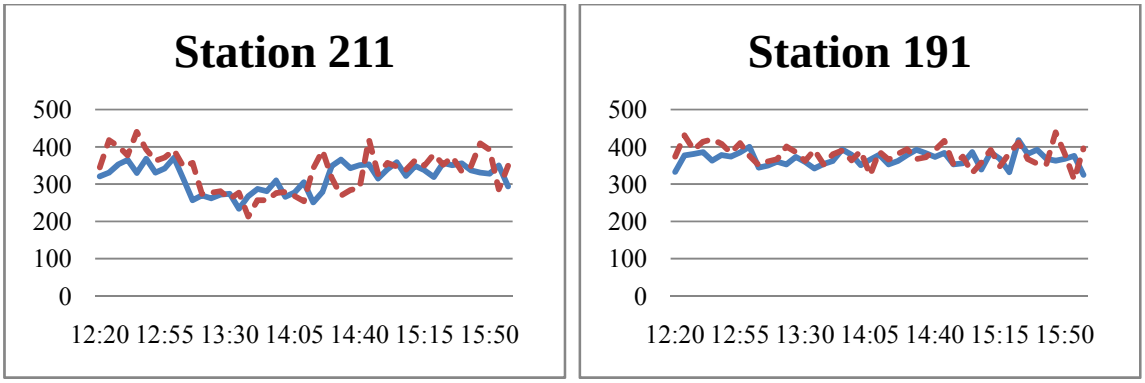

Figure 5.13 Traffic counts (veh/5min) upstream of the incident location on freeway measurement stations and ramps for incident 1(Solid line: field data; Dashed line: simulation results)

The flow drop and flow rise at some stations which can be easily identified from the figures above indicate the arrival and clearance of the queue at that location. The corresponding times can also be obtained from the figures and the time difference between sequential stations implies the queue propagation speed. Based on the station distance information, the queue length can also be computed from these flow plots. For example, according to Figure 5.13, the queue arrived at Station 241 at 12:50 and dissipated at13:55. Its arrival time at Station 211 is 13:00 and clearance time is 14:10. The distance between these two stations is about 1.6 mile. Therefore, the queue propagation speed is estimated as 0.16 mile/min.

From Figure 5.13, the queue propagation speed and queue length properly follow the field data. The time difference of the queue arrival and dissipation time is no more than five minutes between the simulation results and detector data. The average MAPE and GEH% values for each upstream station are listed in Table 5.17. Data involved cover the vehicle counts ranging from 12:20 pm to 14:25 pm with a resolution of 5-min. Since the queue clearance time for each station is no later than 14:10 pm, this time range covers the incident duration along with queue clearance period.

Table 5.17 MAPE and GEH% of Incident 1

Mainline	261	241	231	221	211	191	161	672
MAPE	10.39%	9.25%	8.90%	18.64%	12.30%	5.86%	6.40%	5.90%
GEH%	96.15%	92.31%	92.31%	84.62%	84.62%	100%	100%	100%
Mainline	151	141	121	111	91	61	51	
MAPE	6.15%	6.80%	7.46%	5.75%	7.10%	6.02%	6.80%	
GEH%	100%	100%	100%	100%	100%	100%	100%	
Ramp	222	623	212					
MAPE	10.06%	29.61%	19.78%					
GEH%	100.00%	100.00%	96.30%					

As indicated from Table 5.17, the MAPE value of all the mainline stations are less than 20%. Meanwhile, most of the GEH% values are greater than 85% except Station 221 and 211 whose

values are very close to the threshold. According to these statistical results, incident 1 is properly simulated based on the calibrated parameters and proper rerouting inputs.

The incident caused about 25% flow drop on the mainline and the queue spilled back about 2.1 miles.

Travel time information is collected by all the vehicles in the network. The incident-related travel time indicates the total time taken to traverse from the vehicle's current location to passing through the incident zone. It is affected by two factors: upstream distance from the bottleneck and elapsed time since the occurrence of the incident. Each vehicle's location at every time step is recorded and individual travel time is calculated based on this information. Output travel time is averaged over the data collected from the vehicles of the same locations and same time.

Figure 5.14 provides the tabular travel time records for incident 1. The column header in the table represents the distance from the downstream edge of the incident zone, in unit of miles. The current location interval is set as 0.2 mile, as shown in Figure 5.14, indicating the vehicles in every 0.2 mile are grouped together and the travel time are averaged over data collected from this group of vehicles. Vertical labels indicate the time of the day. The value in the table indicates the incident-related travel time, in units of minutes. When the location and time are determined, the corresponding travel time can be directly read from these tables. The table not only provides the travel time during the incident clearance duration but also in the queue dissipation period until the flow recovers to the normal condition.

	0.2	0.4	0.6	0.8	1.0	1.2	1.4	1.6	1.8	2.0	2.2	2.4	2.6	2.8	3.0	3.2	3.4	3.6	3.8	4.0	4.2	4.4	4.6	4.8
12:50	0.28	0.80	1.40	2.76	4.58	2.79	2.76	2.72	2.60	2.89	3.14	3.49	3.53	4.06	4.38	4.89	5.11	5.84	5.83	5.79	5.68	5.69	5.70	5.98
12:51	0.43	1.17	2.07	4.56	4.64	3.17	2.41	2.62	3.03	3.26	3.72	4.07	4.51	4.60	4.86	5.03	5.25	5.02	5.14	5.46	5.76	6.11	6.74	7.06
12:52	0.51	1.59	3.90	5.45	4.32	3.13	3.26	3.57	3.67	3.97	4.15	4.45	4.53	4.79	5.29	5.53	5.84	5.91	6.21	6.74	6.89	7.11	6.98	7.17
12:53	0.42	1.89	4.95	5.10	5.54	3.46	3.63	3.57	3.92	4.39	4.75	5.03	5.39	5.76	5.91	6.09	6.05	6.01	6.16	6.16	6.73	7.34	8.07	8.49
12:54	0.24	1.67	4.69	5.26	4.95	4.07	4.10	4.65	4.82	5.03	5.21	5.06	5.35	5.66	5.71	6.23	6.90	7.28	7.47	7.50	7.52	7.86	8.06	8.21
12:55	0.44	1.92	4.22	4.96	5.92	4.92	4.14	4.52	4.73	4.89	5.37	6.21	6.36	6.53	6.85	7.04	7.32	7.10	7.37	7.73	8.22	8.78	9.03	9.70
12:56	0.39	1.92	4.52	4.70	5.32	5.22	5.34	5.42	5.64	5.86	6.22	6.48	6.70	7.00	7.38	7.99	8.46	8.23	8.84	9.12	9.16	8.97	8.84	8.97
12:57	0.32	2.25	4.50	4.91	4.72	6.00	5.54	5.97	6.05	6.54	7.26	7.55	8.16	8.69	8.94	8.80	8.83	7.75	8.09	8.87	9.92	10.42	10.75	10.98
12:58	0.48	2.71	4.38	4.43	4.88	6.58	6.81	7.35	7.79	7.88	7.80	7.78	7.94	8.44	8.89	9.57	9.56	10.00	9.78	10.11	9.42	9.30	9.80	10.44
12:59	0.48	2.42	4.11	4.54	5.18	7.43	6.88	7.02	7.31	8.19	8.89	8.78	9.08	8.96	8.92	8.71	9.16	8.96	9.74	9.84	10.37	10.78	10.87	10.34
13:00	0.45	2.31	3.53	4.64	6.23	7.32	7.64	8.08	8.17	7.86	8.03	8.34	8.70	9.15	9.32	9.50	9.93	9.73	9.18	9.58	9.67	9.86	11.06	11.73
13:01	0.46	2.19	3.71	4.60	7.51	6.82	8.38	8.02	8.12	8.41	8.75	9.01	8.61	8.67	9.27	9.36	9.25	10.26	10.60	10.68	10.31	9.94	8.73	9.20
13:02	0.44	2.10	3.70	4.62	8.02	6.56	8.94	7.49	8.17	8.31	8.18	9.21	10.18	10.64	10.37	10.26	9.46	7.85	8.45	9.21	11.23	11.34	12.00	12.78
13:03	0.40	1.98	3.80	4.52	7.88	6.73	9.88	10.22	9.45	9.41	9.17	8.04	7.54	8.12	10.03	10.45	10.95	11.37	11.89	11.49	10.54	10.71	10.63	9.71
13:04	0.48	2.05	3.12	4.66	8.30	7.83	9.17	7.86	7.97	9.48	9.49	9.61	10.50	10.34	9.09	8.83	9.68	8.96	9.23	10.17	10.74	11.13	11.38	11.70
13:05	0.38	2.02	3.00	4.28	8.21	9.65	8.48	9.96	8.74	7.73	8.00	9.01	8.31	9.52	10.06	11.02	11.56	10.81	10.40	9.47	8.57	9.21	9.34	9.60
13:06	0.37	1.76	3.09	4.41	7.99	10.29	7.85	8.40	9.00	9.28	10.50	10.71	10.88	10.22	9.60	8.80	8.07	8.52	8.39	8.48	9.07	8.71	9.15	10.51
13:07	0.41	1.61	3.07	4.77	7.27	10.06	8.38	10.90	8.64	8.95	7.54	7.11	7.30	7.13	7.56	7.71	7.49	8.82	9.59	9.62	9.37	9.61	10.16	9.18
13:08	0.39	1.79	2.66	4.36	7.38	10.50	8.78	6.82	6.19	6.81	6.57	6.50	8.12	8.53	8.37	8.60	9.05	8.77	8.43	9.65	10.08	10.21	9.97	10.26
13:09	0.49	1.97	2.68	4.03	8.41	10.10	8.14	7.38	7.49	7.50	7.80	8.09	7.07	7.82	8.39	8.88	9.42	8.75	9.52	9.32	9.54	9.80	9.90	9.56
13:10	0.48	1.76	3.49	4.36	7.48	12.62	7.70	6.21	7.03	7.64	8.00	8.45	8.65	8.67	8.87	9.12	8.87	9.04	8.45	8.87	9.25	9.22	9.34	9.26
13:11	0.35	1.63	3.41	5.02	7.78	9.92	8.64	7.70	7.77	7.90	8.19	7.93	7.64	7.91	8.04	8.62	8.63	8.31	8.25	8.17	7.69	7.55	8.29	8.67
13:12	0.46	1.73	3.40	4.99	8.52	10.10	8.74	6.55	7.04	7.46	7.55	7.81	7.84	8.00	8.06	7.46	7.62	7.57	7.82	8.31	8.62	8.98	9.22	9.48
13:13	0.46	1.73	3.35	5.20	9.25	10.10	7.88	6.98	7.05	6.67	6.60	6.79	7.19	7.75	8.46	8.84	9.17	8.30	8.53	8.20	8.25	8.08	8.20	8.22
13:14	0.39	1.82	3.36	5.01	9.75	8.86	7.71	6.42	7.12	7.55	7.98	8.46	8.64	8.49	8.09	8.08	7.88	7.23	7.57	8.33	9.33	10.10	10.15	10.42
13:15	0.44	1.82	2.94	5.31	9.40	8.40	8.14	7.73	7.37	7.09	6.98	6.89	6.69	7.05	7.80	8.83	9.43	9.27	9.38	9.15	8.85	8.34	8.50	8.94
13:16	0.32	1.47	3.61	4.26	10.08	8.73	7.46	5.67	6.44	7.18	8.08	8.46	8.54	8.60	8.60	8.25	7.94	7.83	7.96	8.25	9.17	9.39	9.20	9.27
13:17	0.23	1.32	3.33	5.32	9.04	8.52	8.60	7.78	7.54	7.49	7.13	7.27	7.92	8.37	8.86	8.92	8.89	8.16	8.52	8.81	7.80	7.78	7.89	8.62
13:18	0.62	1.72	3.44	5.11	10.02	8.49	7.89	7.07	7.53	8.00	7.90	7.89	7.74	7.75	7.71	7.19	7.02	6.92	8.08	8.46	8.62	9.33	9.48	9.91
13:19	0.73	2.25	3.48	5.20	9.56	8.50	8.34	6.69	6.91	6.29	6.20	5.81	5.92	7.07	7.32	7.58	8.39	8.67	8.77	8.74	8.98	8.63	8.62	8.10
13:20	0.60	1.88	4.70	5.23	9.20	8.78	6.61	5.61	6.23	6.16	6.96	7.34	7.80	7.69	7.70	7.88	7.41	7.46	7.22	7.67	7.89	8.14	8.53	8.47

Figure 5.14 Tabular travel time records for incident 1

5.5.2 Incident 2: Weekday Off-peak

The description of Incident 2 is listed as follows:

- Incident ID: 31852
- Duration: 13:00 - 14:10, Apr 5, 2007, Thursday
- Location: Between SR28 On-ramp and SR7100 Off-ramp
- Type: Road Work
- Severity: Major
- Lane closure status:

  13:00 – 14:10 (70 min) Two lanes were blocked

The location of incident 2 is displayed in Figure 5.15.

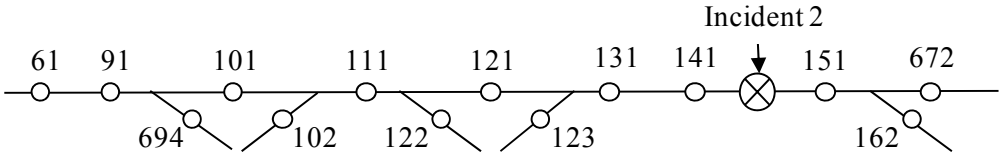

Figure 5.15 Location of Incident 2

The rerouting inputs are initially undefined in this simulation due to lack of ramp data on that day. The flow plots comparing the detector data and simulation results for upstream stations are presented in Figure 5.16.

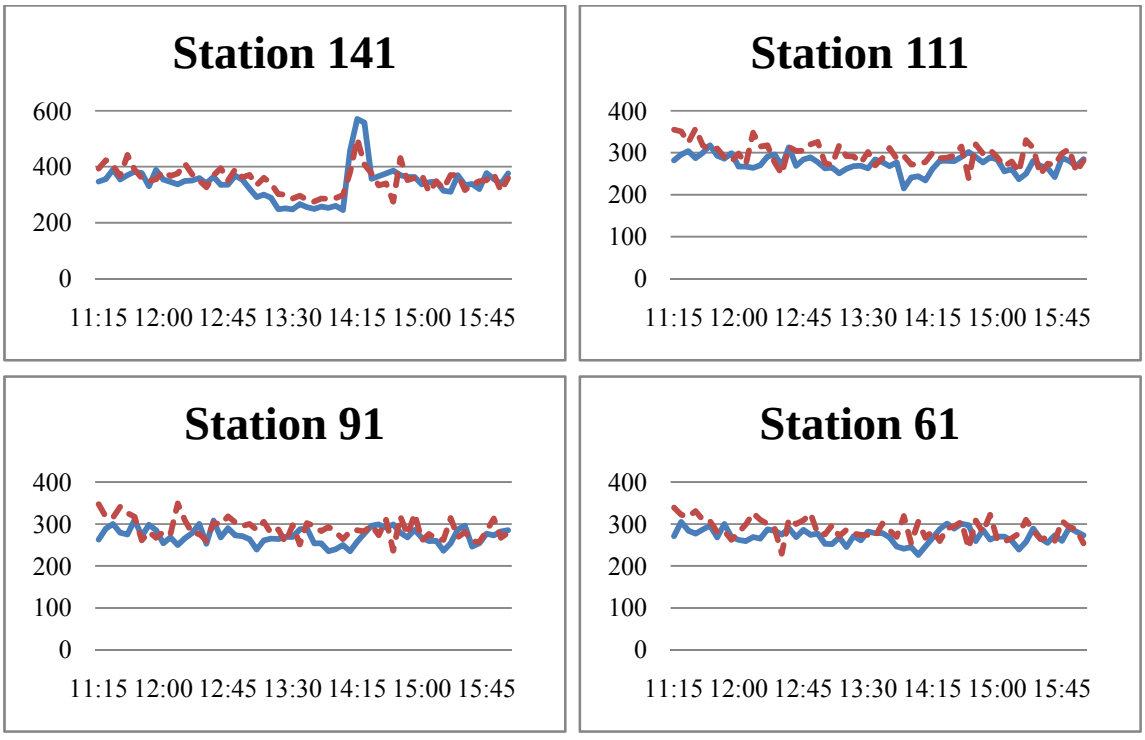

Figure 5.16 Traffic counts (veh/5min) at upstream of incident location on freeway measurement stations for incident 2 (Solid line: field data; Dashed line: simulation results)

The average MAPE and GEH% for each upstream station are listed in Table 5.18. Data involved cover the vehicle counts from 12:30 pm to 14:40 pm with a resolution of 5-min. Since the queue clearance time for each station is no later than 14:20 pm, this time range covers the incident duration along with queue clearance period.

Table 5.18 MAPE and GEH% of Incident 2

	141	111	91	61	51
MAPE	13.12%	9.55%	9.79%	8.97%	9.74%
GEH%	92.59%	100%	100%	100%	100%

Without rerouting inputs, the simulation results are highly consistent with the field data since the average MAPE value for upstream stations is 10.23% and GEH% is about 98.52%. Figure 5.17 provides the tabular travel time records for incident 2.

	0.0	0.2	0.4	0.6	0.8	1.0	1.2	1.4	1.6	1.8	2.0	2.2	2.4	2.6	2.8	3.0	3.2	3.4	3.6	3.8	4.0	4.2	4.4	4.6
13:00	0.01	0.13	0.31	0.50	0.71	0.93	1.13	1.30	1.47	1.64	1.86	2.09	2.30	2.48	2.62	2.78	2.93	3.10	3.31	3.51	3.70	3.88	4.05	4.23
13:01	0.01	0.14	0.34	0.53	0.72	0.92	1.13	1.33	1.52	1.72	1.88	2.04	2.22	2.39	2.58	2.77	2.95	3.14	3.32	3.49	3.66	3.85	4.04	4.22
13:02	0.01	0.16	0.38	0.58	0.78	0.95	1.11	1.29	1.48	1.66	1.85	2.04	2.22	2.39	2.56	2.74	2.93	3.12	3.32	3.54	3.75	3.96	4.16	4.36
13:03	0.01	0.15	0.35	0.53	0.72	0.91	1.12	1.29	1.46	1.64	1.82	2.01	2.20	2.42	2.63	2.84	3.05	3.25	3.43	3.61	3.77	3.93	4.11	4.32
13:04	0.01	0.14	0.33	0.51	0.70	0.89	1.10	1.29	1.51	1.73	1.94	2.14	2.33	2.51	2.68	2.84	3.00	3.20	3.40	3.62	3.83	4.03	4.22	4.41
13:05	0.01	0.14	0.36	0.58	0.80	1.01	1.24	1.42	1.60	1.77	1.92	2.09	2.30	2.50	2.71	2.91	3.12	3.30	3.49	3.67	3.85	4.02	4.23	4.44
13:06	0.01	0.21	0.48	0.67	0.84	0.99	1.17	1.38	1.60	1.81	2.00	2.19	2.38	2.57	2.75	2.92	3.11	3.33	3.53	3.73	3.95	4.19	4.41	4.62
13:07	0.01	0.19	0.46	0.69	0.94	1.13	1.30	1.51	1.69	1.87	2.01	2.21	2.41	2.61	2.82	3.06	3.28	3.51	3.71	3.89	4.06	4.22	4.45	4.64
13:08	0.01	0.34	0.67	0.85	1.05	1.16	1.34	1.54	1.73	1.96	2.17	2.37	2.61	2.78	2.97	3.13	3.32	3.53	3.75	3.95	4.15	4.40	4.51	4.64
13:09	0.01	0.32	0.67	0.88	1.14	1.31	1.50	1.71	1.89	2.07	2.21	2.42	2.61	2.85	3.04	3.26	3.45	3.58	3.71	4.00	4.27	4.57	4.82	5.09
13:10	0.01	0.45	0.84	1.04	1.26	1.38	1.55	1.74	1.95	2.15	2.38	2.50	2.64	2.86	3.13	3.40	3.69	3.94	4.19	4.36	4.54	4.81	5.07	5.16
13:11	0.01	0.51	0.95	1.13	1.33	1.47	1.59	1.82	2.10	2.38	2.58	2.80	3.08	3.28	3.43	3.63	3.96	4.12	4.20	4.47	4.75	4.77	4.83	5.05
13:12	0.01	0.56	0.99	1.28	1.60	1.82	1.98	2.26	2.43	2.59	2.81	3.05	3.15	3.26	3.61	3.81	3.75	3.92	4.22	4.56	4.70	4.91	5.18	5.41
13:13	0.01	0.79	1.73	1.82	2.14	2.17	2.24	2.27	2.51	2.74	2.81	2.81	3.02	3.40	3.64	3.77	4.03	4.30	4.42	4.56	4.77	5.08	5.35	5.56
13:14	0.01	1.35	1.80	1.94	2.16	1.97	1.95	2.29	2.72	2.91	2.93	3.16	3.39	3.46	3.62	3.90	4.25	4.41	4.73	5.18	5.44	5.56	5.96	6.35
13:15	0.01	1.41	1.90	2.07	2.33	2.43	2.58	2.91	3.10	3.29	3.23	3.35	3.51	3.91	4.34	4.56	4.61	5.27	5.32	5.02	5.20	5.52	5.41	5.57
13:16	0.01	1.38	2.22	2.61	2.85	2.78	2.75	2.85	3.17	3.46	3.57	3.88	4.37	4.18	4.06	4.32	4.60	4.42	4.64	4.93	5.16	5.36	5.60	5.83
13:17	0.01	1.55	2.27	2.63	3.00	2.82	3.31	3.51	3.32	3.50	3.64	3.41	3.55	3.76	4.04	4.24	4.49	4.67	4.97	5.39	5.88	6.45	7.10	7.59
13:18	0.01	1.74	2.29	2.52	2.67	3.15	2.70	2.87	3.13	3.44	3.46	3.58	3.81	4.15	4.64	5.05	5.75	6.29	6.70	6.83	7.09	7.07	6.84	6.95
13:19	0.01	1.78	2.15	2.61	2.84	2.82	2.87	3.15	3.43	3.86	4.31	5.02	5.53	5.76	5.97	6.17	5.90	5.90	6.09	6.38	6.59	6.97	7.42	7.71
13:20	0.01	1.67	2.11	2.92	3.31	3.62	4.18	4.61	4.82	5.01	5.11	4.86	4.94	5.29	5.46	5.75	6.18	6.53	6.75	6.87	7.11	7.39	7.44	7.67
13:21	0.01	1.50	2.57	3.86	4.16	4.03	3.83	4.00	4.29	4.58	4.93	5.37	5.68	5.77	5.97	6.22	6.42	6.56	6.79	7.08	7.36	7.47	7.77	8.05
13:22	0.01	1.33	2.83	3.71	4.04	4.25	4.49	4.84	4.98	5.21	5.43	5.45	5.64	5.94	6.21	6.41	6.57	6.91	7.15	7.19	7.49	7.73	7.98	8.23
13:23	0.01	1.55	2.58	4.03	4.51	4.60	4.72	4.85	5.12	5.37	5.47	5.73	6.02	6.18	6.29	6.59	6.87	7.08	7.29	7.52	7.64	7.97	8.18	8.50
13:24	0.01	1.64	2.62	3.91	4.57	4.63	4.95	5.27	5.34	5.64	5.74	5.98	6.21	6.38	6.55	6.79	7.07	7.36	7.55	7.99	8.33	8.69	8.87	8.91
13:25	0.01	1.67	2.60	4.05	4.86	4.93	5.05	5.24	5.46	5.59	5.93	6.14	6.49	6.71	7.17	7.49	7.81	7.86	8.05	8.08	8.11	8.20	8.46	8.87
13:26	0.01	1.67	2.43	4.07	4.94	5.05	5.28	5.54	5.91	6.28	6.65	6.88	6.87	7.10	7.10	7.14	7.30	7.65	7.95	8.27	8.50	8.80	8.94	9.11
13:27	0.01	1.52	2.39	4.21	5.33	5.65	5.89	6.12	6.29	6.32	6.28	6.42	6.84	7.09	7.38	7.62	7.89	8.01	8.25	8.33	8.56	8.70	8.84	9.22
13:28	0.01	1.42	2.34	4.30	5.35	5.52	5.80	6.03	6.32	6.54	6.75	6.95	7.08	7.30	7.43	7.61	7.76	8.02	8.24	8.42	8.70	8.91	9.27	9.49
13:29	0.01	1.21	2.39	4.40	5.58	5.83	6.02	6.16	6.27	6.49	6.68	6.81	7.16	7.28	7.52	7.82	8.04	8.34	8.69	9.12	9.58	9.97	10.36	10.46
13:30	0.01	1.22	2.36	4.45	5.57	5.79	5.89	6.21	6.41	6.77	6.94	7.21	7.50	7.91	8.33	8.73	9.16	9.37	9.47	9.68	9.84	10.04	10.18	10.47

Figure 5.17 Tabular travel time records for incident 2

As indicated in the Table 5.18 and Figure 5.17, the incident has minor influence on the traffic flow and travel time since it occurred in the off-peak on a weekday.

5.5.3 Incident 3: Weekday Peak

The description of Incident 3 is shown as follows:

- Incident ID: 32099
- Duration: 7:45 – 8:10, Apr 9, 2007, Monday
- Location: Between SR28 On-ramp and SR7100 Off-ramp

- Type: Collision
- Severity: High profile
- Lane closure status:

  7:45 – 8:10 (25 min) Two lanes were blocked

The location of the incident is displayed in Figure 5.18.

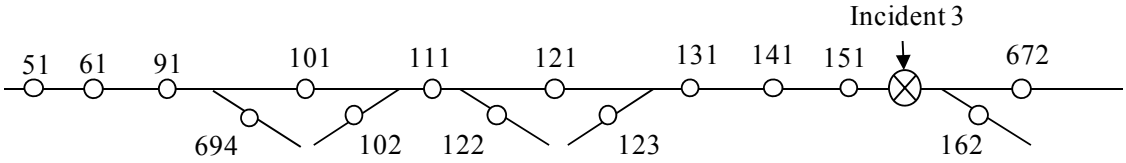

Figure 5.18 Location of Incident 3

One off-ramp and one-onramp upstream of the incident location are affected by the incident including SR28 Off-ramp (Station 122) and SR28 On-ramp (Station 123). Rerouting inputs for relevant ramps are listed in Table 5.19.

Table 5.19 Rerouting start time, end time and percentage for Incident 3

	SR28 Off (122)	SR28 On (102)
Start Time	8:00	8:00
End Time	8:20	8:30
Percentage	40%	20%

The flow plots comparing the detector data and simulation results are presented in Figure 5.19.

Ramps:

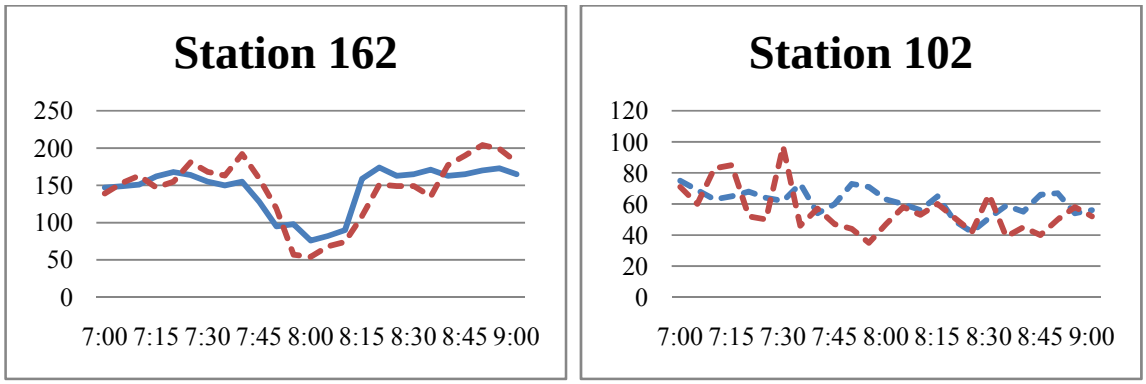

Mainline:

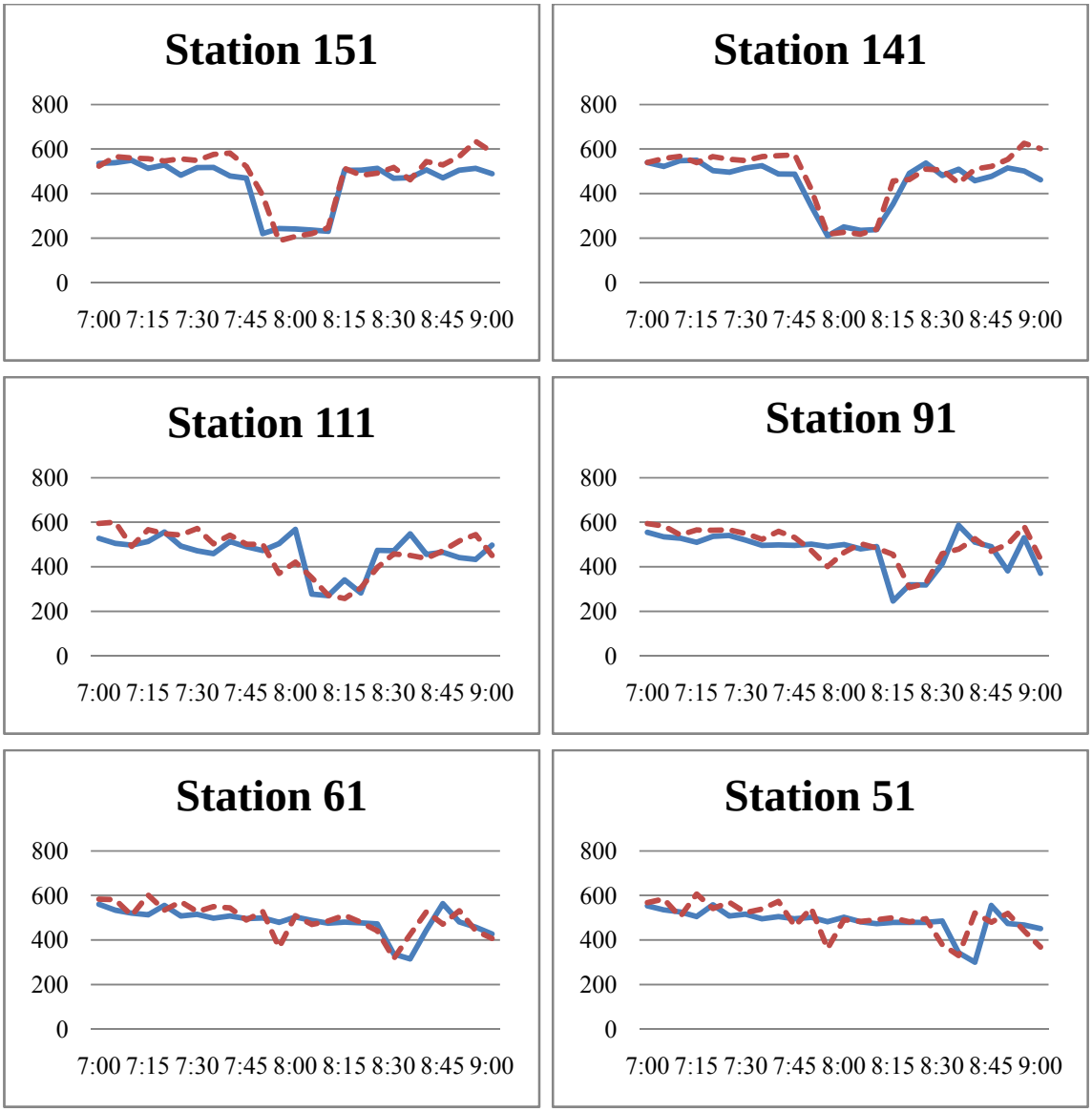

Figure 5.19 Traffic counts (veh/5min) at upstream of incident location on freeway measurement stations for incident 3 (Solid line: field data; Dashed line: simulation results)

According to flow plots in Figure 5.19, the queue propagation speed properly follows the field data. The queue arrival time and dissipation time at each station are within five-minute difference between the simulation results and detector data.

The average MAPE and GEH% values for each upstream station are listed in Table 5.20. The data involved covers the vehicle counts from 7:15 am to 8:50 am with a resolution of 5-min. Since the queue clearance time for each stations is no later than 8:45 pm, this time range covers the incident duration along with queue clearance period.

Table 5.20 MAPE and GEH% of Incident 3

Mainline	151	141	111	91	61	51
MAPE	11.20%	9.30%	12.79%	10.28%	9.17%	10.65%
GEH%	95.00%	95.00%	90.00%	90.00%	90.00%	85.00%
Ramp	162	102	694			
MAPE	20.16%	31.47%	16.65%			
GEH%	100.00%	100.00%	100.00%			

As indicated from Table 5.20, the MAPE values of all the mainline stations are less than 20%. Meanwhile, the GEH% values are greater than 85% for all the stations on the mainline and ramps. According to these statistical results, incident 3 is properly simulated based on the calibrated parameters and proper rerouting inputs.

The incident caused about 50% flow drop on the mainline and the queue spilled back from Station 151 to Station 51 which is about 5.5 miles in length. Figure 5.20 provides the tabular travel time records for incident 3.

	0.2	0.4	0.6	0.8	1	1.2	1.4	1.6	1.8	2	2.2	2.4	2.6	2.8	3	3.2	3.4	3.6	3.8	4	4.2	4.4	4.6	4.8
7:45	1.45	2.86	2.93	4.18	5.37	5.83	7.86	9.97	11.90	12.76	13.76	14.89	15.41	16.78	17.53	18.19	18.82	19.65	20.20	20.89	21.52	21.58	22.09	21.79
7:46	1.75	2.55	3.72	4.86	6.46	7.03	8.35	10.81	12.80	13.96	14.78	15.67	16.24	17.65	19.52	19.95	20.41	20.88	20.99	21.37	21.56	21.91	22.19	22.54
7:47	1.53	2.74	4.39	5.73	7.06	8.13	9.35	11.76	13.73	14.89	15.73	17.51	18.95	19.55	20.36	20.68	21.08	21.26	21.70	21.92	22.24	22.38	22.39	22.74
7:48	1.79	2.57	4.81	6.52	7.51	9.43	11.23	12.62	14.39	16.36	17.88	18.85	19.86	20.63	21.00	21.29	21.35	21.57	21.73	21.80	22.06	22.28	22.56	22.77
7:49	1.62	2.48	4.65	6.96	9.01	9.98	12.18	14.42	15.49	17.34	18.70	19.90	20.40	20.75	20.89	21.17	21.36	21.65	21.83	22.03	22.12	22.24	22.37	22.52
7:50	1.27	2.54	4.67	7.06	9.37	10.84	12.69	15.47	17.07	17.70	18.90	19.65	20.59	20.83	21.08	21.14	21.27	21.43	21.63	21.79	21.92	22.09	22.24	22.33
7:51	1.07	2.46	4.60	7.13	9.27	11.73	14.03	16.24	17.69	17.93	18.55	19.50	20.25	20.66	20.83	20.98	21.18	21.27	21.39	21.51	21.72	21.87	21.99	22.15
7:52	0.98	2.34	4.44	6.89	9.24	12.05	15.83	17.31	17.83	18.17	18.45	19.12	20.03	20.38	20.60	20.80	20.90	21.05	21.19	21.37	21.52	21.62	21.76	21.92
7:53	0.94	2.29	4.53	6.87	9.20	12.12	15.94	17.65	17.90	18.19	18.41	18.84	19.55	20.19	20.44	20.56	20.68	20.82	20.98	21.00	21.01	21.01	21.04	21.21
7:54	0.97	2.14	4.39	6.64	9.28	12.39	15.91	17.49	17.82	18.23	18.46	18.76	19.21	19.82	19.98	20.02	19.98	20.12	20.27	20.45	20.69	20.89	21.07	21.26
7:55	0.72	2.27	4.33	6.52	9.26	12.53	15.63	17.24	17.85	18.06	18.41	18.83	18.95	19.14	19.56	19.74	20.00	20.13	20.33	20.48	20.58	20.73	20.86	20.87
7:56	0.70	2.37	4.28	6.53	9.07	12.42	15.24	16.95	17.73	17.94	18.11	18.27	18.85	19.08	19.38	19.68	19.73	19.89	19.86	19.96	20.23	20.41	20.58	20.81
7:57	0.81	2.32	4.31	6.70	9.02	12.18	14.77	16.59	17.40	17.70	17.99	18.43	18.59	18.84	19.06	19.29	19.48	19.67	19.90	20.14	20.10	20.22	20.33	20.47
7:58	0.72	2.51	4.11	6.63	8.97	11.88	14.16	16.21	17.28	17.80	18.02	18.27	18.48	18.92	19.13	19.17	19.26	19.40	19.50	19.62	19.75	19.86	20.03	20.14
7:59	1.09	2.26	4.58	6.43	8.89	11.58	13.59	15.73	17.20	17.54	17.81	18.15	18.41	18.53	18.65	18.82	18.93	19.06	19.21	19.39	19.43	19.52	19.49	19.55
8:00	1.25	2.22	4.49	6.46	8.84	11.07	13.09	15.30	16.73	17.20	17.55	17.86	18.12	18.28	18.42	18.46	18.51	18.50	18.59	18.67	18.69	18.75	18.88	18.99
8:01	1.00	2.36	4.29	6.43	8.71	10.58	12.45	14.70	16.13	16.75	17.30	17.46	17.58	17.63	17.70	17.71	17.80	17.93	18.01	18.10	18.22	18.39	18.50	18.68
8:02	0.90	2.41	4.17	6.46	8.32	10.08	11.90	14.18	15.49	16.16	16.59	16.75	16.97	17.05	17.14	17.29	17.43	17.56	17.74	17.86	17.99	18.08	18.23	18.36
8:03	1.06	2.27	4.23	6.38	8.03	9.55	11.32	13.67	14.92	15.46	15.70	16.21	16.64	16.78	16.93	17.01	17.15	17.32	17.40	17.54	17.62	17.74	17.86	17.87
8:04	1.33	2.26	4.26	6.10	7.65	9.08	10.83	13.09	14.29	14.60	14.95	15.64	16.25	16.47	16.57	16.66	16.79	16.87	16.90	16.98	17.14	17.22	17.39	17.55
8:05	1.45	2.21	4.23	5.78	7.17	8.54	10.39	12.48	13.55	13.69	14.28	14.98	15.72	15.91	16.05	16.19	16.27	16.44	16.64	16.84	16.95	17.07	17.10	17.12
8:06	1.15	2.20	4.01	5.45	6.61	7.94	9.89	11.88	12.59	12.97	13.54	14.34	15.06	15.64	15.87	16.00	16.09	16.11	16.13	16.15	16.32	16.47	16.59	16.72
8:07	0.96	2.16	3.64	4.96	6.07	7.44	9.43	11.25	11.99	12.28	12.79	13.69	14.45	15.04	15.24	15.39	15.51	15.62	15.77	15.90	15.91	16.08	16.22	16.36
8:08	0.81	2.00	3.25	4.47	5.53	6.92	8.88	10.55	11.22	11.59	12.18	12.87	13.76	14.46	14.88	14.97	15.15	15.31	15.38	15.55	15.74	15.88	15.95	16.10
8:09	0.77	1.60	2.81	3.85	4.98	6.40	8.29	9.85	10.62	10.93	11.58	12.01	12.92	13.75	14.46	14.82	14.90	14.99	15.20	15.36	15.50	15.67	15.92	16.15
8:10	0.39	1.17	2.33	3.31	4.46	5.96	7.71	9.17	10.14	10.57	10.80	11.45	12.23	13.09	14.03	14.54	14.76	14.99	15.23	15.44	15.69	15.87	16.08	16.28
8:11	0.20	0.81	1.75	2.76	3.93	5.47	7.09	8.55	9.58	9.86	10.11	10.73	11.49	12.41	13.51	14.55	14.97	15.17	15.35	15.65	15.88	16.13	16.30	16.48
8:12	0.27	0.63	1.25	2.23	3.36	4.89	6.50	8.02	8.93	9.15	9.64	10.11	10.73	11.82	13.02	14.39	15.18	15.37	15.54	15.57	15.68	15.83	16.01	16.14
8:13	0.20	0.55	1.03	1.78	2.89	4.33	5.83	7.40	8.10	8.58	9.08	9.56	10.15	11.15	12.61	14.08	14.73	15.04	15.22	15.42	15.69	15.89	16.09	16.40
8:14	0.26	0.62	1.03	1.50	2.39	3.78	5.15	6.77	7.69	7.99	8.38	9.00	9.80	10.67	12.14	13.49	14.47	15.20	15.51	15.70	15.84	16.09	16.30	16.42
8:15	0.24	0.68	1.05	1.49	2.14	3.16	4.51	6.13	6.92	7.33	7.70	8.46	9.42	10.64	11.85	12.90	14.04	15.05	15.48	15.65	15.80	15.90	15.95	16.11

Figure 5.20 Tabular travel time records for incident 3

Though both incident 2 and incident 3 have two lanes blocked, the increase of travel time in incident 3 is greater than that in incident 2 due to the different incident occurrence time of the day.

5.5.4 Incident 4: Weekday Peak

The description of Incident 4 is shown as follows:

- Incident ID: 33910
- Duration: 8:20 – 8:45, May 2, 2007, Wednesday
- Location: Between SR28 On-ramp and SR7100 Off-ramp
- Type: Collision
- Severity: High profile
- Lane closure status:

  8:20 – 8:45 (25 min) Three lanes were blocked

The location of the incident is displayed in Figure 5.21.

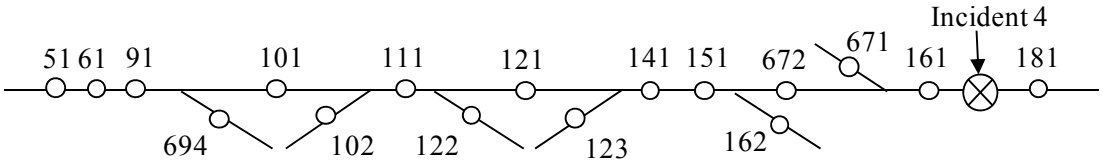

Figure 5.21 Location of Incident 4

Three off-ramps and two on-ramps upstream of the incident location are affected by the incident including SR7100 Off-ramp (Station 162), SR28 On-ramp (Station 123), SR28 Off-ramp (Station 122), US29 On-ramp (Station 102) and US29 Off-ramp (Station 694). Rerouting inputs for relevant ramps are listed in Table 5.21.

Table 5.21 Rerouting start time, end time and percentage for Incident 4

	SR7100 Off (162)	SR28 On (123)	SR28 Off (122)	US29 On (102)	US29 Off (694)
Start Time	8:25	8:45	8:35	8:55	8:45
End Time	8:50	8:55	9:05	9:10	9:05
Percentage	20%	40%	10%	40%	10%

The flow plots comparing the detector data and simulation results are presented in Figure 5.22.

Ramps

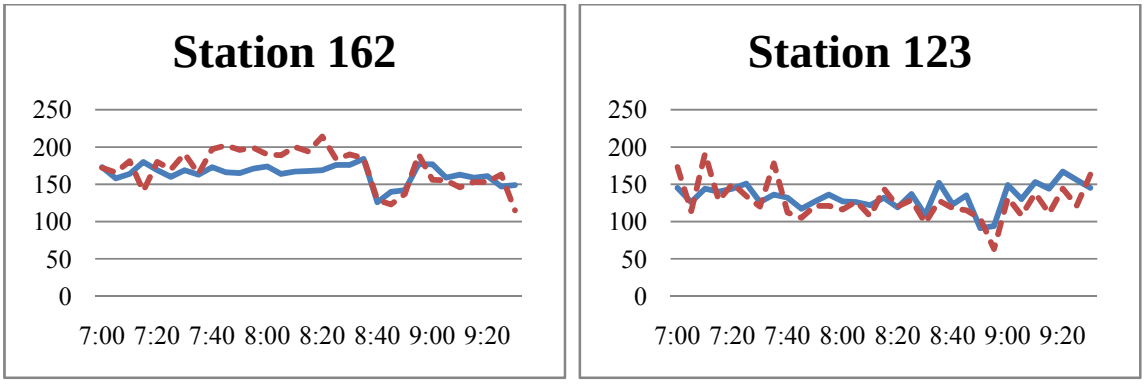

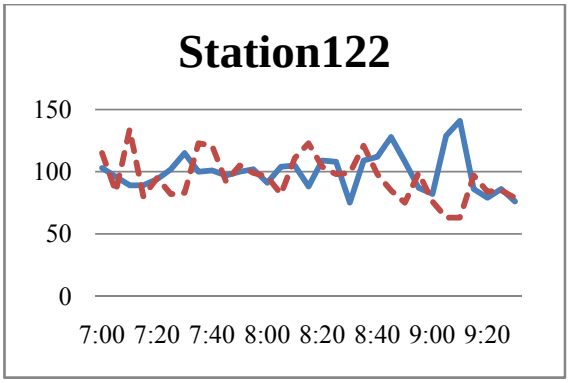
Station122
150
100
50
0
7:00 7:20 7:40 8:00 8:20 8:40 9:00 9:20

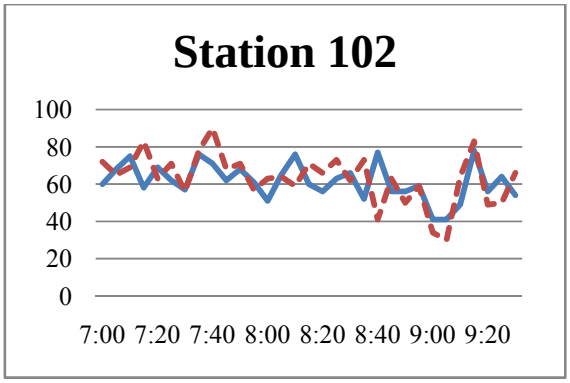
Station 102
100
80
60
40
20
0
7:00 7:20 7:40 8:00 8:20 8:40 9:00 9:20

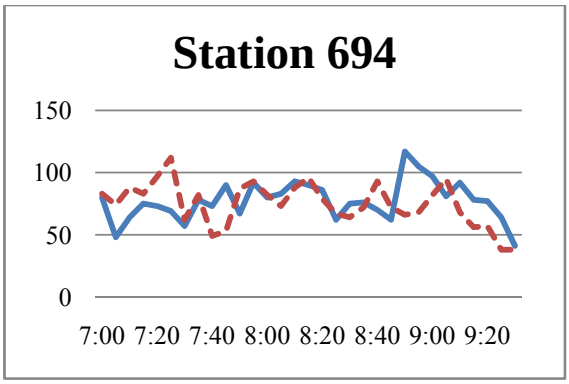
Station 694
150
100
50
0
7:00 7:20 7:40 8:00 8:20 8:40 9:00 9:20

Mainline:

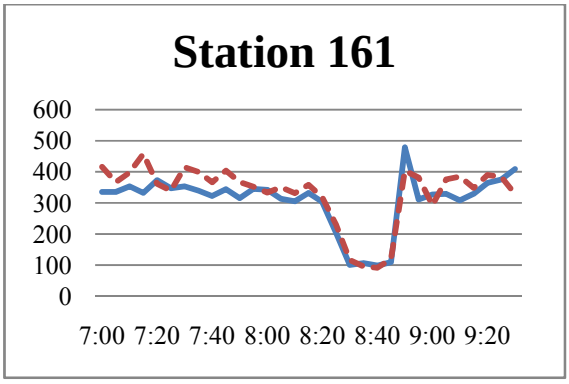
Station 161
600
500
400
300
200
100
0
7:00 7:20 7:40 8:00 8:20 8:40 9:00 9:20

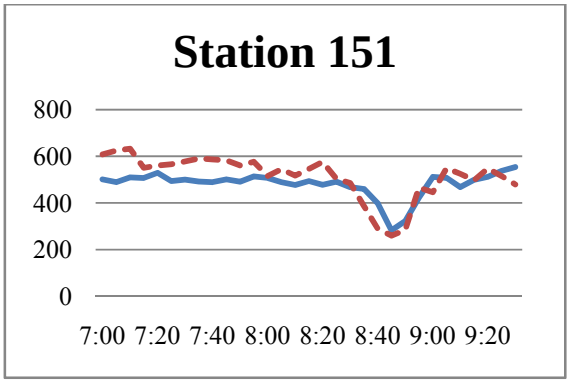
Station 151
800
600
400
200
0
7:00 7:20 7:40 8:00 8:20 8:40 9:00 9:20

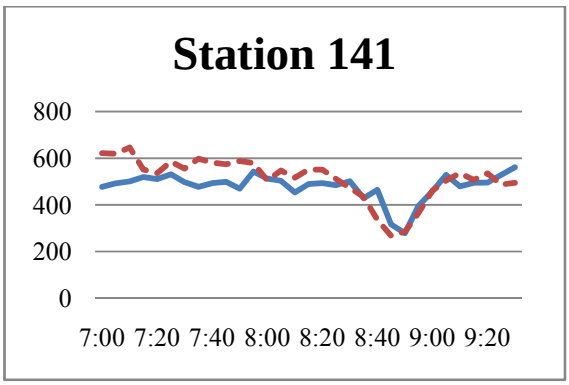
Station 141
800
600
400
200
0
7:00 7:20 7:40 8:00 8:20 8:40 9:00 9:20

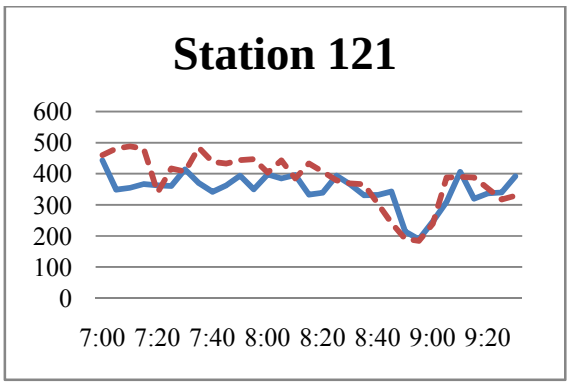
Station 121
600
500
400
300
200
100
0
7:00 7:20 7:40 8:00 8:20 8:40 9:00 9:20

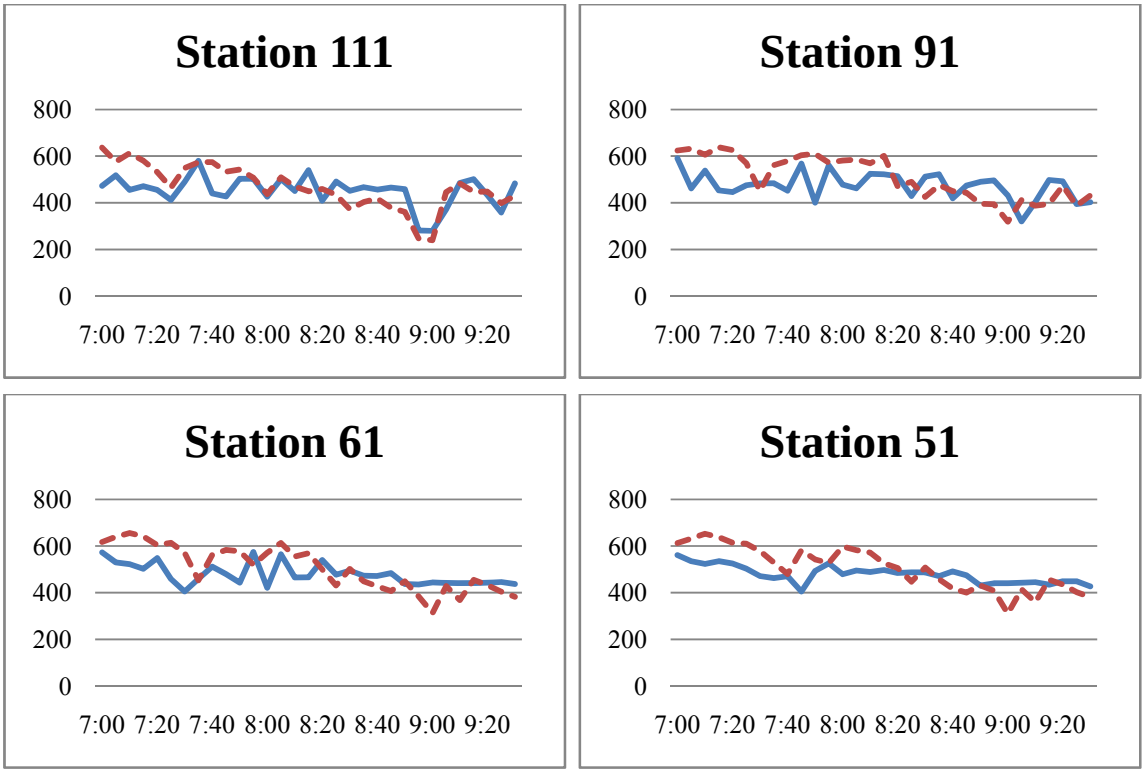

Figure 5.22 Traffic counts (veh/5min) at upstream of incident location on freeway measurement stations for incident 4 (Solid line: field data; Dashed line: simulation results)

According to flow plots in Figure 5.22, the queue propagation speed, arrival time and dissipation time at each station are consistent with the field data. The average MAPE and GEH% for each upstream station are listed in Table 5.22. The data involved covers the vehicle counts ranging from 7:50 am to 9:15 am with a resolution of 5-min. Since the queue clearance time for each station is no later than 9:15 pm, this time range covers the incident duration along with queue clearance period.

Table 5.22 MAPE and GEH% of Incident 4

Mainline	161	151	141	121	111	91	61	51
MAPE	10.53%	10.99%	9.35%	11.99%	12.03%	16.61%	13.39%	11.47%
GEH%	100.0%	100.0%	100.0%	100.0%	100.0%	100.0%	100.0%	100. 0%
Ramp	162	123	122	102	694			
MAPE	9.61%	13.57%	27.31%	18.77%	20.51%			
GEH%	100.0%	100.0%	100.0%	100.0%	100.0%			

As indicated from Table 5.22, the MAPE values of all the mainline stations are less than 20%. MAPE values greater than 20% for some ramps are due to the small values of ramp flow. As indicated in previous section, MAPE will exaggerate the difference between two inputs if their values are small. The GEH% values are 100% for all the stations on the mainline and ramps,

indicating good match between the simulation results and detector data. The incident caused about 50% flow drop at the incident bottleneck. Figure 5.23 provides the tabular travel time records for incident 4.

	0.2	0.4	0.6	0.8	1	1.2	1.4	1.6	1.8	2	2.2	2.4	2.6	2.8	3	3.2	3.4	3.6	3.8	4	4.2	4.4	4.6
8:20	14.31	14.05	15.39	18.37	15.56	16.87	13.12	8.14	5.80	7.98	9.14	10.38	12.13	14.87	15.92	16.24	16.59	19.00	22.27	23.83	24.65	25.11	25.31
8:21	18.82	14.77	14.49	13.90	13.73	12.04	6.81	6.30	7.88	9.20	10.47	11.58	14.47	15.53	15.82	16.58	17.54	20.32	23.29	24.63	24.91	25.37	25.57
8:22	18.84	8.69	6.64	5.31	4.56	5.51	6.62	7.64	9.48	10.87	12.27	13.86	14.78	15.97	17.50	17.88	19.97	21.44	23.48	24.52	24.88	24.96	24.96
8:23	17.19	3.98	4.62	5.51	6.13	7.40	8.36	8.94	10.91	12.61	13.18	14.41	17.30	17.70	19.05	19.89	21.16	22.68	23.45	23.88	24.19	24.44	24.65
8:24	15.93	5.28	6.83	7.08	7.74	9.44	10.08	11.38	11.85	12.45	13.87	16.01	18.24	19.86	20.54	21.52	22.09	22.65	22.83	23.21	23.58	23.76	24.02
8:25	15.12	6.06	8.20	9.37	10.04	11.31	11.08	11.58	12.13	13.19	15.13	17.33	19.76	20.74	21.14	21.46	21.83	22.03	22.35	22.71	22.82	23.09	23.27
8:26	14.57	6.48	9.38	9.91	10.27	11.29	11.86	12.85	14.09	15.10	16.33	18.36	19.92	20.61	20.90	21.14	21.38	21.52	21.83	21.90	22.20	22.30	22.68
8:27	13.87	6.59	9.43	10.54	11.12	12.53	13.09	14.90	15.81	16.50	17.16	18.55	19.62	20.00	20.46	20.52	20.77	21.04	21.06	21.33	21.44	21.70	21.77
8:28	13.38	6.48	10.15	12.27	12.73	14.16	14.83	15.49	16.79	17.54	17.87	18.47	19.00	19.45	19.66	19.96	20.17	20.43	20.59	20.61	20.81	20.81	21.11
8:29	12.40	6.40	10.96	13.66	14.16	15.13	15.65	16.43	17.02	17.67	17.90	18.08	18.40	18.74	19.00	19.20	19.54	19.73	19.90	19.95	20.04	20.11	20.21
8:30	11.53	6.28	11.65	14.65	14.89	15.51	15.96	16.58	16.89	17.08	17.29	17.70	17.86	18.00	18.21	18.58	18.79	18.96	19.07	19.20	19.26	19.42	19.44
8:31	10.87	6.16	11.91	14.55	14.93	15.42	15.83	16.03	16.21	16.45	16.78	16.98	17.21	17.39	17.60	17.73	17.94	18.26	18.29	18.47	18.55	18.66	18.90
8:32	10.34	5.94	11.80	14.40	14.83	15.15	15.11	15.47	15.74	15.91	15.95	16.32	16.52	16.62	16.86	16.91	17.11	17.35	17.69	17.88	17.87	17.84	17.92
8:33	9.90	5.71	11.47	13.87	14.21	14.38	14.58	14.82	14.94	15.13	15.35	15.61	15.80	15.92	16.00	16.12	16.31	16.64	16.80	16.98	17.17	17.23	17.31
8:34	9.06	5.55	11.11	13.18	13.66	13.78	13.93	14.03	14.29	14.44	14.57	14.82	15.02	15.14	15.22	15.33	15.48	15.80	16.05	16.32	16.51	16.81	16.97
8:35	8.14	5.63	10.63	12.45	12.93	13.10	13.14	13.43	13.55	13.69	13.82	13.98	14.22	14.39	14.58	14.69	14.89	14.94	15.27	15.81	16.34	16.62	16.93
8:36	7.49	5.56	10.12	11.72	12.28	12.39	12.54	12.58	12.76	12.92	13.00	13.24	13.45	13.71	13.89	14.00	14.07	14.29	14.63	15.37	16.04	16.84	17.44
8:37	6.70	5.42	9.43	10.94	11.48	11.61	11.68	11.86	11.93	12.05	12.26	12.45	12.81	12.95	13.12	13.29	13.68	13.90	14.30	15.00	16.12	16.97	17.57
8:38	5.93	5.22	8.77	10.08	10.61	10.82	10.88	11.04	11.27	11.31	11.34	11.72	11.99	12.23	12.42	12.76	13.53	14.11	14.42	14.94	16.02	16.90	17.88
8:39	5.20	4.91	8.00	9.24	9.81	9.99	10.12	10.27	10.33	10.57	10.74	10.94	11.26	11.52	12.06	12.56	13.24	14.52	15.12	15.36	15.79	16.96	17.96
8:40	4.54	4.55	7.19	8.39	8.97	9.19	9.24	9.49	9.70	9.74	9.99	10.22	10.70	11.38	11.77	12.38	13.32	14.53	15.65	16.05	16.40	16.86	17.60
8:41	3.72	4.18	6.36	7.55	8.11	8.31	8.45	8.67	8.95	9.09	9.19	9.67	10.47	11.16	11.92	12.60	13.31	14.49	15.76	16.45	16.64	16.77	17.09
8:42	2.93	3.71	5.55	6.70	7.24	7.42	7.62	7.91	8.14	8.36	8.72	9.48	10.38	11.27	12.03	12.70	13.63	14.55	15.57	16.11	16.57	16.76	16.98
8:43	2.19	3.16	4.70	5.85	6.35	6.57	6.80	7.06	7.45	7.82	8.31	9.35	10.97	11.59	12.22	12.87	13.62	14.51	15.21	15.97	16.40	16.76	16.95
8:44	1.39	2.48	3.88	5.02	5.63	5.76	5.93	6.21	6.69	7.49	8.34	9.58	10.99	11.97	12.42	13.00	13.61	14.14	14.89	15.56	16.17	16.55	16.95
8:45	0.63	1.75	3.03	4.16	4.73	4.88	5.11	5.48	6.05	7.00	8.45	9.88	11.13	12.02	12.54	12.89	13.40	14.09	14.71	15.20	15.82	16.51	16.81
8:46	0.21	0.99	2.20	3.32	3.83	4.04	4.29	4.77	5.54	6.63	8.15	9.99	11.03	11.72	12.43	12.88	13.33	13.91	14.46	15.00	15.60	16.03	16.83
8:47	0.11	0.53	1.37	2.48	3.01	3.25	3.57	4.19	5.07	6.31	7.77	9.52	10.82	11.46	12.15	12.85	13.28	13.79	14.41	14.81	15.24	15.97	16.25
8:48	0.11	0.29	0.81	1.67	2.25	2.44	2.88	3.77	4.81	6.05	7.42	9.02	10.54	11.36	11.73	12.52	13.51	13.90	14.30	14.79	15.07	15.41	15.92
8:49	0.11	0.29	0.49	1.04	1.48	1.79	2.34	3.31	4.57	5.77	7.05	8.57	10.15	11.15	11.63	12.15	13.17	14.01	14.30	14.55	14.78	15.14	15.48
8:50	0.11	0.29	0.47	0.73	0.96	1.42	2.02	2.97	4.29	5.51	6.64	8.12	9.68	10.78	11.56	12.03	12.70	13.59	14.21	14.41	14.70	15.23	15.69

Figure 5.23 Tabular travel time records for incident 4

5.6 Queue Length

The end of the queue propagation is the time when the queue reaches the farthest location. This time spot is also the initial time of queue dissipation. The end time of queue dissipation is when the queue is cleared and flow recovers to the normal conditions. This time information can be determined from the speed contour plots and be arranged in a graph, such as that shown in Figure 5.24, indicating the length of the queue over time and its recovery time.

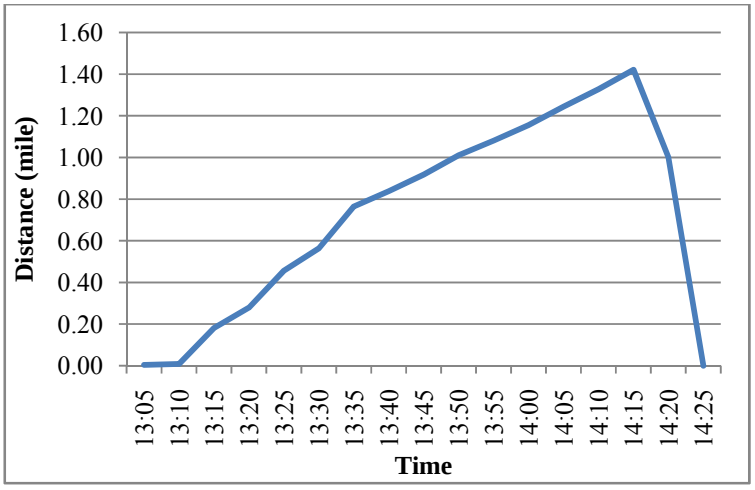

Figure 5.24 Queue length and beginning recovery for Incident 2

As can be seen from the figure, the maximum queue length is approximately 1.4 miles. The queue builds over 70 minutes and then begins to dissipate at 14:15. The traffic flow recovers to normal conditions where queues disappear within ten minutes.

5.7 Computational Efficiency

Table 5.23 lists the computational time of four incidents simulation. "Incident Time" shows the incident occurrence and clearance time, time interval between which is indicated as "Incident Duration". "Simulation Time" indicates the period of the day simulated. "Simulation Duration" is the length of the time interval simulated. Computational Time is the time taken by the computer to finish the whole simulation process. The computer used is Dell Optiplex GX620. CPU is Pentium(R) D, 3.00 GHz and RAM is 2.99 GHz, 3.00GB.

Table 5.23 Computational time of four incidents simulation

Incident	Incident Time	Incident Duration	Simulation Time	Simulation Duration	Computational Time
1	12:50 – 13:55	1h 5min	10: 30 – 16:00	5h 30min	538sec (9min)
2	13:00 – 14:10	1h 10min	11:00 – 16:00	5h	429sec (7min)
3	7:45 – 8:10	25 min	5:30 – 9:30	4h	1729sec (29min)
4	8:20 – 8:45	25 min	5:30 – 10:00	4h 30min	1794sec (30min)

The computational time for peak hour incidents (Incident 3 and 4) is much longer than the off-peak incidents (Incident 1 and 2). The system at the beginning of simulation is empty. However, if snapshots are loaded, the simulation duration will be reduced. Take incident 3 as an example. When snapshots of 7:40 are loaded into the network, indicating the simulation time is from 7:40 to 9:30,

the computational time becomes 1085 sec (18min), a drop of 40% compared to the case without loading snapshots.

5.8 Summary

In this chapter, the proposed model is tested to simulate incident-free and incident conditions. Sensitivity analysis on each parameter provides an intuitive idea of how it affects the results given different values while holding other parameters constant.

Calibration is based on trial-and-error with application of different parameter values. MAPE value and GEH analysis are the two quantitative measurements applied to evaluate the simulation results and the thresholds selected are 20% and 85%, respectively. Speed contour plots are used as supplementary tool to evaluate the weekday morning recurring congestions. Since the speed contours are consistent with field observation in terms of initial time, end time of the congestion and queue length at each bottleneck, the choice of the parameters is indicated properly in reproducing the morning traffic pattern. Both of the evaluation standards are met in the study, implying that the model for incident-free condition is properly calibrated.

Based on the incident-free model, four incidents covering different types including disabled, road work and collision and severity including major and high profile, have been successfully simulated and the results well fit the field data in terms of flow, queue length and propagation speed given the proper rerouting inputs for each ramps. MAPE and GEH% analysis is also used to evaluate the results. Since the results meet the threshold, the CA model is validated in the incident-related traffic simulation.

Based on the calibrated and validated models, travel time information covering the whole period from incident clearance duration to queue dissipation is easily obtained from the simulator. Results of travel time are provided in tabulated forms in terms of two factors affecting the travel time: upstream distance from the bottleneck and elapsed time from the start of the incident. Travel time and distance is averaged over data collected from the vehicles of the same locations and same time.

Computational time for incident simulation depends on the amount of time simulated and the occurrence time of the incident. For the same amount of simulated time, peak incident simulation requires longer time than the off-peak one. If snapshots are loaded prior to the simulation, the computational time will decrease, which is appropriate for real time application.

Chapter 6 Summary, Conclusions and Future Work

6.1 Summary and Conclusions

Numerous studies have contributed to the field of incident-related travel time forecasting. Macroscopic approaches such as shock wave analysis and queuing theory are capable of capturing traffic features under congestion condition especially when a bottleneck exists. However, a study compared the travel times from field observations to those estimated by shock wave analysis and queuing theory and revealed the underestimation of these approaches. Meanwhile, these approaches generally have difficulties in estimating the travel time when ramps are involved. Existing microscopic simulation packages are capable of forecasting travel time with high fidelity, however, they are not flexible to simulate the real-time incident due to difficulty in making rapid changes or setting some features in the software. To prevent these discrepancies, this study explored a microscopic simulation approach based on CA models to address the problems. For the purpose of practical use, many real driving behaviors are incorporated into the model, which can be summarized as:

1. Slow-to-start model
2. Mandatory lane changing behaviors of exit vehicles near their intended off-ramps
3. Mandatory lane changing behavior of merging vehicles from onramps
4. Merging behavior in the upstream of the incident locations
5. Discretionary lane changing behavior on the freeway
6. Braking light effects
7. Driving behavior on shoulder lanes
8. Speed oscillation in ramp influence zones

Different rules of driving behavior 1 to 6 have been explored in this study compared to previous research. Meanwhile, new driving behavior 7 and 8 were initially proposed. In terms of the functionality of the system, the advantages can be concluded as:

1. Flexible in making changes and setting features in the model

In the proposed incident simulator, the change on every incident-related input can be easily achieved through the interface of the system. No additional manual operations are required to change the network. The incident information can be either input via interface or by loading a flat file with defined formats. The loading process can also be accessed via the interface.

2. Adaptable to near-real time simulation

Due to flexibility in making changes in the model and efficiency in computational time, the model could be used for near-real time simulation.

3. Readable format of travel time outputs

The outputs of travel time information are presented in a readable table. Once two variables, which are time and distance from the downstream edge of the incident zone, are determined, the corresponding travel time can be directly read from the table. The travel time table may not only provide travel time information covering the incident clearance duration but also in the queue dissipation period until the flow comes back to the normal conditions. However, this should be determined by the users and specified as simulation end time.

The deficiency of the simulator is that it requires three sources of inputs which are not easily defined before the end of the incident, which include:

1. Duration of the incident

2. Lane closure status and timing

3. Rerouting start time, end time and percentage for each ramps upstream the incident location

The first issue is out of the scope of this study. However, the practical use, this problem along with the second one has been addressed when snapshots are introduced into the simulator. The duration of the incident can use any estimated value initially. When the simulator runs the first time, snapshots including all the prevailing network-related information are saved every five minutes. Once the lane status has been changed, for example, all lanes are open when the incident has been cleared, the simulator can be stopped halfway via the “Stop” button on the interface and the correct information of lane closure status and incident end time can be retyped in via interface. Meanwhile, the snapshots corresponding to the time slot that the simulator was stopped should be loaded into the network. This function increases the feasibility of the system, adapted to the near real-time incident simulation.

The third input information for each incident simulation is currently defined based on the detector data from the corresponding days, however, this is not realistic in real-time simulation and travel time forecasting. Therefore, further research is required on this aspect.

The simulation results verified that the developed CA model is capable of reproducing traffic congestions under incident conditions given proper inputs such as start time, end time and location of the incident, etc. By tracking each vehicle, the CA model can easily provide travel time information in a tabular format. The model is promising to be used on site.

6.2 Future Work

As indicated above, the major issue for further study will focus on rerouting inputs for the model. A driver-perception-based rerouting model should be incorporated into the current simulator without requiring any other information. Driver-perception-based means the drivers will make up their own minds whether to reroute on the basis of their perception of prevailing traffic conditions. The possible factors which affect their decisions may include the average speed, the time waiting in the queue and anticipated waiting time. Once the model has been validated, this model along with current models will constitute a complete incident simulator.

Apart from developing a rerouting model, other recommended future works include:

1. Incorporate HOV lane control into the model;
2. Use multiple vehicle types in the model instead of homogeneous one;
3. Compare CA model with shockwave and queuing analysis;
4. Compare CA model with other simulators such as VISSIM; and
5. Test the simulation results with field travel times.

Task 1 and 2 aim at improving the models for practical use. Tasks 3,4 and 5 compare the proposed model with several classical methods and field observation to evaluate the performance of the model. These future works will prepare the model for field deployment.

Reference

Ahmed, K.I. Modeling Drivers' Acceleration and Lane Changing Behavior. Department of Civil and Environmental Engineering, Massachusetts Institute Of Technology. Doctor of Science, 1999.

Barlovic, R., Santen, L., Schadschneider, A. and Schreckenberg, M. Metastable states in cellular automata for traffic flow. *European Physical Journal B,* Vol.5, No.3, 1998, pp.793-800.

Benjamin, S.C., Johnson, N.F. and Hui, P.M. Cellular automata models of traffic flow along a highway containing a junction. *J. Phys. A: Math.Gen.,* Vol.29, 1996, pp.3119-3127.

Brockfeld, E., Barlovic, R., Schadschneider, A. and Schreckenberg, M. Optimizing traffic lights in a cellular automaton model for city traffic. *Physical Review E (Statistical, Nonlinear, and Soft Matter Physics),* Vol.64, No.5, 2001, pp.056132-1.

Byungkyu, P. and Hongtu, Q. Microscopic simulation model calibration and validation for freeway work zone network - a case study of VISSIM, Piscataway, NJ, USA, IEEE.2006, pp.1471-1476.

Campari, E.G. and Levi, G. A cellular automata model for highway traffic. *European Physical Journal B,* Vol.17, No.1, 2000, pp.159-66.

Chowdhury, D., Wolf, D.E. and Schreckenberg, M. Particle hopping models for two-lane traffic with two kinds of vehicles: effects of lane-changing rules. *Physica A:,* Vol.235, No.3-4, 1997, pp.417-439.

Chu, L., Liu, H.X., Oh, J.-S. and Recker, W. A calibration procedure for microscopic traffic simulation, Piscataway, NJ, USA, IEEE.2003, pp. 1574-9.

Coifman, B. Estimating travel times and vehicle trajectories on freeways using dual loop detectors. *Transportation Research, Part A (Policy and Practice),* Vol.36A, No.4, 2002, pp.351-64.

Corbin, J., Vásconez, K. and Helman, D. Unifying incident response. *Public Roads,* Vol.71, No.2, 2007, pp.23-29.

Cremer, M. and Ludwig, J. A fast simulation model for traffic flow on the basis of Boolean operations. *Math. Comput. Simul.,* Vol.28, No.4, 1986, pp.297-303.

Diedrich, G., Santen, L., Schadschneider, A. and Zittartz, J. Effect of on- and off-ramps in cellular automata models for traffic flow. *International Journal of Modern Physics C,* Vol.11, No.2, 2000, pp.335-345.

Ez-Zahraouy, H., Benrihane, Z. and Benyoussef, A. The effect of off-ramp on the one-dimensional cellular automation traffic flow with open boundaries. *International Journal of Modern Physics B,* Vol.18, No.16, 2004, pp.2347-60.

Fouladvand, M.E. and Lee, H.W. Exactly solvable two-way traffic model with ordered sequential update. *Physical Review E (Statistical Physics, Plasmas, Fluids, and Related Interdisciplinary Topics),* Vol.60, No.6, 1999, pp.6465-79.

Garib, A., Radwan, A.E. and Al-Deek, H. Estimating Magnitude and Duration of Incident Delays. *Journal of Transportation Engineering,* Vol.123, No.6, 1997, pp.459-466.

Giuliano, G. Incident Characteristics, Frequency, and Duration on a High Volume Urban Freeway. *Transportation Research – A,* Vol.23A, No.5, 1989, pp.387-396.

Gomes, G., May, A. and Horowitz, R. Congested freeway microsimulation model using VISSIM. *Transportation Research Record,* No.1876, 2004, pp.71-81.

Golob, T.F., Recker, W.W. and Leonard., J.D. Severity and Incident Duration of Truck-Involved Freeway Accidents. *Accident Analysis & Prevention,* Vol.19, No.4, 1987, pp.375-395.

Hafstein, S.F., Chrobok, R., Pottmeier, A., Schreckenberg, M. and Mazur, F.C. A high-resolution cellular automata traffic simulation model with application in a freeway traffic information system. *Computer-Aided Civil and Infrastructure Engineering,* Vol.19, No.5, 2004, pp.338-350.

Hall, R.W. Incident dispatching, clearance and delay. *Transportation Research, Part A (Policy and Practice),* Vol.36A, No.1, 2002, pp.1-16.

Hobeika, A. and Dhulipala, S. Estimation of travel times on Urban freeways under incident conditions. *Transportation Research Record,* No.1867, 2004, pp.97-106.

HCM2000 *Highway Capacity Manual 2000*. Transportation Research Board, 2000, pp. 5-7.

IMS *Incident Management System*, https://vdotim.cattlab.umd.edu/index.php. Accessed January 27, 2008.

Jia, B., Jiang, R. and Wu, Q. The traffic bottleneck effects caused by the lane closing in the cellular automata model. *International Journal of Modern Physics C,* Vol.14, No.10, 2003, pp.1295-303.

Jia, B., Jiang, R. and Wu, Q. Traffic behavior near an off ramp in the cellular automaton traffic model. *Physical Review E,* Vol.69, No.5 1, 2004, pp.056105-1.

Jia, B., Jiang, R., Wu, Q. and Hu, M. Honk effect in the two-lane cellular automaton model for traffic flow. *Physica A: Statistical Mechanics and its Applications,* Vol.348, 2005, pp.544-552.

Jia, B., Jiang, R. and Wu, Q. The effects of accelerating lane in the on-ramp system. *Physica A: Statistical Mechanics and its Applications,* Vol.345, No.1-2, 2005, pp.218-226.

Jia, B., Gao, Z., Li, K. and Li, X. *Models and Simulations of Traffic System Based on the Theory of Cellular Automaton*. Science Publication, Beijing, 2007.

Jiang, R., Wu, Q. and Wang, B. Cellular automata model simulating traffic interactions between on-ramp and main road. *Physical Review E - Statistical Physics, Plasmas, Fluids, and Related Interdisciplinary Topics,* Vol.66, No.3 2A, 2002, pp.036104-1.

Jiang, R. and Wu, Q. Cellular automata models for synchronized traffic flow. *Physica A: Statistical Mechanics and its Applications,* Vol.36, 2003, pp.381-390.

Jiang, R., Jia, B. and Wu, Q. The stochastic randomization effect in the on-ramp system single-lane main road and two-lane main road situations. *Journal of physics. A, mathematical and general* Vol.36, 2003, pp.11713-11723.

Khan, A.M. Intelligent infrastructure-based queue-end warning system for avoiding rear impacts. *IET Intell. Transp. Syst.,* Vol.1, No.2, 2007, pp.138-143.

Khattak, A.J., Schofer, J.L. and Wang, M. A Simple Time Sequential Procedure for Predicting Freeway Incident Duration. *IVHS Journal,* Vol.2, No.2, 1995, pp.113-138.

Knospe, W., Santen, L., Schadschneider, A. and Schreckenberg, M. Disorder effects in cellular automata for two-lane traffic. *Physica A:,* Vol.265, No.3, 1999, pp.614-633.

Knospe, W., Santen, L., Schadschneider, A. and Schreckenberg, M. Towards a realistic microscopic description of highway traffic. *International Journal of Modern Physics C,* Vol.33, No.48, 2000, pp.L477-85.

Larraga, M.E., del Rio, J.A. and Alvarez-lcaza, L. Cellular automata for one-lane traffic flow modeling. *Transportation Research Part C: Emerging Technologies,* Vol.13, No.1, 2005, pp.63-74.

Lawson, T.W., Lovell, D.J. and Daganzo, C.F. Using input-output diagram to determine spatial and temporal extents of a queue upstream of a bottleneck. *Transportation Research Record,* No.1572, 1996, pp.140-147.

Li, X., Jia, B., Gao, Z. and Jiang, R. A realistic two-lane cellular automata traffic model considering aggressive lane-changing behavior of fast vehicle. *Physica A: Statistical Mechanics and its Applications,* Vol.367, 2006, pp.479-486.

Li, X., Wu, Q. and Jiang, R. Cellular automaton model considering the velocity effect of a car on the successive car. *Physical Review E,* Vol.64, No.6, 2001, pp.066128.

Liu, M. Traffic Flow Modeling and Forecasting Using Cellular Automata and Neural Networks. Computer Science, Palmerston North, Massey University. M.S., 2006.

M. Van Aerde & Assoc. *QUEENSOD Rel. 2.10 - User's Guide: Estimating Origin - Destination Traffic Demands from Link Flow Counts,* M. Aerde and Associates, Ltd., Blacksburg, Virginia, 2005.

MUTCD *Manual on Uniform Traffic Control Devices*. 2003, pp. 4H-1.

Nagel, K. and Schreckenberg, M. A cellular automaton model for freeway traffic. *Journal de Physique I (General Physics, Statistical Physics, Condensed Matter, Cross-Disciplinary Physics),* Vol.2, No.12, 1992, pp.2221-9.

Nagel, K., Wolf, D.E., Wagner, P. and Simon, P. Two-lane traffic rules for cellular automata: a systematic approach. *Physical Review E. Statistical Physics, Plasmas, Fluids, and Related Interdisciplinary Topics,* Vol.58, No.2-A, 1998, pp.1425.

Nam, D.H. and Drew, D.R. Automatic measurement of traffic variables for intelligent transportation systems applications. *Transportation Research, Part B (Methodological),* Vol.33B, No.6, 1999, pp.437-57.

Nam, D. and Mannering, F. An Exploratory Hazard-Based Analysis of Highway Incident Duration. *Transportation Research – A,* Vol.34A, No.2, 2000, pp.85-102.

Nassab, K., Schreckenberg, M., Boulmakoul, A. and Ouaskit, S. Effect of the lane reduction in the cellular automata models applied to the two-lane traffic. *Physica A: Statistical Mechanics and its Applications,* Vol.369, No.2, 2006, pp.841-852.

Oh, J., Jayakrishnan, R., Recker, W. Section travel time estimation from point detection data. In: Transportation Research Board 81st Annual Meeting, Washington DC, 2003.

Ohta, S., Kurebayashi, R. and Kobayashi, K. Minimizing false positives of a decision tree classifier for intrusion detection on the internet. *Journal of Network and Systems Management,* Vol.16, No.4, 2008, pp.399-419.

Ozbay, K. and Kachroo, P. *Incident Management in Intelligent Transportation Systems.* Artech House, 1999.

Petty, K.F., Bickel, P., Ostland, M., Rice, J., Schoenberg, F., Jiming, J. and Ritov, Y. Accurate estimation of travel times from single-loop detectors. *Transportation Research, Part A (Policy and Practice),* Vol.32A, No.1, 1998, pp.1-17.

Rakha, H., Van Aerde, M., Bloomberg, L. and Huang, X. Construction and calibration of a large-scale microsimulation model of the Salt Lake area. *Transportation Research Record,* No.1644, 1998, pp.93-102.

Rakha, H. and Zhang, W. Consistency of Shock-wave and Queuing Theory Procedures for Analysis of Roadway Bottlenecks. *Transportation Research Board 84 th Annual Meeting, Washington D.C., CD-ROM [Paper 05-1763]*. 2005.

Rickert, M., Nagel, K., Schreckenberg, M. and Latour, A. Two lane traffic simulations using cellular automata. *Physica A:,* Vol.231, No.4, 1996, pp.534-550.

Schadschneider, A. and Schreckenberg, M. Traffic flow models with 'slow-to-start' rules. *Annalen der Physik* Vol.6, 1999, pp.541.

Schrank, D. and Lomax, T. *2007 Urban Mobility Report*. United States, 2007.

Simon, P.M. and Gutowitz, H.A. Cellular automaton model for bidirectional traffic. *Physical Review E (Statistical Physics, Plasmas, Fluids, and Related Interdisciplinary Topics),* Vol.57, No.2, 1998, pp.2441-4.

Smith, K. and Smith, B.L. *Forecasting the Clearance Time of Freeway Accidents*. UVACTS-15-0-35. United States, 2001.

Sullivan, E.C. New Model for Predicting Incidents and Incident Delay. *ASCE Journal of Transportation Engineering,* Vol.123, 1997, pp.267-275.

Takayasu, M. and Takayasu, H. 1/f noise in a traffic model. *Fractals,* Vol.1, 1993, pp.860-866.

Ulam, S. Random process and tranformations. *Proceedings of the International Congress of Mathematicians,* Vol.2, 1952, pp.264-275.

Vanajakshi, L.D. Estimation and prediction of travel time from loop detector data intelligent transportation systems applications, Civil Engineering, Texas A&M University. Doctor of philosophy, 2004.

VDOT *Incident Management System*, https://vdotim.cattlab.umd.edu/index.php. Accessed 2007.

VDOT. *High Occupancy Vehicle (HOV) Systems*, http://www.virginiadot.org/travel/hov-novasched.asp. Accessed December 29, 2008.

Wei, C. and Lee, Y. Sequential forecast of incident duration using Artificial Neural Network models. *Accident Analysis and Prevention,* Vol.39, No.5, 2007, pp.944-954.

Wikipedia. http://en.wikipedia.org/wiki/Mean_absolute_percentage_error. Accessed 2009.

Wolfram, S. Statistical mechanics of cellular automata. *Reviews of Modern Physics,* Vol.55, No.3, 1983, pp.601 - 644.

Xia, J. and Chen, M. *Freeway Travel Time Forecasting Under Incident*. Lexington, KY, 2007.

Yahoo. http://maps.yahoo.com/. Accessed 2009.

Yeon, J. and Elefteriadou, L. Comparison of Travel Time Estimation Using Three Previously Developed Methods to Field Data Along Freeways. *5th International Symposium on Highway Capacity and Quality of Service*, 2006, pp. 229-238.

Zhu, L.-H., Chen, S.-D., Kong, L.-J. and Liu, M.-R. The influence of tollbooths on highway traffic. *Acta Physica Sinica,* Vol.56, No.10, 2007, pp.5674-8.

Zhang, W. Freeway Travel Time Estimation Based on Spot Speed Measurements. Department of Civil and Environmantal Engineering, Blacksburg, Virginia Polytechnic Institute and State University. Doctor of Philosophy, 2006.